

This item was submitted to Loughborough's Institutional Repository (<https://dspace.lboro.ac.uk/>) by the author and is made available under the following Creative Commons Licence conditions.



CC creative commons
COMMONS DEED

Attribution-NonCommercial-NoDerivs 2.5

You are free:

- to copy, distribute, display, and perform the work

Under the following conditions:

 **Attribution.** You must attribute the work in the manner specified by the author or licensor.

 **Noncommercial.** You may not use this work for commercial purposes.

 **No Derivative Works.** You may not alter, transform, or build upon this work.

- For any reuse or distribution, you must make clear to others the license terms of this work.
- Any of these conditions can be waived if you get permission from the copyright holder.

Your fair use and other rights are in no way affected by the above.

This is a human-readable summary of the [Legal Code \(the full license\)](#).

[Disclaimer](#) 

For the full text of this licence, please go to:
<http://creativecommons.org/licenses/by-nc-nd/2.5/>

SYNTHESIS AND CHARACTERISATION OF
SIZE-SELECTIVE NANOPOROUS
POLYMERIC ADSORBENTS FOR BLOOD
PURIFICATION

by

Chris Webb

A Doctoral Thesis submitted in partial fulfillment of the
requirements for the award of the degree of Doctor of
Philosophy of Loughborough University

November 2009

© by Chris Webb, 2009

Abstract

This thesis is concerned with the development and characterisation of polymeric nanoporous adsorbents to be used for blood purification. Current treatment methods for suffers of chronic renal failure are limited to haemodialysis, peritoneal dialysis and organ transplant. Organ transplant is the most efficient option however lack of donor organs mean that the majority of suffers rely on dialysis. Unfortunately both dialysis treatments are lacking when it comes to the removal of middle molecular weight molecules (MMs) (500 - 60000 Da) and the accumulation of these molecules has been attributed to a number of additional ailments suffered by those on long term dialysis. Sorbent augmented dialysis has been identified as a potential avenue to remove these MMs, an additional column would be introduced to the haemodialysis loop this would contain adsorbent particles to remove these unwanted molecules. Styrene-divinylbenzne copolymers have been identified as suitable for this task as they will non-specifically adsorb a wide range of molecules. One major concern with the introduction of a polymeric adsorbent is the potential removal of human serum albumin HSA from the patient's blood, this essential blood protein is present in very high concentrations typically 40g/l and this will potentially swamp the surface of any adsorbent. Fortunately HSA is a large blood protein (69kDa) and as such the method to combat this limitation as explored in this thesis is to tailor the pore structure of the polymeric adsorbent to size exclude albumin while retaining sufficient adsorption capacity to remove the MMs. To achieve these goals a number of polymeric adsorbents were generated using different porogens and degrees of crosslinking to control the porous structure. These adsorbents were analysed using a number of characterisation methods to assess their dry and swollen state porosities and molecular weight cut offs. Once a suitable material had been developed protein adsorption studies were carried out to confirm the size exclusion of HSA and the uptake of MMs.

KEYWORDS: Adsorption, blood purification, nanoporosity, porosity characterisation, polymerisation

Acknowledgments

I would like to thank my supervisors Prof. Richard Holdich and Dr Danish Malik for their support during my study.

I would also like to thank the technical staff of the Chemical Engineering Department for providing advice and technical assistance during the practical aspects of this work. In particular I would like to thank Dave Smith and Sean Creedon for their time and patientce.

Finally I would like to thank my Family and particularly my long suffering partner Victoria Cole for always being there for me and believing in me.

Table of Contents

<i>Abstract</i>	<i>i</i>
<i>Acknowledgments</i>	<i>ii</i>
<i>Table of Figures</i>	<i>vi</i>
<i>Table of Tables</i>	<i>x</i>
<i>1 Introduction</i>	<i>- 1 -</i>
<i>1.1 Introduction to Renal Failure and its Treatment Methods</i>	<i>- 1 -</i>
1.1.1 <i>Kidney Function and Renal Failure</i>	<i>- 1 -</i>
1.1.2 <i>Haemodialysis and Peritoneal Dialysis</i>	<i>- 2 -</i>
1.1.3 <i>The Uremic Syndrome</i>	<i>- 4 -</i>
<i>1.2 Adsorbent Augmented Haemodialysis</i>	<i>- 6 -</i>
1.2.1 <i>Augmented Haemodialysis: Use of Adsorbents</i>	<i>- 6 -</i>
1.2.2 <i>Commercial Sorbents Currently Available or Under Development</i>	<i>- 8 -</i>
<i>1.3 Conclusions</i>	<i>- 10 -</i>
<i>1.4 Research Objectives</i>	<i>- 10 -</i>
<i>2 Literature Review of the Synthesis of Porous Spherical Adsorbents</i>	<i>- 12 -</i>
<i>2.1 What are Polymers?</i>	<i>- 12 -</i>
<i>2.2 Classification of Polymers</i>	<i>- 14 -</i>
<i>2.3 General Review Of Synthesis Methods</i>	<i>- 19 -</i>
2.3.1 <i>Bulk Polymerisation</i>	<i>- 19 -</i>
2.3.2 <i>Solution Polymerisation</i>	<i>- 20 -</i>
2.3.3 <i>Precipitation Polymerisation</i>	<i>- 21 -</i>
2.3.4 <i>Emulsion Polymerisation</i>	<i>- 21 -</i>
2.3.5 <i>Suspension Polymerisation</i>	<i>- 22 -</i>
<i>2.4 Particle Size Control During Suspension Polymerisation</i>	<i>- 22 -</i>
2.4.1 <i>Agitation</i>	<i>- 23 -</i>
2.4.2 <i>Membrane Emulsification</i>	<i>- 23 -</i>
2.4.3 <i>Polymeric Stabilisers</i>	<i>- 25 -</i>
2.4.4 <i>Inorganic Particulate Stabilisers</i>	<i>- 25 -</i>

2.4.5 Viscosity Effects _____	- 26 -
2.5 Controlling Porosity Within Polymer Networks _____	- 27 -
2.5.1 Solvents and Degree of Crosslinking _____	- 27 -
2.4.2 Determination of the Porosity in Porous Polymer Beads _____	- 38 -
2.4.2.1 Introduction _____	- 38 -
2.4.2.2 Gas Adsorption _____	- 39 -
2.4.2.3 Mercury Porosimetry _____	- 41 -
2.4.2.4 Inverse Size Exclusion Chromatography _____	- 43 -
3 Experimental Materials and Methods _____	- 48 -
3.1 Membrane Emulsification and Drop Size Control _____	- 48 -
3.2 Suspension Polymerisation _____	- 51 -
3.2.1 Separation of particles from the reaction mixture _____	- 54 -
3.2.2 Removal of porogens and un-reacted monomers from particles ____	- 55 -
3.3 Measurement of Particle Size Distributions _____	- 57 -
3.4 Measurement of Porosity in Polymer Adsorbents _____	- 59 -
3.4.1 Nitrogen porosimetry _____	- 59 -
3.4.2 Inverse Size Exclusion Chromatography (ISEC) _____	- 60 -
3.5 Protein Adsorption Studies _____	- 63 -
4 Results and Discussion - Synthesis and Analysis of Porous Spherical Polymer Adsorbents _____	- 65 -
4.1 Synthesis of Polymer Adsorbents _____	- 65 -
4.2 Membrane Emulsification and Droplet Size _____	- 66 -
4.2.1 Stirrer Agitation Rate and Stabiliser Concentration _____	- 67 -
4.2.2 Effect of the addition of sodium chloride to the continuous phase ____	- 75 -
4.3 Effect on Droplet/Particle Size During Polymerisation _____	- 77 -
4.4 Porous structure of polymer adsorbents _____	- 79 -
4.4.1 Effect of Porogen and Monomer Composition on Adsorbent Internal Pore Structure _____	- 79 -
4.5 Influence of Swelling on Pore Structure _____	- 85 -
4.5.1 Inverse Size Exclusion Chromatography _____	- 85 -
4.5.2 Protein Size Analysis – Superdex 75 _____	- 89 -

4.5.3 Inverse Size Exclusion Chromatography of Polystyrene Adsorbents	- 90 -
4.5.4 Vacuum Drying of Polymer Adsorbents	- 96 -
4.5.5 Drying at Ambient Temperature	- 96 -
4.5.6 Freeze Drying of Polymer Adsorbents	- 97 -
4.6 Choosing the most suitable adsorbent	- 100 -
4.7 Conclusions	- 100 -
5 In Vitro Evaluation of Size Exclusion Principle: Adsorption Studies	- 103 -
5.1 Analysis of Protein Uptake Data	- 103 -
5.2 Single Solute Batch Adsorption Dynamics	- 107 -
5.3 Multiple Solute Batch Adsorption Dynamics	- 113 -
5.4 Modelling Batch Adsorption Dynamics Data	- 117 -
5.5 Conclusions	- 120 -
6 Conclusions and Recommendations for Further Work	- 122 -
6.1 Control of Internal Porous Structure of Polymeric Adsorbents	- 122 -
6.1.1 Exclusion of human serum albumin	- 122 -
6.1.2 Optimisation of pore structure	- 123 -
6.3 Analysis of Porous Structure	- 127 -
6.4 Adsorption of Marker Proteins	- 129 -
6.5 Conclusions	- 130 -
6.6 Further Work	- 131 -
7 References	- 133 -
8. Appendices	- 143 -
8.1 Appendix I Standard operating procedures	- 143 -
8.2 Appendix II Toluene droplet micrographs	- 158 -
8.3 Appendix III Irreversible adsorption batch kinetics model	- 175 -
8.4 Appendix IV Publications	- 182 -

Table of Figures

Figure 2.1: Simple representations of linear, branched and crosslinked networks, where X represents a repeating unit and Y a crosslinking unit.	- 13 -
Figure 2.2: Variation of molecular weight with percentage monomer conversion during chain polymerisation.	- 18 -
Figure 2.3: Variation of molecular weight with percentage monomer conversion during step polymerisation.	- 18 -
Figure 2.4: Phase separation and the generation of pores during polymerisation	- 29 -
Figure 2.5: Phase diagram for determining the type of polymer generated; regions correspond to I - Gel type resins, II – Macroporous resins and III – Microgel powder.	- 36 -
Figure 2.6: Pseudo phase diagram showing how the macroporous resin envelope moves depending on the type of porogen.	- 37 -
Figure 2.7: Mercury porosimetry (a) intrusion; (b) extrusion curves of porous silica (Vydac TP 15) (Hagel, 1988).	- 41 -
Figure 2.8: Sample chromatogram showing the relationship between totally included, excluded and partially excluded probes and their relationship to K_d	- 45 -
Figure 2.9: Pore size distribution of porous silica (Vydac TP 9) from ISEC and nitrogen sorption data (*) (Taken from Hagel, 1988).	- 47 -
Figure 3.1: Schematic of Micropore Technologies Ltd. membrane emulsification cell and a micrograph of the membrane surface.	- 48 -
Figure 3.2: Schematic diagram of the suspension polymerisation reactor (showing orientation of heating and cooling water flows and stirrer position).	- 52 -
Figure 3.3: Schematic of Shaft stirrer gland used for suspension polymerisation.	- 53 -
Figure 3.4: Schematic diagram of a Soxhlet extraction system	- 56 -
Figure 3.5: Schematic diagram of the freeze drier system.	- 60 -
Figure 3.6: Schematic of batch protein adsorption apparatus	- 63 -
Figure 4.1: Toluene droplet size distributions with 0.5% PVA continuous phase at various stirrer speeds.	- 69 -

Figure 4.2: Toluene droplet size distributions with 1% PVA continuous phase at various stirrer speeds.....	- 69 -
Figure 4.3: Toluene droplet size distributions with 2% PVA continuous phase at various stirrer speeds.....	- 70 -
Figure 4.4: Toluene droplet size distributions with 3% PVA continuous phase at various stirrer speeds.....	- 70 -
Figure 4.5: Toluene droplet size distributions with 4% PVA continuous phase at various stirrer speeds.....	- 71 -
Figure 4.6: Toluene droplet, photographs clockwise from top left 0.5% PVA & 335 rpm, 1% PVA & 1345 rpm, 2% PVA & 335 rpm and 4% PVA & 335 rpm	- 72 -
Figure 4.7: Surface and contour plots for approximating a median droplet diameter for a given PVA concentration and stirrer speed.	- 74 -
Figure 4.8: Toluene droplet size distributions, comparing the effect of adding sodium chloride to the continuous phase, generation conditions 1% PVA and 1010 rpm stirrer speed.....	- 76 -
Figure 4.9: Polystyrene-divinylbenzene emulsion generation and droplet/particle size progression during polymerisation, 2% PVA, 3.3% sodium chloride and 335rpm stirring.	- 78 -
Figure 4.10: Effect of porogen on pore volume distribution of poly(styrene-divinylbenzene) copolymer adsorbent particles measured using nitrogen gas adsorption.	- 80 -
Figure 4.11: Effect of monomer to porogen ratio on pore volume distribution of a poly(styrene-divinylbenzene) copolymer adsorbent with a nominal 50% crosslinking degree and toluene as the porogen, analysed with nitrogen gas adsorption.	- 81 -
Figure 4.12: Effect of nominal crosslinking degree on poly(styrene-divinylbenzene) adsorbents utilising adsorbents generated using toluene as porogen and assessed using nitrogen gas adsorption.	- 82 -
Figure 4.13: Comparison of pore volume size distributions using nitrogen gas adsorption for two identically specified polymer adsorbents of differing particle size.	- 85 -
Figure 4.14: Particle size distribution for Superdex 75 Prep Grade.	- 86

Figure 4.15: ISEC chromatogram for Superdex 75 packed in a 4.6 mm diameter column 250 mm in length, ultra pure water as the eluent, flow rate of 0.1 ml/min, probing with dextran standards size 180 Da – 1.4 MDa.....	- 87 -
Figure 4.16: ISEC chromatogram for Superdex 75 packed in a 10 mm diameter column 250 mm in length, ultra pure water as the eluent, flow rate of 0.1 ml/min, probing with dextran standards size 180 Da – 1.4 MDa.....	- 88 -
Figure 4.17: Normalised cumulative pore volume distributions for Superdex 75 comparing column size	- 88 -
Figure 4.18: Dextran calibration curve for Superdex 75 (10mm diameter column)....	- 89 -
Figure 4.19: ISEC chromatogram for adsorbent PSDVB3:5TolUn1:0, polystyrene standards in THF.....	- 91 -
Figure 4.20: ISEC chromatogram for adsorbent PSDVB1:1TolUn9:1, polystyrene standards in THF.....	- 92 -
Figure 4.21: ISEC chromatogram for adsorbent PSDVB3:5TolNap5:2, polystyrene standards in THF.....	- 92 -
Figure 4.22: Molecular weight calibration curves for polystyrene in THF for three polymer adsorbents.....	- 94 -
Figure 4.23: Percentage accessible pore volume distributions for three polymer adsorbents generated from ISEC with polystyrene standards in THF, with indicators for the size of albumin and lysozyme.	- 95 -
Figure 4.24: Nitrogen gas adsorption cumulative pore volume distributions for PSDVB3:5TolNap5:2 dried under vacuum from different solvents, and normalised cumulative pore volume distributions for the same samples. Arrows indicate which axis for each set of results.....	- 98 -
Figure 4.25: Normalised nitrogen gas adsorption cumulative pore volume distributions for PSDVB3:5TolNap5:2 freeze dried from benzene and cyclohexane with toluene thermally dried as a comparison.....	- 99 -
Figure 4.26: Comparison between 50% and 80% crosslinking for an adsorbent using toluene and naphthalene for a porogen.	- 100 -
Figure 5.1: Lysozyme adsorption kinetics for XAD4, varying particle diameter (sauter mean) at stirrer speed 826 rpm to minimise external film diffusion effects.	- 108 -

Figure 5.2: Lysozyme adsorption kinetics for PSDVB3:5TolNap5:2, varying particle diameter (sauter mean) at stirrer speed 826 rpm to minimise external film diffusion effects. - 108 -

Figure 5.3: Lysozyme adsorption kinetics for XAD4, y-axis plotted as $q(t)/q(f)$ (normalised uptake) against dimensionless time. - 110 -

Figure 5.4: Lysozyme adsorption kinetics for PSDVB3:5TolNap5:2, y-axis plotted as $q(t)/q(f)$ (normalised uptake) against dimensionless time. - 110 -

Figure 5.5: HSA adsorption kinetics for XAD4, varying particle diameter (sauter mean) at stirrer speed 826 rpm to minimise external film diffusion effects. - 112 -

Figure 5.6: HSA adsorption kinetics for PSDVB3:5TolNap5:2, varying particle diameter (sauter mean) at stirrer speed 826 rpm to minimise external film diffusion effects. - 112 -

Figure 5.7: Lysozyme adsorption kinetics for 15g of PSDVB3:5TolNap5:2, 420 μm particle diameter (sauter mean), comparing the uptake kinetics in the presence of 200 mg/l HSA. At a stirrer speed of 826 rpm to minimise external film diffusion effects. - 115 -

Figure 5.8: Lysozyme adsorption kinetics for 15g of PSDVB3:5TolNap5:2, 420 μm particle diameter (sauter mean), comparing the uptake kinetics in the presence of 1000 mg/l HSA. At a stirrer speed of 826 rpm to minimise external film diffusion effects. - 116 -

Figure 5.9: Fractional uptake ($q(t)/q^*$) versus adsorption time, comparison of PSDVB3:5TolNap5:2 (open triangles – lysozyme data; solid triangles – HSA data) and XAD4 (open diamonds – lysozyme data; solid diamonds – HSA data). Solid lines are the irreversible isotherm model predictions for the data. - 120 -

Table of Tables

Table 2.1: <i>Polystyrene solvents and non-solvents solubility parameters.....</i>	- 32 -
Table 2.2: <i>Solvent-polymer interaction parameters.....</i>	- 33 -
Table 2.3: <i>Average pore diameter of porous polymer beads generated using three different porogens and varying concentrations of crosslinking agent (divinylbenzene), adapted from Poinescu et al (1984).</i>	- 33 -
Table 2.4: <i>Surface area varying with divinylbenzene concentration</i>	- 35 -
Table 2.5: <i>Inverse size exclusion probe molecules - molecular weight and viscosity radius.</i>	- 44 -
Table 3.1: <i>Dextran probe molecular weight (M_P), polydispersity index (PDI) and viscosity radius (R_η).</i>	- 61 -
Table 3.2: <i>Polystyrene probe molecular weight (M_P), polydispersity index (PDI) and viscosity radius (R_η).</i>	- 62 -
Table 4.1: <i>Polymer adsorbent composition, all ratios are weight for weight.....</i>	- 66 -
Table 4.2: <i>Stirrer speeds and PVA concentrations</i>	- 67 -
Table 4.3: <i>Toluene droplet size distribution data.....</i>	- 73 -
Table 4.4: <i>Nitrogen porosimetry results for polymer adsorbents, refer to Table 4.1 for compositional information.</i>	- 83 -
Table 4.5: <i>Comparison of BET surface area for poly(styrene-divinylbenzene) adsorbents with varying nominal crosslinking degree and values obtained for similar materials reported by Durie et al (2002).</i>	- 84 -
Table 4.6: <i>Determination of lysozyme and human serum albumin viscosity radii by use of size exclusion chromatography, Superdex 75 and dextran standards</i>	- 90 -
Table 4.7: <i>Inverse size exclusion chromatography adsorbents particle size distribution data.....</i>	- 91 -
Table 4.8: <i>Nitrogen gas adsorption porosity data for a poly(styrene-divinylbenzene) adsorbent (PSDVB3:5TolNap5:2) dried under vacuum at ambient temperature or freeze dried at -20°C from different solvents.....</i>	- 97 -
Table 5.1: <i>Lysozyme and human serum albumin (HSA) total adsorption capacity q^* and Γ values for selected adsorbent materials.</i>	- 104 -

Table 5.2: *Mass of adsorbent required for the removal of 1g of lysozyme and the mass of the consequential removal of human serum albumin (HSA).* - 106 -

Table 5.3: *Summary of experimental variables used for measuring lysozyme (LYZ) and HSA batch adsorption dynamics.....* - 119 -

1 Introduction

1.1 Introduction to Renal Failure and its Treatment Methods

1.1.1 Kidney Function and Renal Failure

With advancements in medical technologies and medicine people are living longer and surviving illness which previously would have been fatal, the upshot of this however is that a number of these patients subsequently require the treatment of chronic illnesses such as kidney failure.

Kidney failure can be one of two types acute and chronic. Acute kidney failure is the sudden and reversible loss of kidney function this can be caused by a number of factors including trauma, septic shock or a multitude of other conditions. Chronic kidney failure is typified by the longer term progressive loss of kidney function, chronic kidney failure will require long term treatment (this will usually last the remainder of the patient's life), this treatment is dialysis.

The most effective treatment for somebody with kidney failure is to have a donor organ transplanted, however there is a general shortage of donor organs and there must be compatibility between the donor and recipient. To understand the treatment methods which are available for patients with kidney failure, who through unavailability of donor organs or other medical conditions which would make operating dangerous, we must first understand what function the kidney performs. The primary role the kidneys play is in the maintenance of the balance of the bodily fluids through the filtering and excretion of excess water, minerals (salts) and metabolites (urea) as urine.

The kidneys also play a role in controlling blood pressure and the generation of red blood cells however these are secondary functions over filtering toxins from blood.

With the major function of the kidney simplified to that of a filter (even be it a very highly efficient one) a review of current treatment methods which are available all focus around membrane filtration. The clinical treatment for renal failure is by dialysis and there are two major methods by which this may be carried out: haemodialysis and peritoneal dialysis.

1.1.2 Haemodialysis and Peritoneal Dialysis

Haemodialysis uses an external unit called a dialyser this incorporates a pump and the filter module, filtration occurs by the diffusion of waste products, excess minerals etc. and the convection of water through a semi-permeable membrane into a dialysate fluid, which contains healthy biological levels of minerals and salts. The dialysate is constantly replaced to maintain a concentration gradient enhancing removal. Haemodialysis is normally carried out in a hospital/haemodialysis clinic and patients are normally treated 3 times a week with each haemodialysis session lasting between 3-5 hours.

Peritoneal dialysis is different to haemodialysis in that it utilises the peritoneal cavity to hold the dialysate fluid (which contains minerals and glucose). The peritoneal membrane acts as a semi-permeable membrane, the dialysate stays in the peritoneal cavity for extended periods of time absorbing waste products and excess fluid, excess liquid is removed through osmotic pressure generated by the presence of glucose in the dialysate. The fluid is then drained and discarded. The process is repeated 4-5 times during the

day and often automated during the night. Peritoneal dialysis is less efficient than haemodialysis, however the longer periods of treatment allow for effective removal of waste products and excess liquid. Peritoneal dialysis can be carried out in the home which allows the patient more freedom as they are not tied to a treatment centre.

Currently over a million people require ongoing dialysis treatment worldwide. Lysaght (2002) estimated an increase in the need for patients requiring dialysis at 7% per year

Haemodialysis is by far the most common treatment (in 2004 88% of long term dialysis patients were treated using haemodialysis (Grassman *et al*, 2005)) and over time the membranes have improved to clean the blood more efficiently however, due to the non-specific nature of the diffusion process important blood proteins for example human serum albumin could also be removed this then becomes a major design criteria in the development of haemodialysis membranes. Albumin is present in blood at concentration levels typically around 40 g/L in a healthy person and it is therefore not practical to include this much albumin in the dialysate to hinder removal by diffusion. Human serum albumin has a molecular weight of 69 kDa to prevent the removal of this molecule haemodialysis membranes typically have a molecular weight cut off of ~50 kDa this helps in the reduction of albumin removal however, this limits the potential to remove middle molecular weight molecules as fouling of the membrane during treatment reduces the molecular weight cut off further.

Further advances in the treatment of renal failure have identified that while dialysis is a good substitute for a kidney in its function of water, mineral, salts and small proteins (e.g. urea) removal there are a large number of other proteins normally removed by the kidneys which accumulate in patients with

renal failure. To describe these molecules they are grouped in terms of their size, low molecular weight molecules <500Da , middle molecular weight molecules 500Da - 60kDa and large molecular weight molecules >60kDa (Winchester et al, 2006). The removal of low molecular weight molecules is efficiently carried out by current dialysis treatment due to their physical size. However the larger middle molecular weight molecules are inefficiently removed (Humes et al, 2006) and may lead to ill health in patients (Vanholder *et al*, 2001) therefore an augmented treatment which combines haemodialysis with a second treatment to remove these middle molecular weight molecules is required.

1.1.3 The Uremic Syndrome

Uremic syndrome is the term associated with complications which arise from retention of molecules normally removed by the healthy kidney that are not removed by current dialysis treatments. These molecules which remain are called the “uremic toxins” and are within the middle molecular weight range (500 – 60000 Da). The small diffusivity of middle molecular weight molecules and reduced effective area available for diffusion through fouling of the membrane are probably the reason for the inherently slower diffusion flux and hence ineffective clearance of the middle molecular weight molecules.

The increases in these uremic toxins within the patient are attributed to declining health in dialysis patients (Vanholder et al, 1996). The precise effect that uremic toxins have on a patient’s health are hard to evaluate due to other morbid conditions associated with renal failure however, there is evidence to support the removal of these toxins. Studies have shown correlation between the length of time a patient has been on dialysis and the onset of dialysis related amyloidosis (DRA) (Vraetz et al, 1999 and Dember and Jaber, 2006). The retention of middle molecular weight toxins is a

suggested cause of DRA. DRA has a wide range of symptoms including osteolytic bone lesions and carpal tunnel syndrome. Direct links to the presence in elevated levels of β_2 -microglobulin have been associated with DRA.

End stage renal disease (ESRD) has also been linked to the elevated presence of middle molecular weight toxins. Winchester et al, (2002) highlights the potential use for sorbents within the field for the removal of these molecules. The HEMO study (Depner et al, 2004) further supports the suggestion of removing middle molecular weight molecules suggesting that greater clearances of small molecules (traditionally well cleared by dialysis) did not relate to improved mortality rates.

Uremic toxins which have been identified in literature to be of particular interest include (Vanholder et al, 2006),

- β_2 -microglobulin
- Cytokines
- Advanced Glycation End Products (AGEs)

Of these the main focus has been β_2 -microglobulin for the removal of which a commercial adsorbent column has been developed (Lixelle) and use of this has demonstrated improved patient health (Hiyama et al, 2002). Additionally strong links between β_2 -microglobulin and DRA have been made, the demonstration of consistently high levels of β_2 -microglobulin in patients suffering from DRA (Gejyo et al, 1993 and Lornoy et al, 2000) and supports the removal of β_2 -microglobulin.

Due to the supporting evidence that β_2 -microglobulin removal is important to the long term health of patients suffering chronic renal failure many papers

have adopted it as a marker molecule for the removal of middle molecular weight molecules.

Uremic syndrome is a complex problem however, evidence suggests that the removal of uremic toxins could result in better patient standard of living. Work has been carried out to assess the effects of specific molecules. However, there is still a strong case for the non-specific removal of all uremic toxins based on their size as no benefit is likely from elevated levels of these molecules.

1.2 Adsorbent Augmented Haemodialysis

1.2.1 Augmented Haemodialysis: Use of Adsorbents

With the problems faced in the removal of middle molecular weight uremic toxins during haemodialysis a potential solution may be adsorbent augmented haemodialysis. Combining adsorption with current dialysis techniques where the adsorbent is designed to remove the middle molecular weight toxins may improve the clinical outcome for the patient (Davankov *et al*, 1997; Davankov *et al*, 2000; Winchester *et al*, 2003 and Winchester and Audia, 2006). All of these techniques share the design in that the dialysis process is augmented rather than replaced. This may be a sensible approach as current haemodialysis is well-suited for the removal of small molecular weight solutes (<500Da), minerals and regulation of water in patients. It also means that the adsorbent can be tailored more specifically for the removal of the middle molecular weight fraction of uremic toxins.

There are two schools of thought regarding the approach to remove middle molecular weight solutes and these are the use of selective and non-selective adsorption methods.

The selective camp are focused on particular middle molecules that have been shown to cause health problems in patients suffering from renal failure e.g β_2 -microglobulin (MW 11.8 kDa). These selective removals are very successful in the treatment of water streams or the recovery of particular minerals for example Uranium. Caro *et al* (2006) discussed the use of molecularly imprinted polymers in the extraction of solutes from complex biological fluids and found that while extraction was possible, removal remained quite low. Mogi *et al* (1993) used immunoaffinity (the immobilization of an antibody) to selectively remove β_2 -microglobulin from the plasma of patients of renal failure, with some success seeing clearances of greater than 90%. The obvious down side to selective removal is that there are a wide range of middle molecular weight molecules which could provide benefit to the quality of life of a patient if they were to be removed.

Non-selective removal utilises an adsorbent which is not tailored to a single molecule. This approach has been investigated by Davankov *et al* (1997 & 2000) Malik *et al* (2005) and the company Medasorb. While these materials can potential remove less of a particular target molecule (e.g. β_2 -microglobulin) they remove a wider ranging selection of molecules which may be of greater benefit to the patient than the selective removal of a single molecule. The majority of these non-selective adsorbents are based around the crosslinked structure of polystyrene-divinylbenzene, some utilising a macroporous (referring to a large number of constant pores) network whilst others have moved towards hyper-crosslinked materials which can have a much larger surface area, however much of this is in the microporous region and of no importance in the removal of middle molecular weight molecules.

Winchester *et al* (2002) discussed the use of three different sorbents including a generic carbon, Betasorb (Renaltech) and Lixelle (Kaneka). Betasorb was a non-ionic resin while the Lixelle device contained a cellulosic bead with ligands to bind β_2 -microglobulin. Of these devices the mode of solute removal by the carbon and Betasorb adsorbents were non-specific whilst the Lixelle adsorbent had been tailored for the removal of β_2 -microglobulin. The conclusions from the work were that advances in haemoadsorbents had been made and further advances were likely focus on size exclusion of larger blood proteins (e.g. Albumin) and pore structures tailored to the removal of middle molecular weight uremic toxins. As a final point they discuss that while the Lixelle device is commercially available and approved for use in Japan for the treatment of dialysis related amyloidosis (a condition linked to high levels of β_2 -microglobulin in renal failure patients) its high cost has been prohibitive to its uptake.

1.2.2 Commercial Sorbents Currently Available or Under Development

Medasorb International - Betasorb™ and Cytosorb™

Betasorb™ is a material under development for the removal of β_2 -microglobulin and has been demonstrated by Winchester *et al*, (2001) to remove ~92% of β_2 -microglobulin in a uremic dog. Further work has indicated that the material possesses the ability to remove some cytokines which has increased interest in its potential use commercially.

Cytosorb™ is a poly(styrene-divinylbenzene) co-polymer which has been coated with polyvinylpyrrolidone to improve biocompatibility. Studies on

animals using Cytosorb™ have been carried out by Kellum (2004) both ex vivo and in vivo studies were carried out. The in vivo study looked at the survival rates of animals experiencing septic shock with and without the use of the Cytosorb™ device. The results showed that survival after 12 hours for the group treated by the Cytosorb™ was much improved over the control group. Ex vivo studies provided evidence to support these findings by demonstrating rapid removal of interleukin-6 and interleukin-10. No precise data for the capacity of this material have been published.

Cytosorb™ received approval for a clinical study for the treatment of sepsis in October 2007.

Kaneka Corporation – Lixelle

The Lixelle device was developed and manufactured by the Kaneka Corporation, Osaka, Japan and is designed specifically to remove β_2 -microglobulin from blood. The device consists of a column packed with cellulose beads of particle size 460 μ m. The cellulose beads have covalently bonded hexadecyl groups on their surface which act as ligands. The material is porous and described as having a porous structure which excludes albumin. The device is marketed towards the removal of β_2 -microglobulin however, Namatani et al (1998) and Tsuchida et al (1998) demonstrated that the device is capable of removing middle molecular weight molecules in the size range 4000-20000Da and cytokines IL-1beta and IL-6 respectively.

The Lixelle device is available for use in Japan and has seen clinical success (Geyjo et al, 2004 and Kutsuki et al, 2005). However its use in Japan is limited to 2 years of treatment and its high cost has limited its commercial success elsewhere. Its clinical success though furthers the cause for the removal of β_2 -microglobulin as advantageous for patient health.

1.3 Conclusions

The presence of middle molecular weight molecules in above healthy concentrations in patients suffering chronic renal failure is well documented. The full range of uremic toxins have yet to be identified, some toxins are linked directly to patient health and secondary conditions prevalent in renal failure patients (β_2 -microglobulin linked to DRA) and as such their removal has been accepted as the next step in renal failure treatment.

Currently available solutions for augmented dialysis are either yet to be approved or are cost prohibitive. As such the development of an adsorbent which was cheap to manufacture would be of benefit.

1.4 Research Objectives

The research study undertaken focused on the development of non-specific polymeric adsorbents with a tailored pore structure for the removal of middle molecular weight uremic toxins (500 Da -20 kDa) while size excluding larger blood proteins for example albumin (69 kDa). In addition to the tailored pore structure methods to control the particle size of manufactured materials will be investigated, the benefit of controlled particle size is two fold firstly by careful control of particle size the final haemoperfusion device can be more easily optimised and secondly by controlling particle size less material is wasted during grading reducing manufacturing costs.

Methods into the determination of pore structures in various states were investigated to determine if the convention of dry state gas adsorption

porosimetry was a reasonable method of analysis for a product used in a wetted state.

Finally proof of concept adsorption experiments were carried out to demonstrate how the adsorbents developed during the research compared with commercially available adsorbents, particularly focusing on the size exclusion of human serum albumin.

In summary, the objectives of the research were:

1. Control the internal pore structure of the adsorbent to size exclude human serum albumin
2. Optimise the adsorbent pore structure and surface area in the region important for the removal of middle molecular weight uremic toxins (2-10nm)
3. Develop a method to increase the yield of particles of a given size distribution
4. Determine whether dry state (gas adsorption) porosimetry is a suitable method for analysing the size exclusion potential of adsorbents to be used in the wet state.
5. Undertake protein adsorption studies with the developed adsorbents and compare with a commercially available adsorbent (XAD4) for human serum albumin uptake minimised through pore size control and a marker for middle molecular weight uremic toxins (lysozyme 14.4 kDa, readily available).

2 Literature Review of the Synthesis of Porous Spherical Adsorbents

The following sections relate to the chemistry and production of polymers for further information and background into this wide ranging subject please refer to the following texts Principles of Polymer Chemistry by PJ Flory (1953), Principles of Polymerisation by G. Odian (1991) and The Chemistry of Polymers by J. Nicholson (1997).

2.1 What are Polymers?

Polymers are described as being macromolecules (large molecules) built up from numerous smaller repeating molecules, which are known as mers. Polymers can be linear, a long chain of mers connected end-to-end e.g. polyethylene (-CH₂-CH₂-). Polymers may be branched, where the mer molecules are connected in a chain as in linear polymers, in addition, some mer molecules are connected laterally to the backbone creating branches from the main chain. The final form the polymers can take is that of highly interconnected crosslinked networks. Crosslinked networks consist of two types of mers a mer with a single active site and a crosslinking mer which contains at least two active sites. The crosslinking units are incorporated into two (or more if more reactive sites are available on the mer) polymer chains connecting them together creating a single larger polymer network. All of these different structures can be seen in Figure 2.1

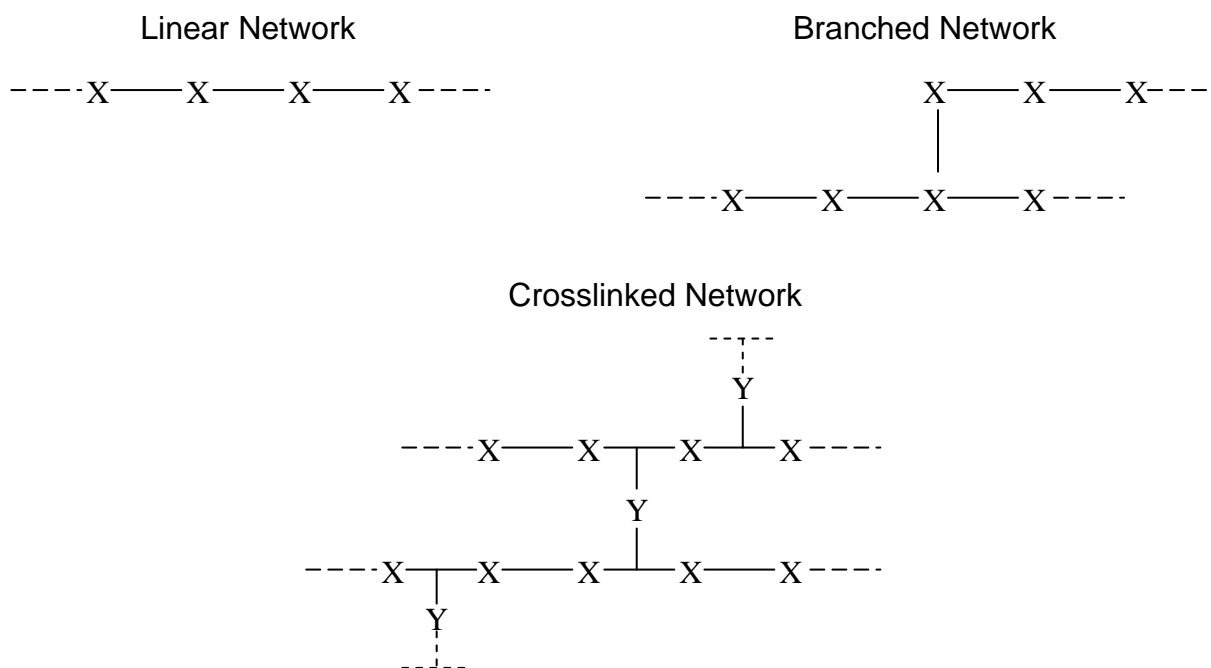


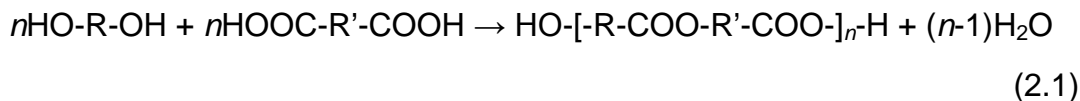
Figure 2.1: Simple representations of linear, branched and crosslinked networks, where X represents a repeating unit and Y a crosslinking unit.

Depending on the degree to which a polymer is branched and crosslinked will highly affect its physical properties including for example how the polymer will react to thermal treatments, solubility in organic solvents etc. Crosslinked polymers are linear and branched molecules bonded covalently together to form a three dimensional network. One major difference between crosslinked polymer molecules made from the same monomer as the linear and branched polymers is that crosslinked polymers will not dissolve in thermodynamically good solvents whereas the latter will. Crosslinked polymers may however, depending on the crosslink density, admit significant quantities of solvent, in doing so they swell and become softer. Unlinked chains and lightly crosslinked polymers are generally soft and reasonably flexible however, in contrast heavily crosslinked polymers tend to be brittle. This brittleness cannot be affected by heating as heavily crosslinked molecules are thermosets (see section 2.2) which will not melt but degrade

irreversibly when a sufficiently high temperature is reached. Another polymer type is known as an interpenetrating polymer network (IPN) which is described by Stepto (1998) as “A polymer comprising of two or more networks which are at least partially interlaced on a molecular scale but not covalently bonded to each other and cannot be separated unless chemical bonds are broken”. These polymers are more easily dissolved in solvents than crosslinked polymers because of the lack of covalent bonds within the polymer molecules.

2.2 Classification of Polymers

Polymers can be classified in a number of ways; these include properties of the polymer such as their response to thermal treatment e.g. thermosetting. Thermoplastic polymers upon heating melt and when cooled re-solidify. Thermosets on the other hand do not melt when heated but at a sufficiently high temperature decompose irreversibly. This difference in behaviour is attributed to the structure of the polymer. Thermoplastics tend to be linear or lightly branched whereas thermosets tend to be highly interconnected molecules (crosslinked). Polymers can also be classified by the reaction method by which the polymers were produced. The classification of polymers by the mechanism of chemical reaction during the polymerisation was first suggested by Carothers (1929). Classification of polymers by this method results in two distinct groups namely condensation polymers and addition polymers. Condensation polymers are created from monomers which when polymerised liberate a small molecule, including but not limited to water, ammonia, HCl and alcohols. An example of a condensation polymerisation reaction would be that of the production of polyesters as shown in Reaction 2.1.

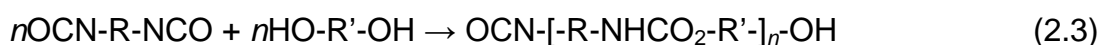


where n represents the number of repeating units, R and R' are potentially different groups.

Addition polymers in contrast are those created by the addition reaction of an unsaturated monomer, e.g. the polymerisation of vinyl chloride shown in Reaction 2.2.



P. J. Flory (1953) modified this system of classification by placing the emphasis on the mechanism of the polymerisation reaction. He reclassified the polymerisations as step and chain reactions. These approximate to Carothers' condensation and addition classification system but there are certain differences. Polymerisation to produce polyurethanes follow step kinetics, the monomers are saturated however, no small molecule is released during the reaction as shown in Reaction 2.3 so this would have been classified as an addition polymer under Carothers' system.



The two polymerisation methods (step and chain) are substantially different in the way in which the polymer molecule is formed. However, the two reactions basically differ in the time scale required for the production of full-sized polymer molecules. Step reactions create large polymer molecules relatively slowly as a monomer molecules join-up with another monomer to produce a dimer, the dimer then joins with another monomer to form a trimer etc. In addition to the use of monomer units growing chains can react

together to form a single chain terminating the polymerisation reaction for that chain this is referred to as radical recombination, this process results in varied polymer molecular weights in the final product. This is in direct contrast with chain polymerisations where full sized polymer molecules are produced almost instantly once the polymerisation begins. Chain polymerisation requires an initiator which has a reactive centre, the reactive centre of the initiator could be a free radical, cation or anion. Polymerisation occurs by the propagation of the reactive centre through the addition of large numbers of monomer molecules. In a chain reaction the monomer can only react with a reactive centre and not other monomer so a few large polymer molecules are formed whilst there is still a high concentration of monomer in solution. An example of chain polymerisation is that of vinyl monomers and can be seen in Reaction 2.4.



Where R represents the initiator and * represents a reactive centre.

This process continues until termination is achieved (Reaction 2.4.3).



The growth of the polymer chain is stopped with the destruction of the reactive centre by way of a number of possible termination reactions.

Despite what has been stated above, it should not be assumed that step polymerisation is slower than chain polymerisation. The rate of monomer reduction (the rate of polymerisation) in step polymerisation can be greater

than that during chain polymerisation. The difference between the two methods is only in the time required to produce large polymer molecules. This happens very quickly in chain polymerisation and is slower in step polymerisation as monomer can react with another monomer rather than having a very limited number of potential reaction centres.

In chain reactions the molecular weight of the polymer is relatively independent of monomer conversion as shown in Figure 2.2. There are actually three phases to this polymerisation stage one is the initiation of polymerisation and the chains are growing rapidly with minimal termination. The second stage combines growth of new chains and termination of larger chains these form an equilibrium keeping the average polymer molecular weight relatively stable. The final phase sees the average molecular weight tail off this is due to the higher viscosity of the polymer/monomer solution resulting in an increased number of more mobile smaller polymer chains being formed and combining to create an overall lower average molecular weight polymer. During step polymerisation the molecular weight of the polymer and monomer conversion are more closely related as shown in Figure 2.3. In step polymerisation, high molecular weight polymers (polymers of high degrees of polymerisation) do not appear until more than 98% of the monomer has been converted (Odián, 1991).

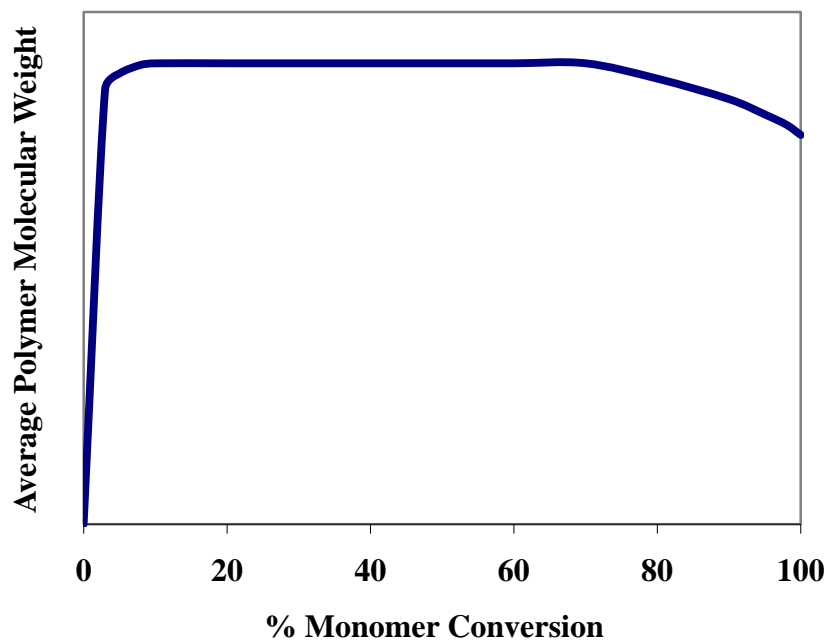


Figure 2.2: Variation of molecular weight with percentage monomer conversion during chain polymerisation.

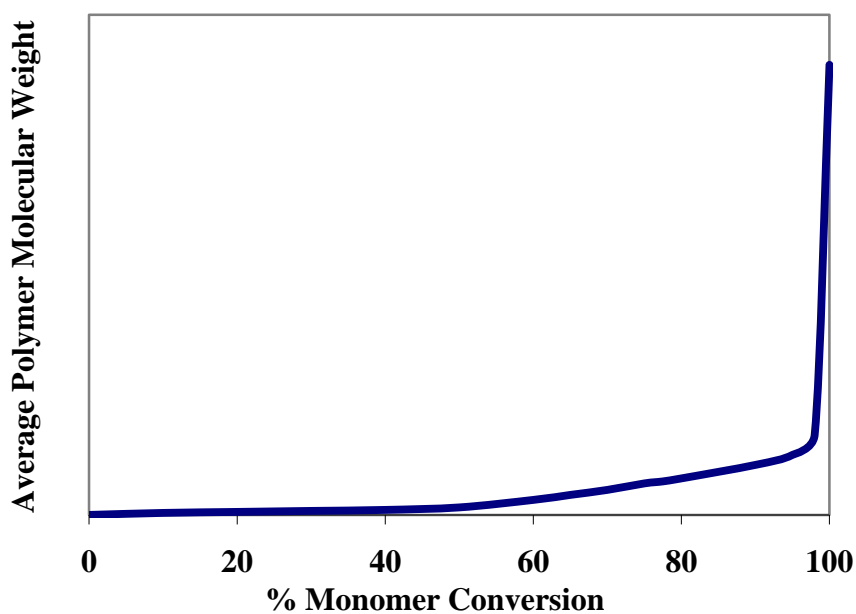


Figure 2.3: Variation of molecular weight with percentage monomer conversion during step polymerisation.

2.3 General Review Of Synthesis Methods

2.3.1 Bulk Polymerisation

Bulk polymerisation of a pure monomer offers the simplest means of obtaining a polymer with a minimum of product contamination. Because of these attributes, bulk polymerisation appears at first glance to be the method of choice for producing chain reaction polymers. All that is required for the polymerisation is the monomer and a small amount of initiator. However, bulk polymerisation has a number of associated problems. As the monomer concentration goes down during polymerisation the concentration of high molecular weight-polymer molecules increases. This results in an appreciable increase in the viscosity of the mixture and this can lead to problems e.g. in transporting the material out of the reactor. The problem of increased viscosity also causes heat transfer problems. Polymerisations tend to be exothermic and the increasing viscosity inhibits good heat dissipation. This can lead to hot spots within the polymerisation bulk, resulting in charring or thermal degradation of the product. Other undesirable side effects include discolouration and a broadening of the molecular weight distribution of the final product. These disadvantages are the main reasons why bulk polymerisation is not widely used for large scale production of polymers. However, bulk polymerisation is still used for the laboratory preparation of vinyl polymers. The exception to this is the production of polystyrene and polymethyl methacrylate which are all produced on a large scale by bulk polymerisation. Polystyrene production has been very well engineered to prevent these problems from occurring. The reaction is initiated in a tank heated to 80 °C (Nicholson, 1997) at this temperature the styrene self initiates and so requires no additional initiator to be present. The polymerisation is allowed to continue until about 35% of the styrene has been converted, at this point the mixture of polymer and monomer is still easily stirred to dissipate heat from the exothermic polymerisation. The

styrene/polystyrene mixture is then passed down a tower in an inert nitrogen atmosphere, with the temperature in the column increasing from 100 °C at the top to 200 °C at the bottom. When the material reaches the bottom of the tower it has completely polymerised and is then extruded, granulated and cooled.

Step polymerisations are often carried out in bulk reactors, as the viscosity does not become a problem until almost all of the monomer has been converted due to the low degree of polymerisation. This enables heat transfer to be carried out effectively during the polymerisation process.

2.3.2 Solution Polymerisation

To overcome the problems of high viscosity a solvent is needed for heat sequestration and better control of the temperature of the reaction mixture . As the name suggests, solution polymerisation utilises a solvent in which the monomer is dissolved and the polymerisation occurs within this solution. There are however a number of disadvantages associated with solution polymerisation a large amount of solvent is required, which subsequently has to be separated from the polymer. The solvent can usually be recycled, this however requires additional processing equipment and increases both capital and operational costs. There may be difficulties in removing all of the solvent from the product and this may adversely affect the polymer properties (Odian, 1991). The choice of solvent ideally requires it to be inert in relation to the polymerisation. However, this is not always possible, thus there are issues with chain transfer to the solvent causing a reduction in the average molecular mass of the product. Another issue in solution polymerisation is that the temperature of the polymerisation is limited to the boiling point of the solvent. This may mean that the polymerisation reaction kinetics is slowed considerably. The main problem here is the reduction in the degree of

polymerisation and this is the main reason why solution polymerisation is rarely used by industry.

2.3.3. Precipitation Polymerisation

Precipitation polymerisation begins as a homogeneous system but quickly develops into a heterogeneous polymerisation. This occurs in the polymerisation of a polymer either in bulk or solution (aqueous or sometimes organic) where the polymer formed is insoluble in the reaction medium. The initiators used in precipitation polymerisations are soluble in the initial reaction medium. After the formation of solid polymer the polymerisation continues either by the transfer of monomer and initiator to the surface of the polymer or reactive sites on the polymer reacting with monomer. Two examples of precipitation polymerisation are bulk polymerisation of vinyl chloride and solution polymerisation of acrylonitrile in water.

2.3.4 Emulsion Polymerisation

Emulsion polymerisation is a versatile method and is widely utilised as a means of polymerisation. The monomer is dispersed in an inert liquid e.g. water. An emulsifying agent (usually a synthetic detergent/surfactant) is used giving rise to small micelles of the order of 0.1-1 μm in diameter. This drop size is significantly smaller than drops formed through the use of mechanical agitation. The micelles contain a small amount of monomer, the rest of the monomer is suspended in the water without the aid of a surfactant. The initiator in this case is required to be water soluble (e.g. persulphate salts) and is dissolved in the continuous phase. The initiator forms free radicals within the water, which induces polymerisation. The growing polymer chains diffuse to the micelles, which allows for the bulk of the polymerisation to occur within these stabilised droplets. The resulting dispersed polymer is not a true emulsion after the polymerisation has

occurred and is in fact now a latex. The main advantage of emulsion polymerisation is that there is virtually no increase in viscosity of the reaction mixture even up to 60% solid's content (Nicholson, 1997). This is due to the lack of interaction between the water and the latex particles. Emulsion polymerisation is used in the production of the latexes required in “emulsion” paints as well as the production of synthetic diene elastomers.

2.3.5 Suspension Polymerisation

Suspension polymerisation is similar in many ways to solution polymerisation (described in section 2.3.2) except that the monomers and the initiator are suspended as a dispersed phase within a continuous phase. Continuous mixing is required to generate the monomer drops (due to mixing induced shear effects) and once the drop viscosity increases due to polymerisation mixing is required to keep the droplets/particles suspended. During suspension polymerisation the individual monomer droplets act as small bulk polymerisation reactors. However, due to the large surface area to volume ratio of the droplet, heat dissipation to the continuous phase prevents the problems faced during bulk polymerisation (see section 2.3.1).

Generation of the dispersed phase (droplets of the reaction mixture) may be produced by a number of methods including use of an agitator or membrane emulsification techniques. These are discussed below.

2.4 Particle Size Control During Suspension Polymerisation

The control of particle size begins with the generation and dispersion of the initial monomer droplets in the continuous phase. There are two distinct methods used for generating the droplets; (i) using an agitator and (ii) by

membrane emulsification. To prevent droplet coalescence use of droplet stabilisers (these may be polymeric or inorganic particulates) is common as well as continuous phase viscosity modifiers.

2.4.1 Agitation

The conventional method by which monomer droplets are produced in a continuous phase is addition of the monomer mixture to the continuous phase and then using an agitator to mix the two phases together. The shear induced drop break-up results in a heterogeneous distribution of monomer droplets. A number of factors affect the size of the droplets produced including the size and type of the stirrer, the power dissipation rate and the effectiveness of the mixing achieved within the reactor (Nicholson, 1997). The speed of the stirrer has a considerable affect on the droplet size distribution. High rotational speeds result in high shear around the blades thereby resulting in smaller average droplet size. This method of producing droplets through mixing suffers from a lack of uniformity of the drop size obtained.

2.4.2 Membrane Emulsification

The production of a dispersed phase using a microporous membrane has been extensively investigated by a number of researchers including Peng and Williams (1998). They investigated the use of a cross-flow membrane to produce droplets forming an oil-in-water emulsion. Dowding *et al* (2001) used a cross-flow membrane to produce styrene divinylbenzene droplets within an aqueous continuous phase. They concluded that by employing a cross-flow membrane system purpose built by Disperse Technologies

(Dorking, UK) the system consisted of a centrifugal pump recirculating the continuous phase and suspended droplets post production. Discontinuous phase was injected using a syringe pump, droplets were generated using a stainless steel plate (0.45mm thick) with laser drilled holes of 100 or 150 μm in a cubic array with an average distance of 323 μm between holes, the active area of the membrane was 20 x 20 mm. Using this system Dowding *et al* (2001) could produce droplets that after polymerisation resulted in particles with a size range between 100–300 μm and that the particle size distribution was significantly narrower than droplets produced by agitation.

Shirasu porous glass (SPG) membranes were used by Hatate *et al* (1995). Their methodology utilised a crossflow system and generated droplets in the sub-10 μm range. Using a different SPG membrane, Yoshizawa *et al* (2004) generated polymer droplets of approximately 50 μm . Micropore Technologies Limited have employed a metal based membrane with a regular array of pores using a stirred batch cell to generate an emulsion with a controlled drop size distribution. Kosvintsev *et al* (2004) utilised these membranes to generate droplets of sunflower oil in water generating mono-sized droplets with the drop size dependent on the shear rates resulting in regular drop ranging from 75 μm to 105 μm .

However, once the drops are generated by using the membrane emulsification process, the continuous phase is still requires agitation to prevent coalescence of the droplets. This agitator induced shear can cause droplet break-up as a result and coalescence cannot be completely avoided. Thus the final drop size distribution is dependent upon the shear history.

After being generated the droplets need to be stabilised to help reduce drop break-up and coalescence. Monomer drops are stabilised using polymeric

stabilisers or inorganic particulate stabilisers (both methods discussed below) and viscosity modifiers (discussed below).

2.4.3 Polymeric Stabilisers

Typical polymeric stabilisers for oil-in-water suspension polymerisation reactions are polyvinyl alcohol co vinyl acetate, which is formed by partial hydrolysis (80-95%) of polyvinyl acetate. The stabilising abilities of these polymers are affected by factors including molecular weight, copolymer composition and the physical structure of the polymer branching. One example of this is the degree of hydrolysis; Goodall and Greenhill-Hooper (1990) used two samples of partially hydrolysed polyvinyl acetate 88% and 98% to stabilise a styrene-in-water system. The 88% hydrolysed sample adsorbed more strongly to the styrene-water interface in comparison with the 98% hydrolysed sample. This resulted in a thicker layer of interfacial polymer and produced a more stable emulsion.

2.4.4 Inorganic Particulate Stabilisers

For inorganic particulate stabilisers to work, they are required to be incompletely wetted by either the oil or the water phase. The particles sit at the oil-water interface and appear to hinder coalescence of oil droplets by hindering their approach. The concentration of particles required depends on the droplet size required, smaller droplet sizes require larger concentrations of particles as the total droplet surface area increases. Examples of inorganic particulate stabilisers include calcium carbonate, aluminium oxide and various clays (Nicholson, 1997).

2.4.5 Viscosity Effects

Increasing continuous phase viscosity can increase droplet stability by decreasing the collision frequency of the droplets, possible viscosity modifiers include xanthan gums, clays and gelatine (Nicholson, 1997).

To increase the viscosity within the monomer phase (e.g. in a styrene water system) polystyrene can be dissolved within the monomer phase. This increased viscosity increases the drop's resistance to coalescence by forming a more rigid drop-water interface.

Combinations of these different methods can be used to help increase drop stability. Dowding *et al* (2001) used an 88% hydrolysed polyvinyl alcohol (0.1 wt/wt %) and sodium chloride (5.7 wt/wt %) in an aqueous phase and added a small amount of polystyrene to their monomer phase. The result of this was a continuous phase including a polymeric stabiliser and a viscosity modifier to the monomer phase. The sodium chloride was used to create a salting out effect reducing/preventing the dissolution of the monomer into the continuous phase. This process is common when the polymer being used is slightly soluble in the continuous phase as in styrene-water systems.

Use of polymeric stabilisers is wide spread as they can easily be removed from the final polymerised product through washing with water. This often outweighs the economic benefits of using inorganic particulate stabilisers which are generally cheaper than their polymeric alternatives.

2.5 Controlling Porosity Within Polymer Networks

2.5.1 Solvents and Degree of Crosslinking

The porosity within a polymer bead can be influenced by the use of porogens added to the polymerisation mixture. Porogens are not incorporated into the final polymer product. The porogens must be soluble with the monomers and in the case of suspension polymerisation, must be reasonably insoluble in the continuous phase although this can be countered by the addition of a salt e.g. sodium chloride to the aqueous phase to lower the solubility of the porogens in the continuous phase by the process of salting out (previously discussed).

In suspension polymerisation systems e.g. styrene divinylbenzene, a diluent is often used as a porogen during the polymerisation reaction. The solvent can then be removed and reused after the polymerisation reaction has been completed. Typical examples of diluents used are, dichloroethane, dichloromethane and toluene (Okay 2000). These are all good solvents for both styrene and divinylbenzene and also polystyrene however they cannot dissolve a crosslinked polymer the result of this reaction.

The solubility of the monomers in the porogen and the concentration of the solvent to the monomer concentration are major factors in determining the scale of the porosity formed within the final product (Beldie *et al*, 1984; Poinescu *et al*, 1984; Coutinho and Rabelo, 1992; Horak *et al*, 1996; Erbay and Okay, 1998; Sherrington, 1998; Erbay and Okay, 1999; Okay, 2000; Santora and Gagne, 2001; Durie *et al*, 2002; Macintyre and Sherrington, 2004).

The solubility of the monomer and the polymer in the porogen determine the predominant size of the pores found in the polymer product. Thermodynamically good solvents like those already mentioned e.g. dichloroethane and toluene result in porous polymers which according to Okay (2000) display considerable surface area in the region of $50 - 500 \text{ m}^2 \text{ g}^{-1}$ but with a relatively low pore volume (typically around $0.8 \text{ cm}^3 \text{ g}^{-1}$) and usually consist of mostly micropores ($<2 \text{ nm}$) with some mesopores (2-50nm). If a porogen is a good solvent for the monomer but not so for the polymer then as the polymerisation reaction proceeds, micro-phase separation is induced (illustrated in Figure 2.4, showing how microspheres of polymer precipitate when the porogen/solvent ratio is no longer sufficient to keep the growing polymer chains solvated). If a poor solvent is used as the porogen, phase separation will happen earlier and the micro-spheres will grow larger creating macropores (greater than 50 nm).

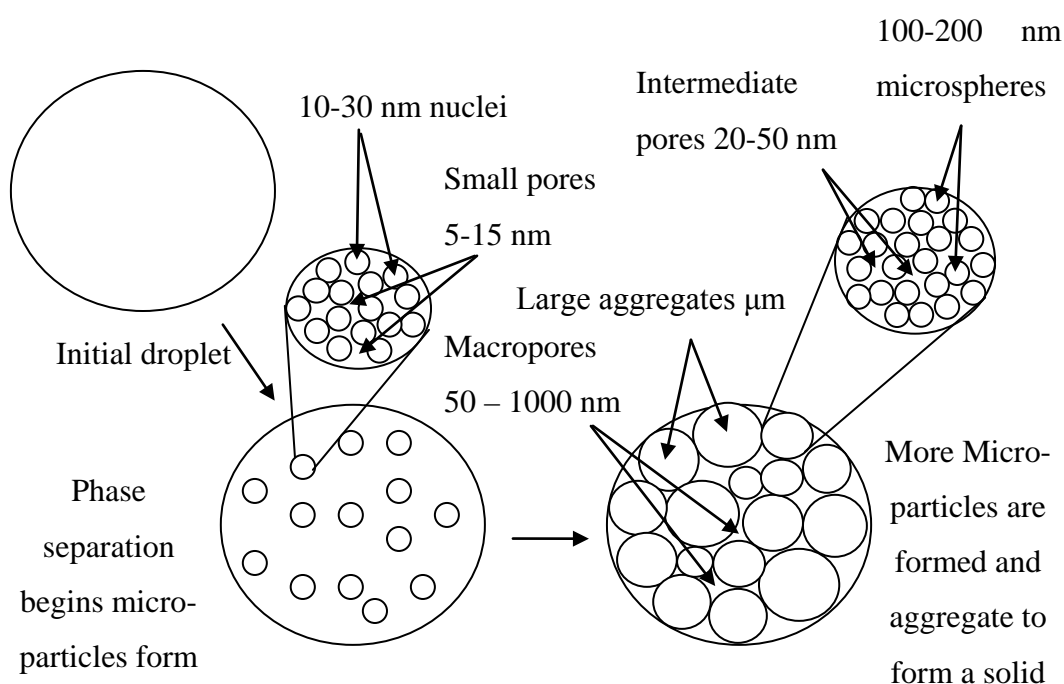


Figure 2.4: Phase separation and the generation of pores during polymerisation

These non-solvating diluents e.g. n-heptane, result in large pore volumes $0.6 - 2.0 \text{ cm}^3 \text{ g}^{-1}$ and possess surface areas between $10 - 100 \text{ m}^2 \text{ g}^{-1}$ (Okay, 2000). The pores within these structures are mostly macropores with some mesopores. If a solvent can be found which falls in the middle of these two cases then it would be expected that such a system would produce mesoporous ($2 - 50 \text{ nm}$) polymer adsorbent beads. Solvents that are in this category range between the thermodynamically good solvents and precipitators of the polymer. They are known as Θ -solvents (Davankov *et al*, 2000). A Θ -solvent for a polymer interacts with the polymer chains with just enough energy to prevent the collapse of the polymer coils and hence prevents precipitation of the polymer. For the production of polystyrene-divinylbenzene beads by suspension polymerisation as reported by Davankov *et al* (2000) a Θ -solvent for polystyrene should be utilised to

produce a mesoporous structure. Cyclohexane is a classical Θ -solvent for polystyrene however, mixtures of a thermodynamically good solvent and a precipitating media can also be used to tailor the adsorbent pore size distribution depending on reaction conditions (temperature etc.).

A final type of porogen that can be used to control the adsorbent pore structure is the addition of a polymeric diluent for example linear polystyrene (Macintyre and Sherrington, 2004). This results in relatively large macropores and as a consequence provide low specific surface areas of between 0.1 - 10 m² g⁻¹ (Okay, 2000; Macintyre and Sherrington, 2004).

In general the concentration of the porogen is usually 50% or more of the total volume of the monomer phase (Davankov *et al*, 2000 and Durie *et al*, 2002).

Porogens for polystyrene and divinylbenzene

Good Solvents

Dichloromethane, dichloroethane, toluene

Θ -Solvents

Cyclohexane

Precipitating media

Hexane, octane, iso-octane, higher aliphatic alcohols

It should be noted that while dichloromethane and dichloroethane are both good solvents for both polystyrene and divinylbenzene the presence of the chlorine can act as a quencher for free radicals required for the

polymerisation to proceed. For this reason toluene is preferred as a good solvent for these polymers.

The values given for surface areas from different porogens are guidelines as other factors also affect the porosity of the beads. Degree of cross-linking can have a significant effect on the surface area with Okay (2000) quoting values of up to $900 \text{ m}^2 \text{ g}^{-1}$ (determined using gas adsorption) for a styrene-divinylbenzene system in the presence of a precipitating diluent with a high crosslinker concentrations.

The solubility parameter (δ) of a solvent is a measure of the attractive strength between molecules. If a solvent solubility parameter matches that of a polymer, then the solvent is likely to be a good solvent candidate for the polymer. Conversely, if the solubility parameters differ considerably, then the likelihood is that the solvent is less good i.e. will encourage early precipitation of the polymer chains. Sherrington (1998) compiled a list of good and bad solvents for polystyrene systems (presented in Table 2.1). The solubility parameter for polystyrene and copolymers of styrene-divinylbenzene is $\sim 17 - 18 \text{ (MPa)}^{0.5}$.

Table 2.1: Polystyrene solvents and non-solvents solubility parameters

Good Solvent	δ - (MPa) ^{0.5}	Poor Solvent	δ - (MPa) ^{0.5}
<i>Aromatic hydrocarbons</i>		Water	47.9
Benzene	18.8	<i>Aliphatic alcohols</i>	
Toluene	18.2	Methanol	29.7
Xylenes	18.0	Ethanol	26.0
<i>Chlorocarbons</i>		2-Ethylhexanol	19.4
1,2-Dichloroethane	20.1	<i>Aliphatic hydrocarbons</i>	
Chloroform	19.0	Hexane	14.9
<i>Cyclic ethers</i>		Dodecane	16.2
Tetrahydrofuran	18.6	<i>Others</i>	
Dioxane	20.5	Diethyl ether	15.1
		Acetic acid	20.7

Some examples from literature show how different porogens and the concentrations of these porogens can affect the porosity within polymeric materials. Poinescu *et al* (1984) investigated styrene divinylbenzene systems using cyclohexane, cyclohexanol and cyclohexanone as porogens. Table 2.2 shows the solvent polymer interaction parameters which are listed in Hildebrandt units δ_H . Hildebrandt units are often used when describing solubility in older literature and when no units are provided it is reasonable to assume this is the case. Hildebrandt units are defined as (calories/cm³)^{0.5} the current SI unit for solubility parameters is MPa^(0.5) the conversion between these two units is δ (MPa^{0.5}) = 2.0455* δ_H (calories/cm³)^{0.5} the SI value can be quickly estimated by multiplying the Hildebrandt unit value by 2.

Table 2.2: Solvent-polymer interaction parameters

Solvent	Interaction Parameter - δ_H [(calories/cm ³) ^{0.5}]
Cyclohexane	7.81
Cyclohexanol	9.94
Cyclohexanone	9.90
Toluene	8.90
Polystyrene	9.10
Polyvinylbenzene	8.80

Table adapted from Poinescu *et al* (1984)

Toluene is a good solvent for polystyrene with solvent-polymer interaction parameter values closely matched (see Tables 2.1 and 2.2). Of the other solvents used cyclohexane, cyclohexanol and cyclohexanone, we would expect cyclohexanone with a difference in δ_H of 0.8 (calories/cm³)^{0.5} (Table 2.2) should be the best solvent for polystyrene where as cyclohexane would be the worst selected with a δ_H difference of 1.29 (calories/cm³)^{0.5} (Table 2.2).

Table 2.3 shows how changing the porogen and crosslinker (divinylbenzene) concentration affects the average pore diameter within synthesised polystyrene adsorbents

Table 2.3: Average pore diameter of porous polymer beads generated using three different porogens and varying concentrations of crosslinking agent (divinylbenzene), adapted from Poinescu *et al* (1984).

Porogen	% DVB and average pore diameter (nm)		
	10%	30%	50%
Cyclohexane	270	21	5
Cyclohexanol	70	14	9
Cyclohexanone	18	61	39

The divinylbenzene used for the study was 55% isomers whilst the remainder was ethylstyrene and non-polymerising material. 50% by weight of the total dispersed phase was porogen. The pore structure was evaluated using nitrogen porosimetry.

Changing the solvent was found to have a significant effect on the average pore size (see Table 2.3). Cyclohexanone-polystyrene solvent-polymer interaction parameters are closely matched. Using this combination of porogen-monomer was found to result in a polymer adsorbent with the smallest average pore size using 10% divinylbenzene. Increasing the divinylbenzene concentration to an value (30%) resulted in an increase in the average pore size (61nm) whereas further increase in the divinylbenzene concentration (50%) reduced the average pore size to 39nm. For porogens cyclohexanol and cyclohexane increasing the divinylbenzene concentration resulted in a reduction in the average pore size (see Table 2.3).

Durie *et al* (2002) altered the composition of the crosslinking agent to alter the porosity of the polymer particles. Experiments were conducted using 50% toluene whilst varying the concentrations of styrene and divinylbenzene. Analysis of the resulting pore structure of the polymer material was carried out using nitrogen porosimetry. A summary of the results of the work are shown in Table 2.4.

Table 2.4: Surface area varying with divinylbenzene concentration

*Divinylbenzene wt/wt %	Surface Area / m ² g ⁻¹
20	<5
30	<5
40	51
50	497
60	562
80	756

*Weight percent refers to the actual divinylbenzene isomers.

Increase in the divinylbenzene crosslinker concentration was shown to result in an increase in the surface area of the resulting polymer material. Employing an alternative porosimetry technique of inverse size exclusion chromatography, the researchers evaluated the 60% divinylbenzene sample and found the surface area to be 1392 m² g⁻¹. The difference between the BET data and that from the inverse size exclusion chromatography measurement was attributed to the swelling of the adsorbent particles in the wet state. Increasing the crosslinker density results in a more rigid polymer structure which does not collapse on drying (nitrogen porosimetry data is evaluated using dry samples under vacuum) and thus provides access to the probe molecule e.g. nitrogen to the internal pore structure.

Sherrington (1998) proposed a phase diagram of sorts (shown in Figure 2.5) which relates the concentration of the crosslinker and the solvent used to categorise the type of polymer resin that is generated. The three types of potential resins are gel, macroporous and microgel powders. Gel resins have no dry state porosity (as typified by the 20 and 30 wt% DVB resins in Table 2.4), however they do swell in solvents producing microporous networks. Macroporous resins have a rigid/semi rigid structure formed by cross-links that provide porosity in the dry state (In Table 2.4 resins with 40% DVB or more). The microgel powder material is similar to the gel resin

however, due to a high solvent concentration employed during synthesis, the microspheres do not fuse together so a very fine powder is formed instead of a single large particle. This is because of the reactivity ratios of the two monomers involved in the copolymerisation, using styrene and divinylbenzene as an example, divinylbenzene is more reactive than styrene because of this it is more likely to join a polymer chain near the start of the reaction, if there is a large volume of porogen then conceivably there will be no available crosslinking sites remaining to join the nuclei resulting in a microgel powder.

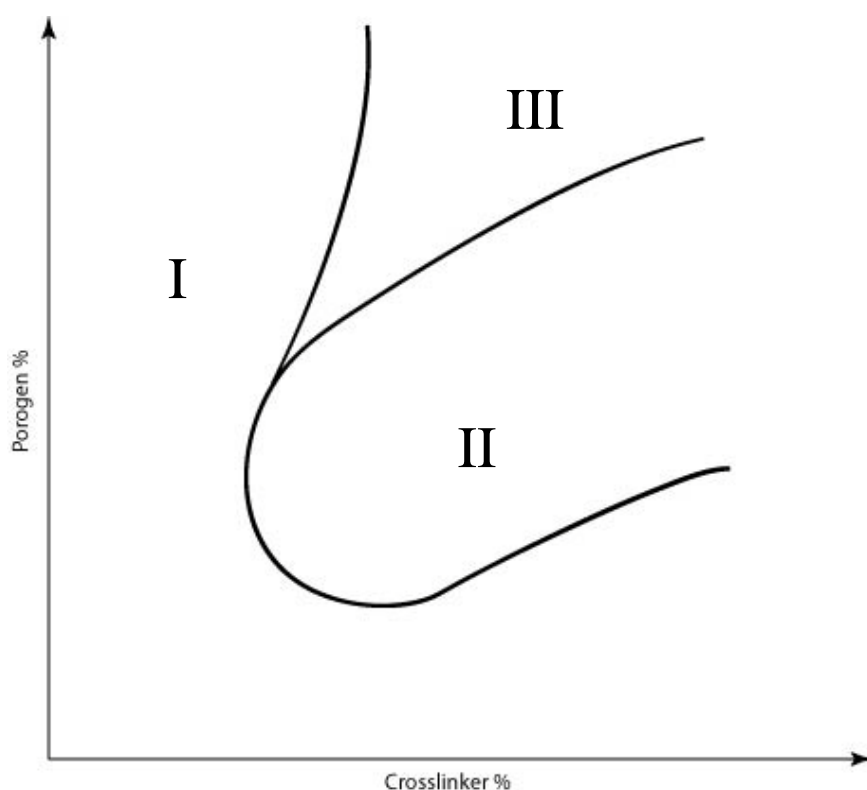


Figure 2.5: Phase diagram for determining the type of polymer generated; regions correspond to I - Gel type resins, II – Macroporous resins and III – Microgel powder.

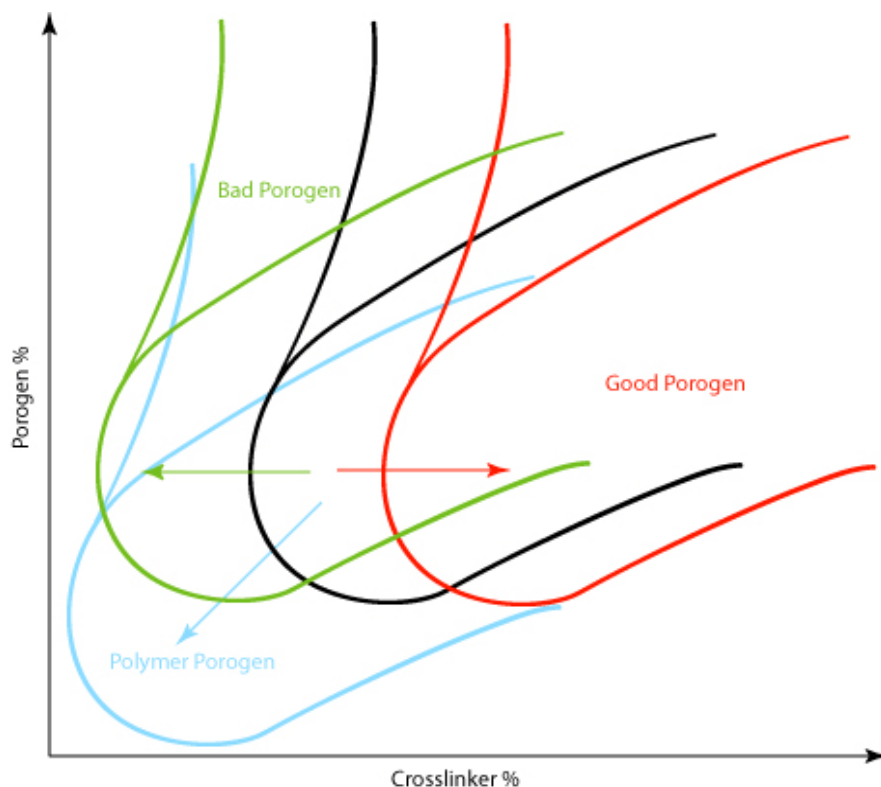


Figure 2.6: Pseudo phase diagram showing how the macroporous resin envelope moves depending on the type of porogen.

The effect of the porogen may be seen in Figure 2.6 using good solvents for the polymer (e.g. toluene for styrene divinylbenzene) moves the macroporous region to the right and requires higher degrees of crosslinking to produce a macroporous resin (Table 2.4 shows how low crosslinking degree results in a gel state polymer). Poor/bad solvents (e.g. undecane for styrene divinylbenzene) moves the macroporous region left-wards requiring lower levels of crosslinker to generate a macroporous resin. Polymeric porogens shift the macroporous window down and towards the left suggesting lower crosslinker and solvent concentrations are required to form a macroporous resin.

2.4.2 Determination of the Porosity in Porous Polymer Beads

2.4.2.1 Introduction

In reviewing the literature on the generation of porous polymeric adsorbents the characterisation of the generated porous structures is of vital importance firstly we need to understand some terminology relating to the size of particular pores.

Adsorbent particles can have a range of pore sizes, which cover three main pore size ranges: Micropores - 0 - 2 nm; Mesopores - 2 - 50 nm; Macropores - >50 nm, (Macintyre and Sherrington, 2004).

A single adsorbent material can have a range of pores in all of these regions however, adsorbents having smaller pore sizes possess greater overall surface area. This is due to the surface area to pore volume ratio two materials with identical pore volumes will have different surface areas if their average pore size is different. Not all the surface area measured using say nitrogen porosimetry may be accessible to larger moieties e.g. MMs or HSA. The Synthesis of adsorbents with a high surface area accessible to the molecules of interest (middle molecular weight molecules) whilst size excluding larger molecules for example HSA should be possible providing suitable synthesis parameters can be obtained.

In the case of kidney failure the harmful waste molecules which are currently not removed with conventional treatments and need to be removed for example β_2 -microglobulin are classed as middle molecules. Winchester *et al* (2002) reviewed these middle molecular weight uremic toxins and found that they may be categorised on the basis of molecular weight range of between 4 - 30 kDa. These target molecules would require pores in the range of 4-10

nm to allow entry within the adsorbent pore structure while excluding entry of larger useful proteins such as HSA (~10nm).

The polymer synthesis conditions may be tailored to alter the resulting pore size distribution of the polymer adsorbents (discussed previously). The influence of synthesis conditions on the resulting pore structure requires rigorous evaluation in order to ensure that the final material possesses the appropriate microstructure.

There are a number of characterisation methods available to determine the internal pore structure of the adsorbent particles and these are discussed below.

1. Gas adsorption
2. Mercury porosimetry
3. Inverse size exclusion chromatography

2.4.2.2 Gas Adsorption

Adsorption of a gas on to a dry solid surface can be described by the use of an adsorption isotherm. The monolayer capacity can be calculated using the Brunauer, Emmet and Teller equation (BET). The surface area of the material can then be calculated on the basis of the size of the adsorbent molecule and the measured monolayer capacity. The standardised tests are carried out using nitrogen at 77 K. The adsorption isotherm allows for the determination of pore sizes by comparing the adsorption and desorption isotherms and using the Kelvin equation (Hagel 1988) in conjunction with the desorption data. The Kelvin equation is:

$$r_k = - 4.10 \log P/P_0 \quad (2.5)$$

Where r_k is the Kelvin radius in Å and the constant is calculated assuming the gas adsorbed is nitrogen at 77 K.

The nature of the adsorption process is such that liquid condensation in large pores occurs when the relative pressure is close to 1. This means that reliable adsorption data for pore sizes can only be achieved with pores less than 100 nm (Hagel, 1988) and the smallest pore size that can be characterised is restricted to the size of the gas molecule which for nitrogen is approximately 0.3 nm. The use of helium will allow for the evaluation of pores <0.3 nm if required however for this work that is not required.

The major disadvantage of nitrogen adsorption as a method of pore structure analysis is that the material is characterised in the dry state at liquid nitrogen temperature (77 K). For materials whose dry state porosity is unchanged by wetting with a solvent, this is not a problem. However, polymer pore structures are known to be influenced by the solvation of the polymer chains and this depends on the solvent-polymer interactions, as well as the crosslinking level of the polymer. Thus, characterisation of polymer pore structure using nitrogen adsorption porosity measurements requires qualification that upon contact with a solvent the polymer physical structure may change.

With the above caveat it is worth noting that nitrogen gas adsorption porosimetry is by far the most widely used method for the analysis of porous structures in the pore size range this work is interested in.

2.4.2.3 Mercury Porosimetry

Mercury porosimetry is a technique that forces liquid mercury under pressure into the pores of a solid substrate. Applied pressure in excess of 4000 bar is used (Hagel, 1988). The volume of liquid which penetrates the pores is plotted against the applied pressure as shown in Figure 2.7. The initial sharp increase in volume at very low pressures is due to the filling of the extra particle volume.

Figure removed due to copyright.

Please refer to the original text.

Hagel L. *Pore Size Distributions*. In: Dubin PL, editor. *Journal of Chromatography Library – Volume 40, Aqueous Size-exclusion Chromatography*. Netherlands: Elsevier, 1988. p. 119-155

Figure 2.7: Mercury porosimetry (a) intrusion; (b) extrusion curves of porous silica (Vydac TP 15) (Hagel, 1988).

The intrusion and extrusion curves do not overlap (see Figure 2.7). This effect has been attributed to the shape of the pores within the material and possible entrapment of the mercury within the substrate. Pressure required to enter a pore can be correlated to the pore entrance diameter using the Washburn equation (Hagel, 1988):

$$r_c = -2 \gamma \cos \theta / P \quad (2.6)$$

r_c is the radius of a cylindrical pore in Å, and P is the pressure in bar. The surface tension (γ) value for mercury is 0.48 N m^{-1} and a contact angle (θ) of 140° is assumed (Hagel, 1988). Incorporating these two values in to the relationship of pore entrance diameter and required pressure, equation 2.6. can be reduced to:

$$r_c = 735 \times 10^2 / P \quad (2.7)$$

The volume of mercury imbibed vs pressure curve can be transformed into a pore size distribution using equation 2.7. The largest pore size that may be determined is limited by the use of 1 bar of pressure and gives a value in the region of 7500 nm (or $7.5 \mu\text{m}$) while the lower pore size limit is determined by the pressure resistance of the material being tested. Partial destruction of silica materials is reported by Hagel (1988) to occur at pressures over 4000 bar. Taking 4000 bar as the limiting pressure the smallest pore size that may be evaluated using mercury porosimetry is 2 nm.

The reliability of the information gathered using mercury porosimetry is dependent on a number of factors including, pore structure (the assumption being that all pores are cylindrical), the nature of the material's surface (which may affect the wetting contact angle between mercury and the material surface) and sample's resistance to the applied pressure. Due to significant variations in these parameters, the uncertainty of mercury porosimetry is estimated to be around 20% (Hagel, 1988).

The strength of the technique is in the characterisation of larger pores which can not be detected reliably with gas absorption. In addition detecting these larger pores requires significantly lower pressures which reduces the problems of damaging the material during the analysis.

In the context of the research to be carried out here mercury porosimetry will be of little use, the main area of interest is pores in the region of 2-50nm and at these sizes nitrogen gas adsorption is a much preferred method of analysis.

2.4.2.4 Inverse Size Exclusion Chromatography

The pore size distribution of a porous granular material may be evaluated using inverse size exclusion chromatography (ISEC). The technique relies on using information on the solute size and the elution/retention times of a number of solute probe molecules injected individually into a packed column of the adsorbent material.

Inverse size exclusion chromatography relies on having a number of well characterised probe molecules, available in a range of sizes (different molecular weight). Commercially available probes used for ISEC include polyethylene glycol, polystyrenes, dextrans, and spherical proteins (Hagel, 1988). The size of the probe is required in order to evaluate the accessibility to the pore structure of a probe of known physical dimensions. ISEC relies on the use of the viscosity radius of the probe molecule. Viscosity radii can be calculated for a molecule of known molecular weight and intrinsic viscosity (dependent on solvent).

$$R = \left(\frac{3[\eta]M}{10\pi N_A} \right)^{\frac{1}{3}} \quad (\text{Dephillips and Lenhoff, 2000}) \quad (2.8)$$

Where R is the viscosity radius (Å), $[\eta]$ the intrinsic viscosity in $\text{cm}^3 \text{g}^{-1}$, M the molecular weight of the polymer, N_A Avogadro's constant. The viscosity

radius accounts for both the solute mass and the molecular shape and thus is used as a universal calibration parameter for SEC. Some examples of probe molecules and their sizes are presented in Table 2.5 additionally a few reference molecules e.g. relevant blood proteins have been included to aid comparison.

Table 2.5: Inverse size exclusion probe molecules - molecular weight and viscosity radius.

Molecular Weight (Da)	Radius (Å)	Molecular Weight (Da)	Radius (Å)
<i>Dextran</i> ¹		<i>Polystyrene</i> ²	
180	3.60	100	1.84
1000	8.45	1000	7.14
10000	26.61	10000	27.66
100000	83.75	100000	107.13
1000000	263.61	1000000	414.86
<i>Polyethylene Glycol</i> ¹		<i>Spherical Proteins</i> ¹	
100	2.76		
1000	9.07	1000	7.94
10000	29.82	10000	17.11
100000	98.07	100000	36.85
1000000	322.51	1000000	79.4
<i>Others</i>			
B ₂ -microglobulin	16.75 ³	Human Serum Albumin	36.00 ⁴
Haemoglobin	32.50 ⁴		

1 – Solvent: water, 2 – Solvent: THF, 3 – Davankov *et al*, 2000, 4- Glynne *et al*, 2002

The pore size distribution is related to the size exclusion chromatography distribution coefficient, K_d which is defined as:

$$K_d = \frac{V_R - V_0}{V_T - V_0} \quad (2.9)$$

Where V_R is the solute elution volume, V_0 is the interparticle void volume and V_T is the total mobile phase volume. By using a probe molecule sufficiently large to prevent access to the pores within the porous granular material the interparticle void volume may be characterised. By using a molecule small enough to enter all the adsorbent internal pores the total solvent volume may be determined. Thus the relation between K_d and retention volumes may be transformed using solute retention times of each probe relative to the retention time of the largest and smallest molecules as shown in equation 2.10:

$$K_d = \frac{t_R - t_0}{t_T - t_0} \quad (2.10)$$

Where t_R is the solute retention time, t_0 is the retention time of the excluded probe and t_T is the retention time of the probe which can access the whole pore volume.

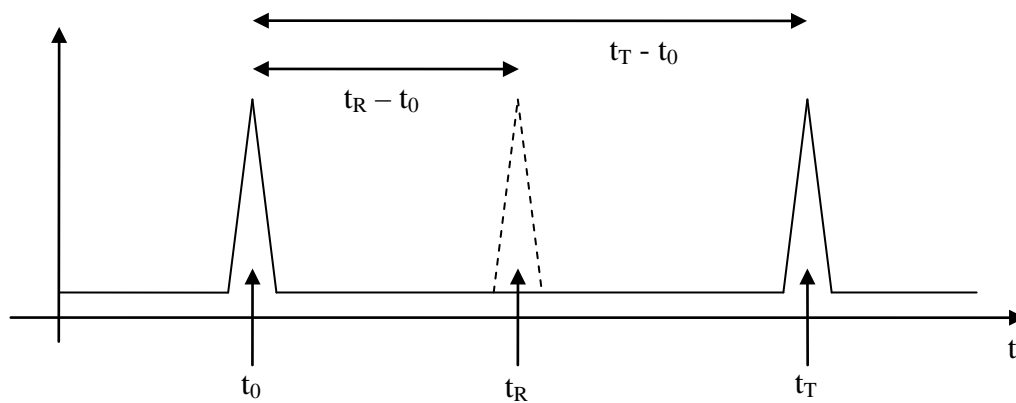


Figure 2.8: Sample chromatogram showing the relationship between totally included, excluded and partially excluded probes and their relationship to K_d .

Passing probe molecules through the packed column and obtaining the retention times allows K_d for each probe solute to be evaluated. Figure 2.8 is a graphical representation of equation 2.10, this shows how K_d for a given probe size represents a fraction of the total pore volume accessible. If t_R of a

probe were found to equal t_0 then the value of K_d would be 0, indicating complete exclusion from the internal pore structure of the adsorbent. If t_R were found to equal to t_T then K_d would equal 1 indicating the solute is small enough to be able to access all the internal pore volume within an adsorbent particle.

Plotting K_d against the probe size provides a calibration curve and represents the fraction of the pores of size greater than a given size. By evaluating $(1 - K_d)$ and plotting this versus the probe size, the resulting curve represents the fraction of the pore volume within the adsorbent particle less than the size of the probe. The calibration curve obtained is the cumulative pore size distribution for the material, a differential pore size distribution can also be evaluated (Figure 2.9 shows a cumulative and a differential pore size distribution for a silica sample based on Inverse size exclusion chromatography). A comparison of the ISEC data with nitrogen sorption data is also provided. The experimental data may be fitted to a model e.g. a Gaussian relationship has been used to describe the pore structure (Dephillips and Lenhoff, 2000) however, this results in pore diameters that are less than zero. An alternative approach is to model the data as a lognormal distribution (Evans et al, 1993) using Equation 2.11,

$$f(r) = \frac{1}{r\sigma(2\pi)^{1/2}} \cdot \exp\left[-\frac{[\ln(r/m)]^2}{2\sigma^2}\right] \quad (2.11)$$

Where m is the median value, σ is the standard deviation. With this formula for the differential pore size distribution can be plotted. This formula may only be used if the pore size distribution data conforms to a lognormal distribution. If the data is not well represented by a log normal distribution then an alternative method of analysis may be recourse to numerical differentiation of the cumulative pore size distribution.

Figure removed due to copyright.

Please refer to the original text.

Hagel L. *Pore Size Distributions*. In: Dubin PL, editor. *Journal of Chromatography Library – Volume 40, Aqueous Size-exclusion Chromatography*. Netherlands: Elsevier, 1988. p. 119-155

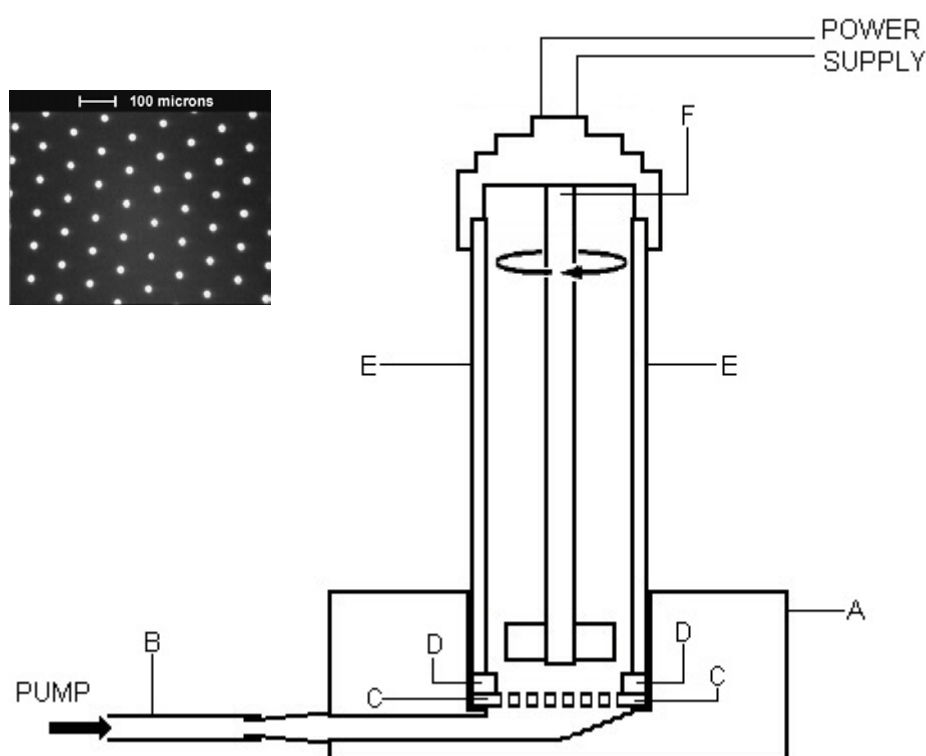
Figure 2.9: Pore size distribution of porous silica (Vydac TP 9) from ISEC and nitrogen sorption data (*) (Taken from Hagel, 1988)

The work of Hagel (1988) focuses on the modelling of porous distributions using silica materials for analysis. In the generation of porous silica particles it is possible to readily generate highly mono-disperse pore size distributions. In these instances it is not an unreasonable assumption to apply a Gaussian or log normal distribution to the ISEC data. Conversely poly(styrene-divinylbenzene) copolymers do not exhibit mono-disperse porous structures and consequently the modelling of ISEC data for these materials using Gaussian or log normal distributions is not backed by a reasonable assumption.

3 Experimental Materials and Methods

3.1 Membrane Emulsification and Drop Size Control

The basis for the membrane emulsification technique was based around the Micropore Technologies Ltd., Membrane Emulsion Cell. The cell utilised a membrane with a regular array of mono-sized pores and a paddle stirrer to generate an emulsion of droplets of tight droplet size distributions. The main features of the cell are shown schematically in Figure 3.1 below as well as an example of a membrane showing the regular array of mono-sized pores.



A – PTFE base, B – PTFE tubing for dispersed phase, C – Membrane, D – O-ring seal, E- Glass Cell and F – Electric stirrer

Figure 3.1: Schematic of Micropore Technologies Ltd. membrane emulsification cell and a micrograph of the membrane surface.

The cell utilised a DC power supply and the stirrer was operated between 3V and 24V. To generate a constant and even flow of dispersed phase into the

cell a Harvard syringe pump was utilised, this allowed adjustment of the flow rate from 0.05 – 10 ml/min. Due to the nature of the organic discontinuous phase a glass syringe was required, a 50ml syringe was purchased from Fisher Scientific for this purpose.

The two phases which were used to generate the emulsion were,

1. The continuous phase – an aqueous solution containing stabilisers (e.g. PVA)
2. The discontinuous phase – an organic solution of monomers, porogens and polymerisation initiator

In all cases, the continuous phase contained polyvinyl alcohol (PVA) (Mowiol 40-88, Sigma Aldrich, Molecular weight 205kDa and degree of hydrolysis 88%) as the droplet stabiliser and sodium chloride was added to reduce the solubility of the monomers and porogens in the aqueous phase. These were dissolved on a weight for weight basis. PVA concentration was varied from 0.5 wt.% to 4.5 wt.% while sodium chloride stayed constant at 3.3 wt.%, as an example a 2 wt.% PVA, 3.3 wt.% sodium chloride solution would comprise of, 20g PVA, 33.3g sodium chloride and 946.7g of ultra pure water.

The discontinuous phase contained a greater variety of potential components, these included monomers styrene (99%, Reagent Plus, Aldrich) and divinylbenzene (DVB) (mixture of isomers, Technical Grade 80%, Aldrich), porogens toluene (99+%, Acros), Undecane (99%, Aldrich) and naphthalene (99%, Aldrich) and the initiator benzoyl peroxide (BPO) (75%, Acros). Mixtures of these were generated on a weight for weight basis. When generating the discontinuous phase the initiator was always added immediately prior to use to delay the polymerisation reaction this is especially important when using the membrane emulsification technique.

The reader is referred to standard operating procedures SOP-01 and SOP-02 in Appendix I for details on the methods used for preparing the two phases.

To generate an emulsion the Micropore Technologies cell was assembled and 100ml of continuous phase was placed in the cell. Using a syringe continuous phase was pushed through the membrane to wet all pores and eliminate any trapped air in the system. Once all air has been eliminated the stirrer was inserted and checked to rotate freely. With the cell and continuous phase readied the discontinuous phase can be prepared. Fill the glass syringe with discontinuous phase and eliminate any air bubbles from the syringe and attach to the cell. Pull a small amount of continuous phase back into the syringe to ensure no air has been trapped. Attach the syringe to the pump and select a flow rate of 0.5 ml min^{-1} . Start the stirrer and engage the pump. Allow the discontinuous phase to be pushed through the membrane when the first droplets appear mark the syringe and allow the emulsion generation to proceed until the required volume of discontinuous phase has been injected. This procedure is detailed in SOP-03 found in Appendix I.

Once the droplet generation has been completed the emulsion was transferred to the suspension polymerisation reactor for the polymerisation stage to be completed.

In addition to generating emulsions of varying monomer-porogen ratios, emulsions were created of pure toluene to determine the effect of the properties of the continuous phase (sodium chloride and PVA concentrations) and stirrer speed (shear rate) on the resulting emulsion properties (droplet size distribution). For these experiments pure toluene was injected at 0.5 ml min^{-1} into a continuous phase consisting of varying

PVA concentrations ranging from 0.5% to 4% the stirrer was operated at four speed settings resulting in varying size distributions. Finally NaCl (3.3%) was added to the continuous phase to assess its effect on droplet distribution

Once the emulsion had been transferred to the polymerisation reactor, the membrane and cell were cleaned following standard operating procedure SOP-04 (Appendix I) to ensure that the membrane remained in good condition for subsequent emulsion generation work.

3.2 Suspension Polymerisation

Suspension polymerisation was used for the synthesis of the nanoporous spherical adsorbents. The equipment and materials used were: (i) a jacketed reaction vessel (volume 500ml), the lid of the reactor had 3 ports (1 central vertical and 2 side slanted) for the shaft stirrer, condenser and for sampling from the reaction vessel. Figure 3.2 shows a schematic diagram of the reaction system.

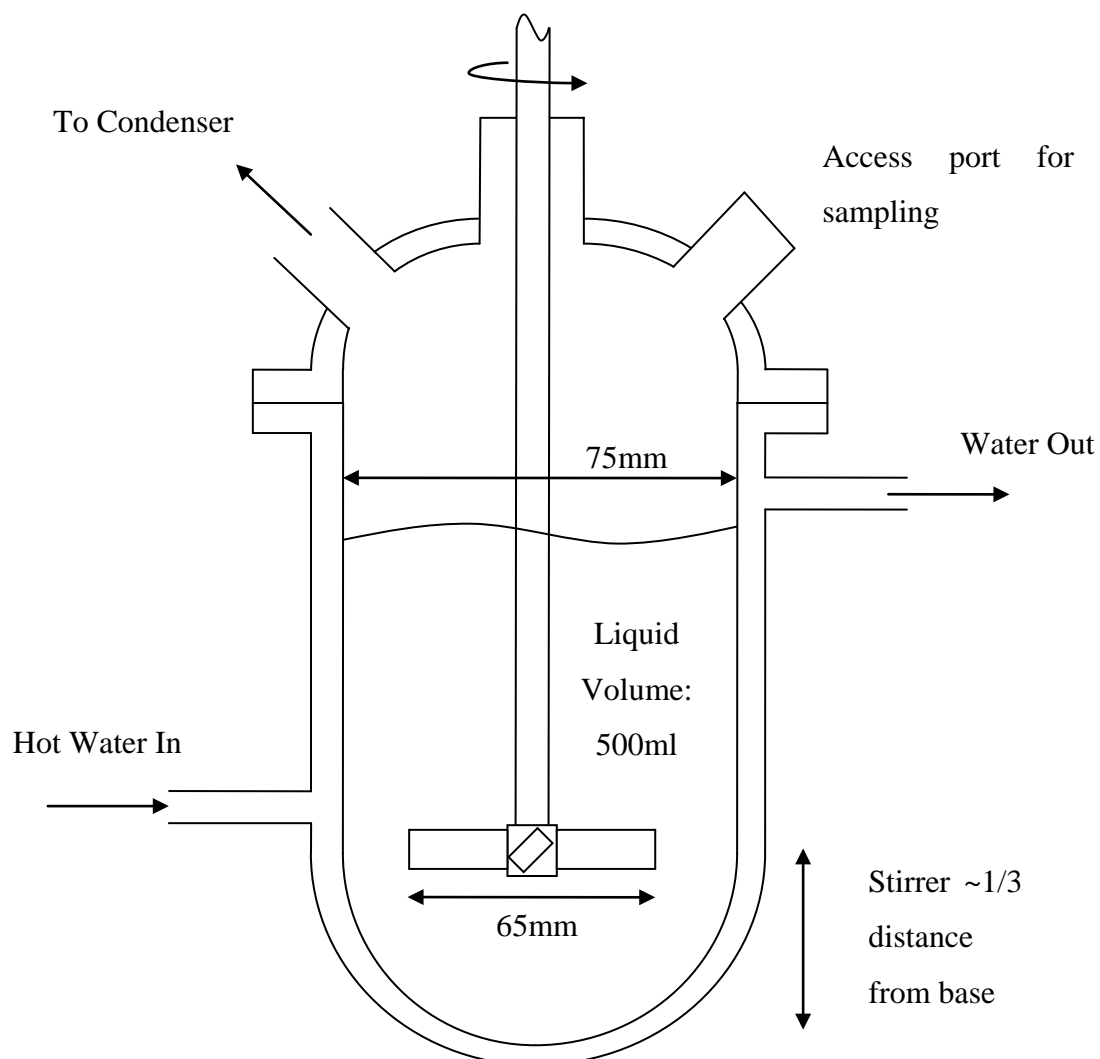


Figure 3.2: Schematic diagram of the suspension polymerisation reactor (showing orientation of heating and cooling water flows and stirrer position).

The reactor was thermostatically controlled through the use of a water bath combined with a pump to circulate hot water through the jacket. The temperature required for the polymerisation reaction to proceed was 80°C. Temperature of the reaction mixture was monitored through the side port throughout the reaction. The exothermic nature of the polymerisation

reaction seemed to have little effect on the temperature of the reaction mixture with this remaining constant throughout the 24 hour reaction period.

To minimise vapour loss from the reaction mixture, a condenser was utilised to capture any vapours which were returned to the reactor. All other ports were sealed using ground glass plugs and silicon grease, the stirrer used a gland to provide an airtight seal and this is shown in detail in Figure 3.3. Silicon oil was used rather than water in the gland to prevent evaporation during the protracted reaction period.

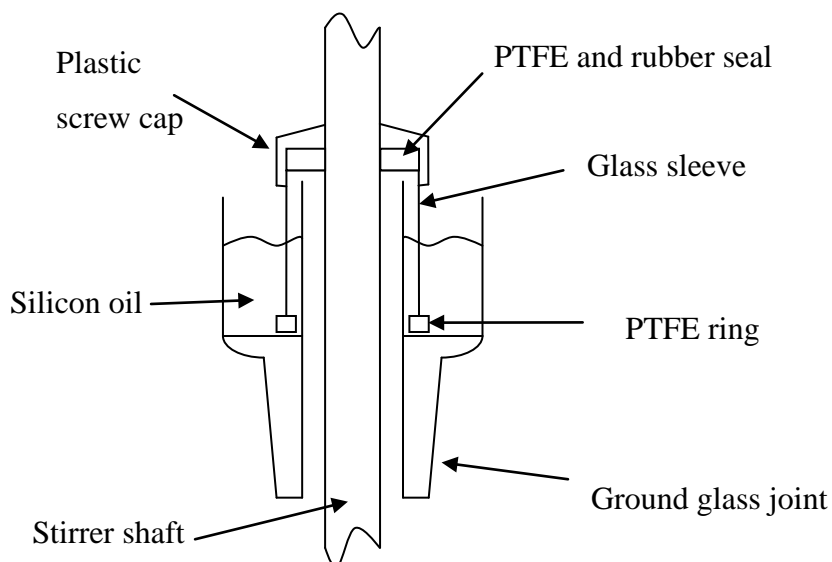


Figure 3.3: Schematic of Shaft stirrer gland used for suspension polymerisation.

The proper mixing of the reaction mixture was considered of importance. During a conventional suspension polymerisation process, a higher stirrer speed may be utilised as the shear induced break-up of the drops may be desirable if a small drop size is required. When controlling the droplet size using the membrane emulsification process it was important that shear due

to the stirrer rotation did not unduly affect the droplet size distribution. Thus a lower stirrer speed (to just suspend the drops) was utilised. Using a traditional paddle style stirrer the rotational speeds required to keep the droplets well suspended were rather high at lower speeds the less dense discontinuous phase tended to rise to the surface causing coalescence of the droplets. To counter this, a screw propeller shaft stirrer was purchased from Fisher Scientific Ltd., (Loughborough, UK). The angled blades on this stirrer force the reaction mixture in an axial direction (i.e. downwards) as well as radially thereby generating better mixing at lower stirring speeds. The stirrer was made of PTFE to minimise interactions between the stirrer and reaction mixture.

During suspension polymerisation the continuous phase was a solution of PVA and NaCl designed to stabilise the monomer/porogen droplets during polymerisation. When using the membrane emulsification method to generate droplets the reactor continuous phase was kept at 4.5% PVA and 3.33% NaCl independent of the continuous phase conditions used in the generation of the droplets. In the situations where the droplets were generated in the more traditional method using the stirrer in the reactor PVA concentrations were varied from 2-4.5% to yield varying droplet sizes NaCl concentrations remained static at 3.33% in all situations.

The reader is directed to standard operating procedure SOP-05 for details of the procedures involved in suspension polymerisation.

3.2.1 Separation of particles from the reaction mixture

Once the reaction had been allowed to reach completion (typically ~ 24 hours) the adsorbent particles were separated from the reaction mixture. Stopping the stirrer resulted in one of two events: either the particles floated

to the surface or, they sank to the bottom of the reaction vessel. In most cases, they floated to the free surface and were skimmed off. The resulting particles were subsequently washed with warm ultrapure water to remove residual PVA and sodium chloride. Depending on the particle size distribution of the materials prepared, either a sintered glass funnel or a Buchner funnel and appropriate filter paper (Whatman GF-B glass fibre filters were found to work well showing a high solvent flux and small pore cut off (2 μ m) ensuring retention of the smallest particles) were used to filter the particles (see SOP-06, Appendix I for further details). Upon elution of the residual PVA and sodium chloride, the particles were soaked with acetone and filtered again this stage removed residual water from the particles.

3.2.2 Removal of porogens and un-reacted monomers from particles

The removal of un-reacted monomers and the porogens was undertaken using a Soxhlet extractor (shown in Figure 3.4). Toluene was used as a good solvent to remove residual monomers as well as small molecular weight oligomer/polymer chains not covalently attached within the adsorbent particle. Toluene was subsequently removed from the particles through thermal or vacuum drying.

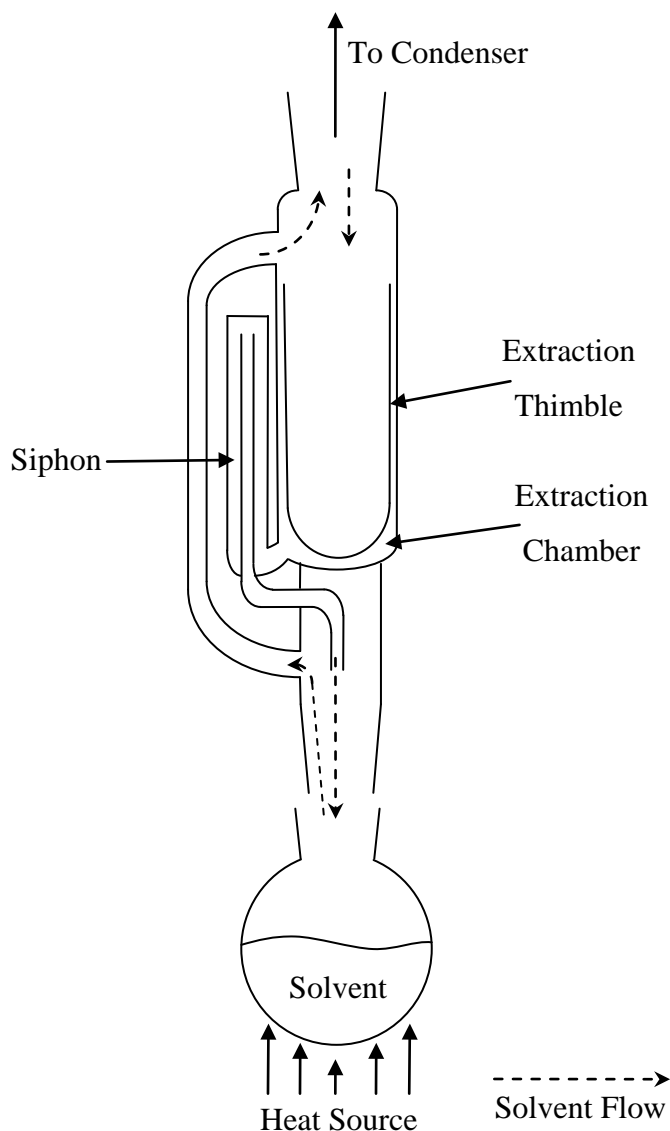


Figure 3.4: Schematic diagram of a Soxhlet extraction system

The Soxhlet extraction process (as described in SOP-07, Appendix I) used the solvent toluene which was heated to boiling point and kept at a gentle boil. The evaporated solvent was then condensed and slowly filled the extraction chamber containing the adsorbent particles in a porous extraction thimble. Once the extraction chamber was full of the solvent it automatically siphoned back to the main solvent evaporation chamber taking with it any dissolved impurities which had been extracted from the adsorbent particles. More pure solvent was continuously evaporated (as toluene has a lower

boiling point than the monomers and naphthalene) the process was continuously repeated. This extraction process was allowed to continue for 8 hours. The adsorbent batch was then removed from the extraction thimble and dried under vacuum overnight to remove the residual toluene.

3.3 Measurement of Particle Size Distributions

Two methods were used for the determination of the adsorbent particle size: Optical microscopy and laser diffraction light scattering.

Optical microscopy utilised an optical microscope fitted with a video camera aiding viewing via a monitor and permitting printing of the image using a photoprinter. It was also possible to record a digital image of the magnified particles. Calibrated graticules were used to accurately compare particle sizes of different samples. The advantages and disadvantages of the system were,

Advantages

1. Actual representation of particles with no modelling required
2. Allowed the shape of the particles to be examined
3. Small sample quantity required

Disadvantages

1. For accurate representation of the particle size distribution, manual measurement of a large number of particles was required and this was time consuming

Laser diffraction/light scattering is a technique where a light source of constant wavelength and intensity (laser) is used to determine the size of the particles. The particles are suspended in a continuous phase and are passed through the path of the laser, the size of the particle directly affects the angle at which the light is scattered and the intensity of the light. Larger

particles scatter light at narrow angles and with high intensity, the angle and intensity of the light is detected and this is used to determine the particle size.

Two light scattering particle sizers were available for use the Coulter LS130 and the Malvern Mastersizer. The Coulter system uses a sample cell which may be easily cleaned and allowed for the use of potentially sticky particles (for example during polymerisation), the cell also allowed a wide range of solvents to be used and a smaller volume of sample was required. In addition, the particles may be easily recovered if necessary for subsequent use (e.g. for structure characterisation and adsorption studies). The Malvern unit was limited to comparing samples in an aqueous environment and required a larger sample size (several ml of suspension rather than drops for use in the Coulter) the sample was also not easily recoverable. With these aspects in mind the Coulter LS130 was chosen as the most suitable instrument.

The advantages and disadvantages of light scattering as a method of particle size analysis are,

Advantages

1. Quick test, providing a complete particle size distribution
2. Easily reproducible

Disadvantages

1. Particle shape and uniformity is not evaluated
2. Agglomerates if present will effect particle size distribution

Obviously a combination of optical microscopy to confirm shape and determine a rough estimate of size and then utilising light scattering to generate a complete particle size distribution provides the most complete picture of the particle size analysis.

For this work samples of the polymer adsorbent particles generated were visually inspected and classified using the Coulter LS130, the Coulter LS130 was used with ultrapure water as the suspending medium when samples were already in aqueous solution for example when looking at droplet generation or the effect of particle size during polymerisation. If a sample was analysed once it had been cleaned and dried acetone was used as the suspending medium this enabled easy wetting of the particles.

3.4 Measurement of Porosity in Polymer Adsorbents

Measuring the porosity of polymer adsorbents can be carried out in a number of ways the most widely used is gas adsorption (as discussed in Chapter 2) the alternative is to investigate the system in the swollen state this requires a completely different approach and Inverse size exclusion chromatography (ISEC) has been used in this capacity.

3.4.1 Nitrogen porosimetry

Nitrogen porosimetry (77K) was carried out using a Micromeritics ASAP 2000 instrument. Samples were dried from toluene under vacuum at ambient temperatures overnight and subsequently degassed at ambient temperature to prevent pore structure change. This analysis provided data on BET surface area, total pore volume, and through DFT analysis of the isotherms pore surface area and volume distributions.

In addition to drying at ambient temperature under vacuum from toluene, acetone and methanol, samples were also freeze dried from two solvents benzene and cyclohexane to observe the effects on the preserved pore structure. For the freeze drying samples were first frozen using liquid

nitrogen and then kept at -20°C to ensure the solvent remained frozen during the drying process. Figure 3.5 shows the freeze drier set up

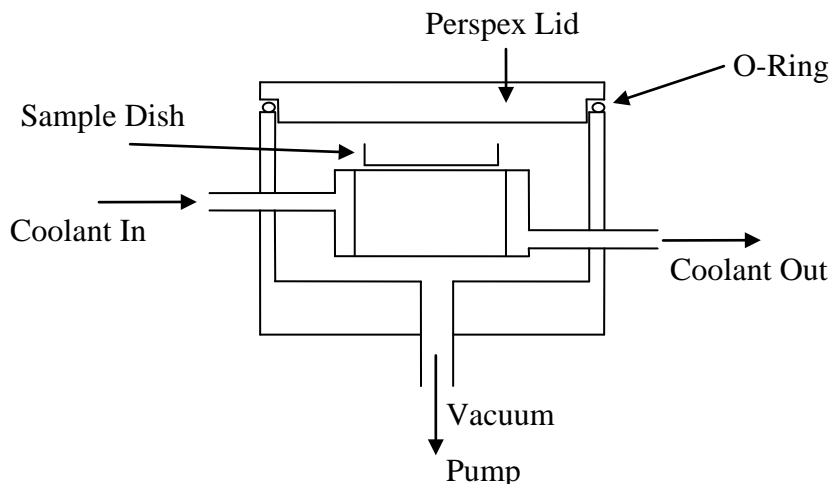


Figure 3.5: Schematic diagram of the freeze drier system

3.4.2 Inverse Size Exclusion Chromatography (ISEC)

Using a commercially available size exclusion material an appropriate method of column packing and analysis could be developed. For this purpose Superdex 75 prep grade (GE Healthcare) was chosen, the resin sample had a particle size range between $22\text{-}44\mu\text{m}$ and was designed to separate proteins between 3 and 70 kDa (equivalent to dextrans of size 500 Da – 30 kDa [Table 2.5]). A series of dextran standards were purchased from Polymer Standards Services for use with the Superdex (Table 3.1 shows the standards used). The standards are defined by a number of physical characteristics firstly molecular weight three values for the molecular weight of a polymer standard are determined these are “weight average molecular weight” M_w , “number average molecular weight” M_n and “molar mass at peak maximum” M_p . The reason behind having three values for molecular weight is that during the polymerisation process a range of molecular weights are generated depending on the use this is of great or little importance, in the

situation of standard materials for ISEC the distribution of molecular weights is important. By measuring three different variations of the average molecular weight we can determine how good a standard material is. The M_P value is the molecular weight that corresponds to the largest peak on the assessment of the standard using a calibrated column and is what will be used for assessing pore size during ISEC. M_n and M_w are number and weight averages respectively these values will differ when a distribution of molecular weights are present because a single large polymer chain can weigh many times that of a large number of small polymer chains. To assess how tight the distribution of molecular weights is for a particular sample a parameter the polydispersity index (PDI) is defined, $PDI = M_w/M_n$ the closer to unity this value the tighter the molecular weight distribution. Generally smaller standards have lower PDI values with pure chemicals for example glucose having a PDI of 1.

Table 3.1: Dextran probe molecular weight (M_P), polydispersity index (PDI) and viscosity radius (R_η).

Probe	M_P (kDa)	PDI	R_η (nm) ^a
Glucose (180 Da)	0.18	1	3.60
Dextran 1.3 kDa	1.05	<1.5	8.66
Dextran 5.2 kDa	4.40	<1.5	17.68
Dextran 12 kDa	9.90	<1.5	26.47
Dextran 25 kDa	21.40	<1.5	28.86
Dextran 50 kDa	43.50	<1.5	55.33
Dextran 150 kDa	124	<1.5	93.22
Dextran 1.3 MDa	1223	2	291.41

a - Calculated using values from Hagel, 1988

Two columns of differing diameter (4.6mm and 10mm) were packed using a slurry column packer, a slurry of particles in water was generated and placed in a reservoir the column to be packed was attached to the reservoir and then the slurry was pumped into the column using a high pressure pump. The column was then removed from the reservoir and sealed for use. The columns were tested with the Dextran standards using ultra pure water as the eluent. Polystyrene adsorbents were packed into columns of 4.6mm diameter in the same fashion however tetrahydrofuran (THF) was used to generate the slurry and pack the column. When evaluating the polystyrene adsorbents using ISEC polystyrene standards and THF as the eluent were utilised, see Table 3.2 for details on the polystyrene standards.

Table 3.2: Polystyrene probe molecular weight (M_p), polydispersity index (PDI) and viscosity radius (R_η).

Probe	M_p (kDa)	PDI	R_η (nm) ^a
Toluene	0.092	1	-
PS 500 Da	0.374	1.22	0.4
PS 1 kDa	0.89	1.12	0.7
PS 2 kDa	1.92	1.06	1.1
PS 5 kDa	4.87	1.05	1.8
PS 10 kDa	9.95	1.03	2.8
PS 20 kDa	24.3	1.02	4.7
PS 70 kDa	76	1.03	9.1
PS 1000 kDa	1044	1.14	42.6

a - Calculated using values from Hagel, 1988

3.5 Protein Adsorption Studies

The protein adsorption studies were carried out in a 500ml reaction vessel suspended in a thermostatically controlled water bath with the temperature controlled at 37.5°C. The experimental apparatus is shown schematically in Figure 3.6.

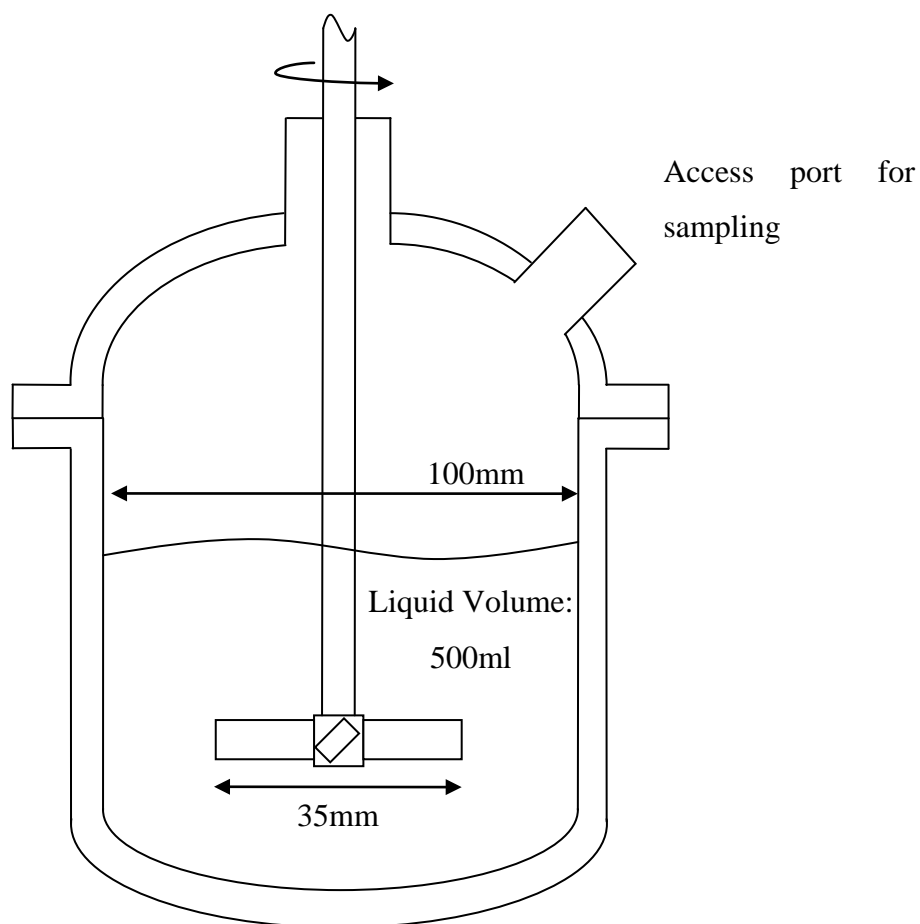


Figure 3.6: Schematic of batch protein adsorption apparatus

The adsorption was carried out using a HEPES buffer solution (10mM HEPES, 100mM NaCl with a pH 7.2) and varying concentrations of either human serum albumin or chicken egg lysozyme, and wetted adsorbent. The adsorption was allowed to proceed for at least 24 hours with samples taken at regular intervals, an example sampling plan used was: 0, 2, 5, 10, 15, 20,

30, 45, 60, 90, 120, 180, 240, 300, 360, 480, 720, 1440 (minutes). For details on buffer preparation and adsorption experiment set up and sampling please see SOP-16 and SOP-17.

Analysis of the protein samples was carried out on an Agilent 1100 series HPLC by reverse phase chromatography on a C18 column (Supelco), this utilised two mobile phases, phase A ultra pure water with 0.5% trifluoroacetic acid (TFA) and phase B acetonitrile with 0.1% TFA. A linear gradient was followed over 60 minutes moving from 2% phase B to 80% phase B, followed by a step change back to 2% phase B for 10 minutes to recondition the column. The flowrate for the entire procedure was kept at a constant 1 ml/min and detection of proteins was accomplished using a diode array detector (detection wavelength λ , 230 and 290 nm for albumin and lysozyme respectively)

4 Results and Discussion - Synthesis and Analysis of Porous Spherical Polymer Adsorbents

4.1 Synthesis of Polymer Adsorbents

The Chapter will begin by outlining the polymer adsorbents synthesised during the research study. A table summarising the synthesis conditions and the associated nomenclature used for identifying the materials is presented in Table 4.1. All adsorbents were synthesised using the membrane emulsification technique detailed in Chapter 3 unless otherwise stated. All adsorbents were produced using styrene and divinylbenzene as monomers. Additionally a selection of porogens toluene (Tol), undecane (Un) and naphthalene (Nap) was used either in combination or individually (see Table 4.1.). Benzoyl peroxide (BPO) was utilised as the polymerisation initiator. Polymerisation was carried out at 80°C and lasted for 24 hours. Samples were subsequently washed and cleaned using a Soxhlet extraction process before being vacuum dried.

Table 4.1: Polymer adsorbent composition, all ratios are weight for weight

Identifier	Monomer Ratio		NDC (%)	Porogen Ratio			M : P Ratio	BPO (%) ^b
	Styrene	DVB ^a		Tol	Un	Nap		
PSDVB1:1TolUn9:1	1	1	40	9	1	0	1:1	1
PSDVB1:1TolUn9:4	1	1	40	9	4	0	1:1	1
PSDVB3:5TolUn1:0	3	5	50	1	0	0	1:1	1
PSDVB3:5TolNap5:2	3	5	50	5	0	2	1:1	1
PSDVB0:1TolUn1:0	0	1	80	1	0	0	1:1	1
PSDVB3:13TolUn1:0	3	13	65	1	0	0	1:1	1
PSDVB3:5TolUn1:0P2	3	5	50	1	0	0	1:2	1
PSDVB0:1TolNap5:2	0	1	80	5	0	2	1:1	1

NDC – Nominal degree of crosslinking

M : P Ratio – Monomer to porogens ratio by weight

a – Divinylbenzene 80% isomers remainder ethylstyrene

b – Based on monomer weight

Nominal degree of crosslinking starts at 40% due to lack of dry state porosity below this value when using toluene as a porogen (see section 2.4.1 and Figures 2.5 and 2.6 specifically for the reasoning behind this).

4.2 Membrane Emulsification and Droplet Size

Initial experiments were designed to determine the range of droplets that can be generated using the Micropore Technologies stirred cell. This work was carried out using pure toluene as the discontinuous phase. A 10µm circular pore hydrophobic membrane was utilised and a constant flow rate of 0.5 ml/min. The two parameters which were altered were the rotational speed of the paddle stirrer and the polyvinyl alcohol (PVA, used as the drop stabiliser) concentration. The stirrer speed was controlled by altering the voltage supplied to the stirrer. The droplet size distributions were measured using the Coulter LS130 and optical microscopy photographs were taken. Table

4.2 shows the applied voltages and the corresponding stirrer speeds for a series of PVA concentrations used.

Table 4.2: Stirrer speeds and PVA concentrations

Voltage (v)	Stirrer Speed (rpm)	PVA Conc ⁿ (%)
3	335	0.5
6	675	1
9	1010	2
12	1345	3
		4

4.2.1 Stirrer Agitation Rate and Stabiliser Concentration

The influence of stirrer agitation rate and PVA concentration on the resulting drop size distribution for pure toluene drops was investigated Figures 4.1 to 4.5 show the effects of stirrer speed on the droplet size distributions at each PVA concentration. Table 4.3 tabulates the generation conditions, as well as the median droplet size, 10 and 90 percent boundaries and the span as an indication of the tightness of the distribution, for each set of conditions. Figure 4.1 details the toluene droplet distributions when using a PVA concentration of 0.5% by adjusting the stirring rate the median droplet diameter is altered from 57-188 μm the distributions are reasonably symmetrical with the mode and median values being very similar. Increasing the PVA concentration to 1% the range of median droplet diameters are 53-180 μm the fastest stirring rate has caused a small amount of break up as is evident from the higher number of droplets in the 20-30 μm range. 2% PVA as shown by Figure 4.3 develops a median particle diameter range of 55-160 μm breakup of droplets is more pronounced with all agitation rates developing a larger proportion of smaller droplets. Figure 4.4 shows the

effect of stirring speed with a PVA concentration of 3% median droplet diameter ranges from 31-132 μm droplet breakup is particularly pronounced at the highest agitation rate however it is present in at all speeds. Figure 4.5 shows PVA concentrations of 4% at this concentration median droplet diameter ranges from 28-119 μm and breakup of the droplets is widespread across all stirrer speeds. Evaluating Figures 4.1 – 4.5 and Table 4.3 we can see that both PVA concentration and agitation rate have an effect on the median size of the droplet generated as well as the distribution of the droplets. From the tabulated data it appears that the distribution span for PVA concentrations <3% PVA remain approximately less than or equal to 0.6 this indicates a tight droplet size distribution. Once the PVA concentration passes 3% the span increases sharply with the loosest distribution being at 4% PVA at the fastest agitation rate. This span data confirms what can be assessed visually in Figures 4.1 - 4.5 that PVA concentrations of 3% start to show wider distributions and at 4% this effect is very pronounced. To confirm these results optical micrographs were taken a selection can be seen in Figure 4.6 and the remainder in Appendix II, as they show the 0.5, 1 and 2% PVA samples all show reasonably mono-sized droplets while the 4% sample even at 335 rpm clearly shows a wide range of droplet sizes.

To provide an overview of the combination of PVA concentration and stirrer speed Figure 4.7 shows the combined effect in the form of a surface/contour plot. Using this as an estimate a desired median droplet size can be targeted through changing PVA concentration and stirrer speed.

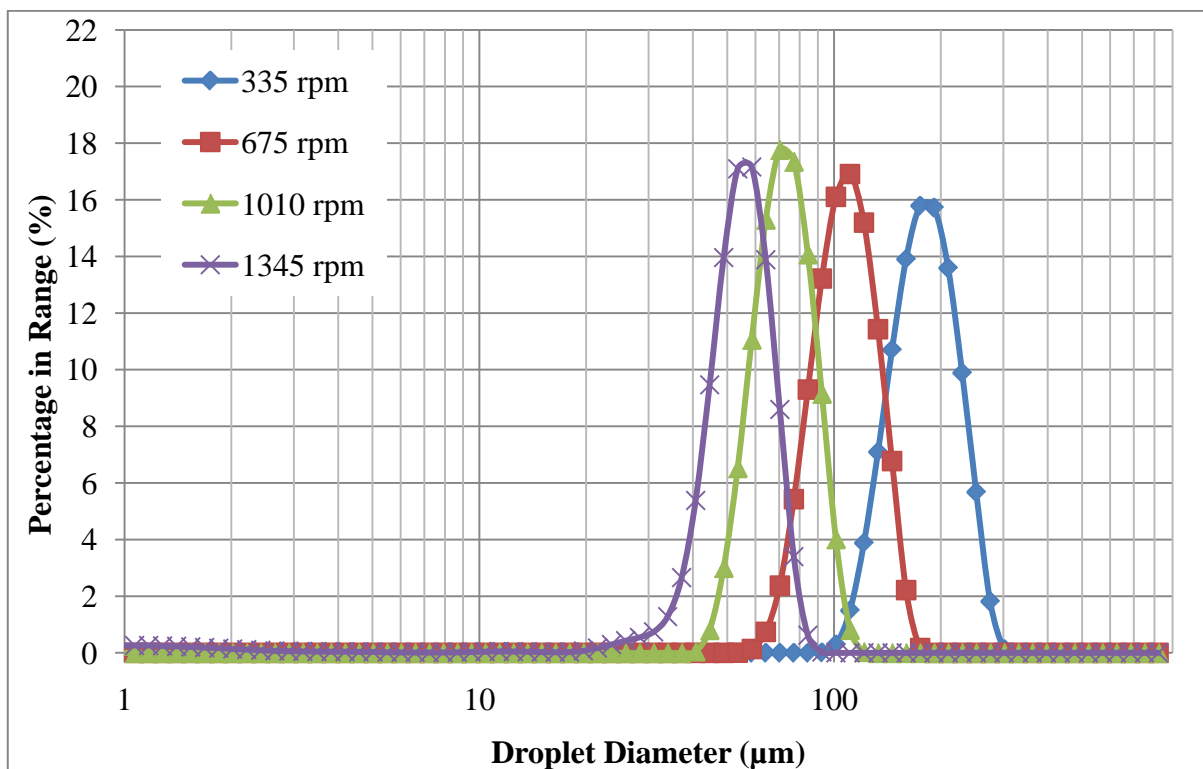


Figure 4.1: Toluene droplet size distributions with 0.5% PVA continuous phase at various stirrer speeds.

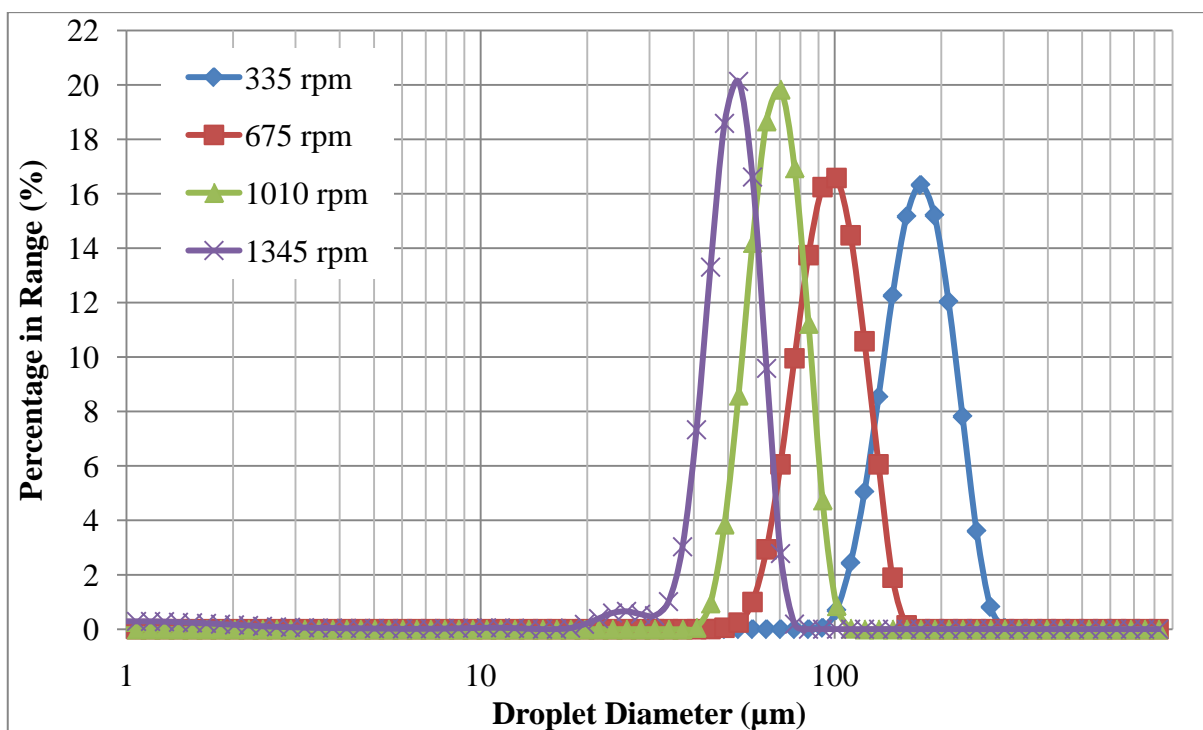


Figure 4.2: Toluene droplet size distributions with 1% PVA continuous phase at various stirrer speeds.

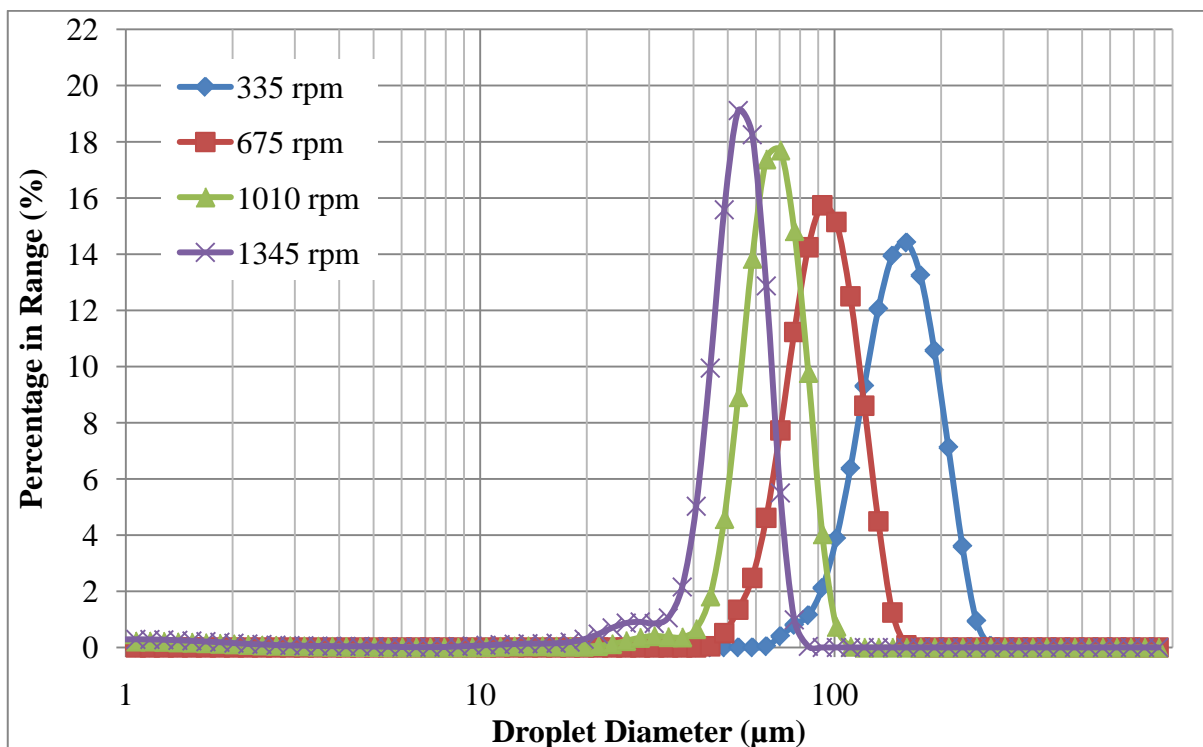


Figure 4.3: Toluene droplet size distributions with 2% PVA continuous phase at various stirrer speeds.

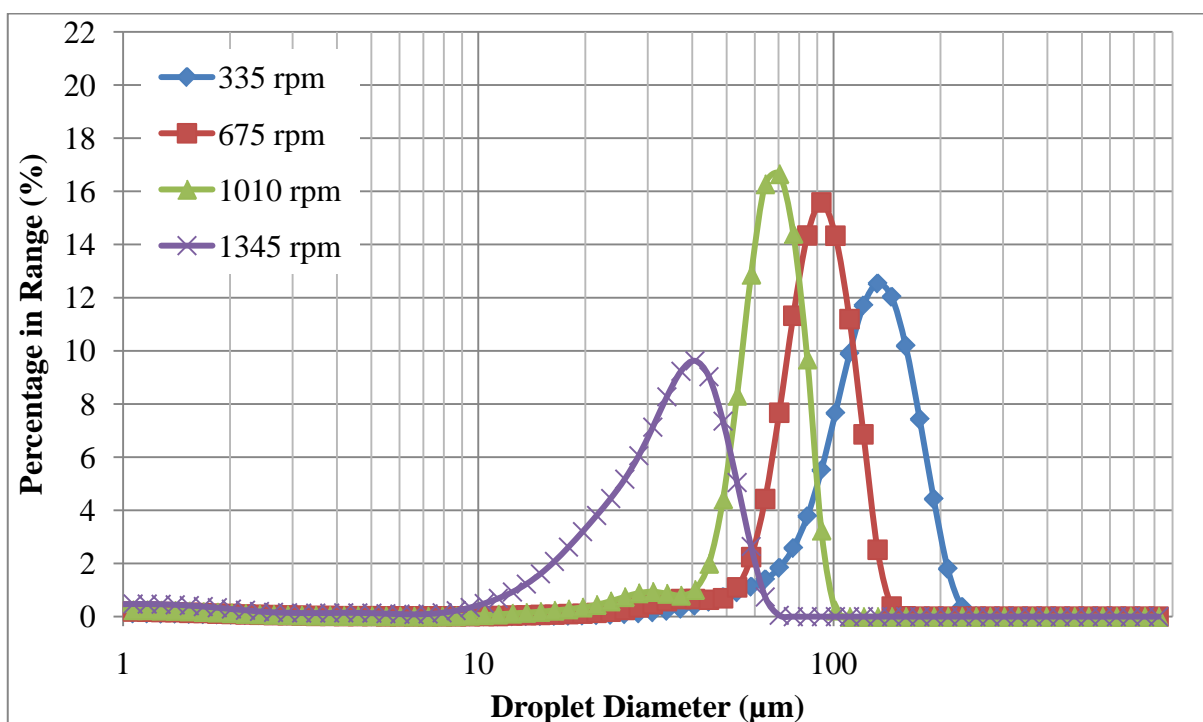


Figure 4.4: Toluene droplet size distributions with 3% PVA continuous phase at various stirrer speeds.

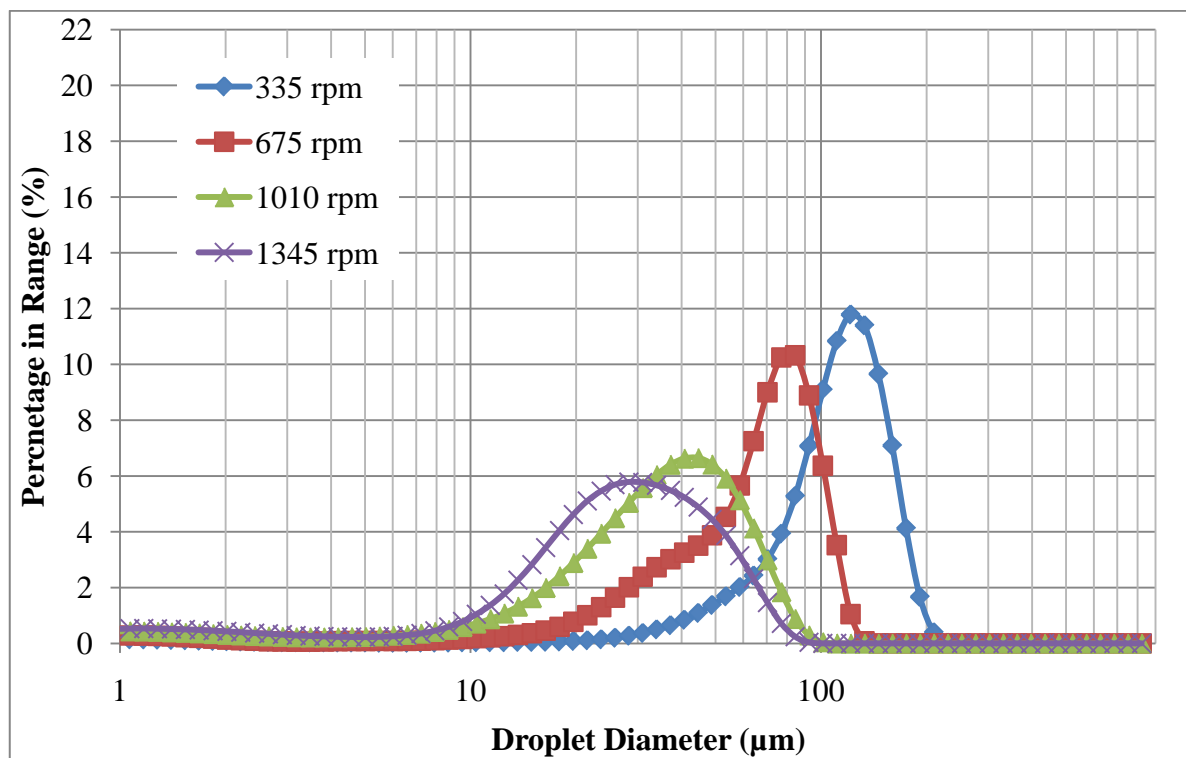


Figure 4.5: Toluene droplet size distributions with 4% PVA continuous phase at various stirrer speeds.

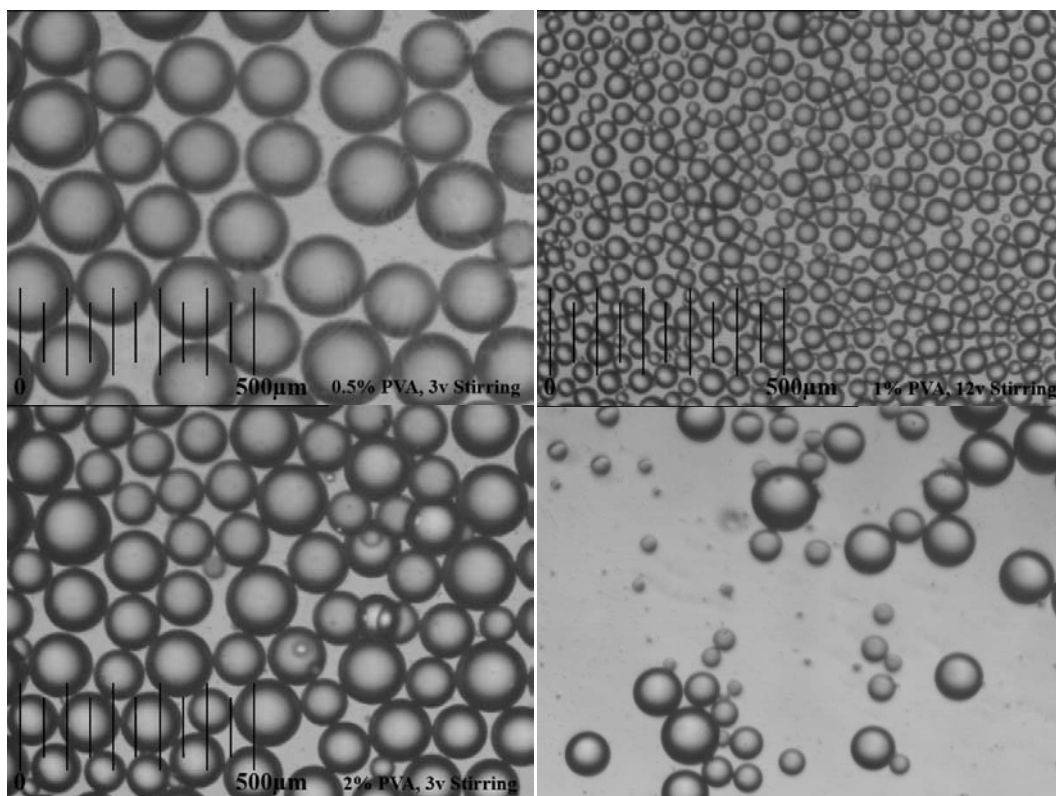


Figure 4.6: Toluene droplet, photographs clockwise from top left 0.5% PVA & 335 rpm, 1% PVA & 1345 rpm, 2% PVA & 335 rpm and 4% PVA & 335 rpm

Table 4.3: Toluene droplet size distribution data

Generation Variables		Droplet Distribution Results (μm)				
PVA Conc ⁿ (%)	Stirrer Speed (rpm)	Mode	Median	x ₁₀	x ₉₀	Span
0.5	335	191.65	188.10	140.75	246.30	0.56
0.5	675	110.95	112.55	85.82	144.75	0.52
0.5	1010	73.59	75.31	58.30	96.27	0.50
0.5	1345	58.67	56.77	40.36	72.04	0.56
1	335	182.90	180.75	135.65	236.05	0.56
1	675	105.90	101.05	76.68	130.95	0.54
1	1010	73.59	71.56	55.34	89.62	0.48
1	1345	56.00	53.34	38.96	65.80	0.50
2	335	167.00	159.60	113.8	214.20	0.63
2	675	96.71	96.79	71.25	127.10	0.58
2	1010	70.39	69.35	51.04	87.93	0.53
2	1345	56.00	55.31	35.56	68.65	0.60
3	335	139.20	131.95	76.63	183.30	0.81
3	675	96.71	92.90	60.70	121.60	0.66
3	1010	70.39	68.17	37.79	86.79	0.72
3	1345	42.62	34.72	12.75	52.53	1.15
4	335	127.10	118.60	58.68	171.00	0.95
4	675	84.45	69.88	24.93	102.75	1.11
4	1010	45.02	31.60	8.529	64.12	1.76
4	1345	31.02	27.90	4.87	55.83	1.83

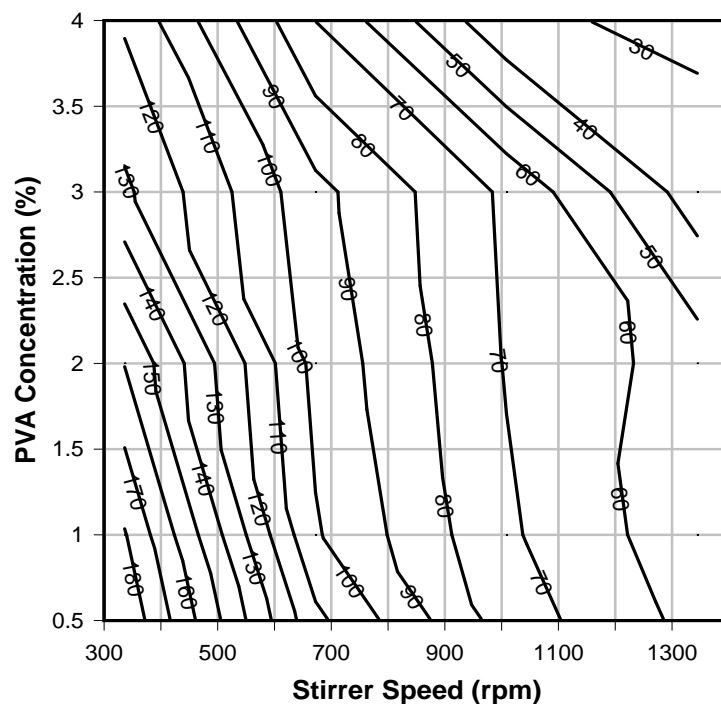
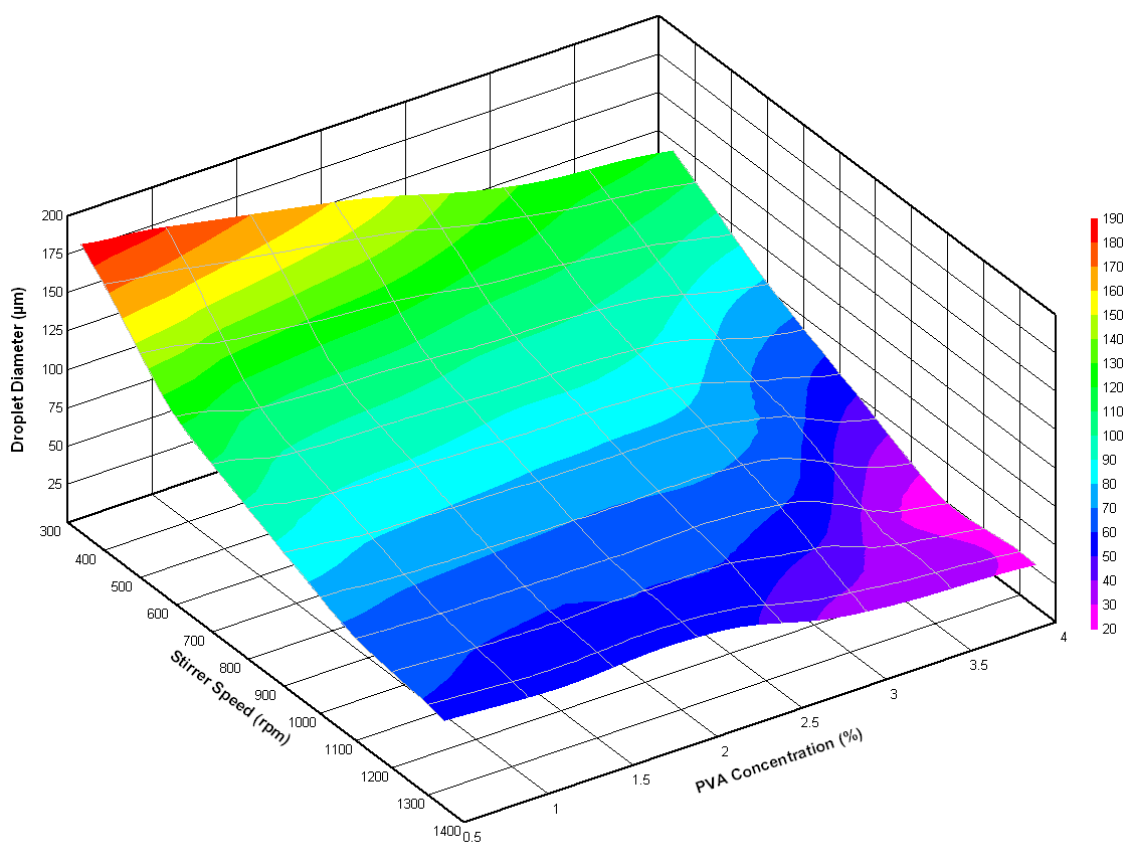


Figure 4.7: Surface and contour plots for approximating a median droplet diameter for a given PVA concentration and stirrer speed.

From the analysis of the droplet size distribution data it is apparent that the use of a membrane emulsification technique to generate a controlled particle distribution can be achieved and tailored to a wide range of droplet sizes. For the current work adsorbent particles are needed for two distinct applications first is for use in ISEC columns and these particles need to be small to increase resolution of the column. Secondly larger particles will be required for use in protein adsorption work and once a final product is ready to be produced a larger particle would be required for a heamoperfusion column to reduce pressure drop through the device.

4.2.2 Effect of the addition of sodium chloride to the continuous phase

The next step in the process was to determine if the addition of sodium chloride to the continuous phase would have an effect on the droplet size distribution, Figure 4.8 clearly shows that the addition of sodium chloride has no noticeable effect on the generation of droplets and the distribution generated.

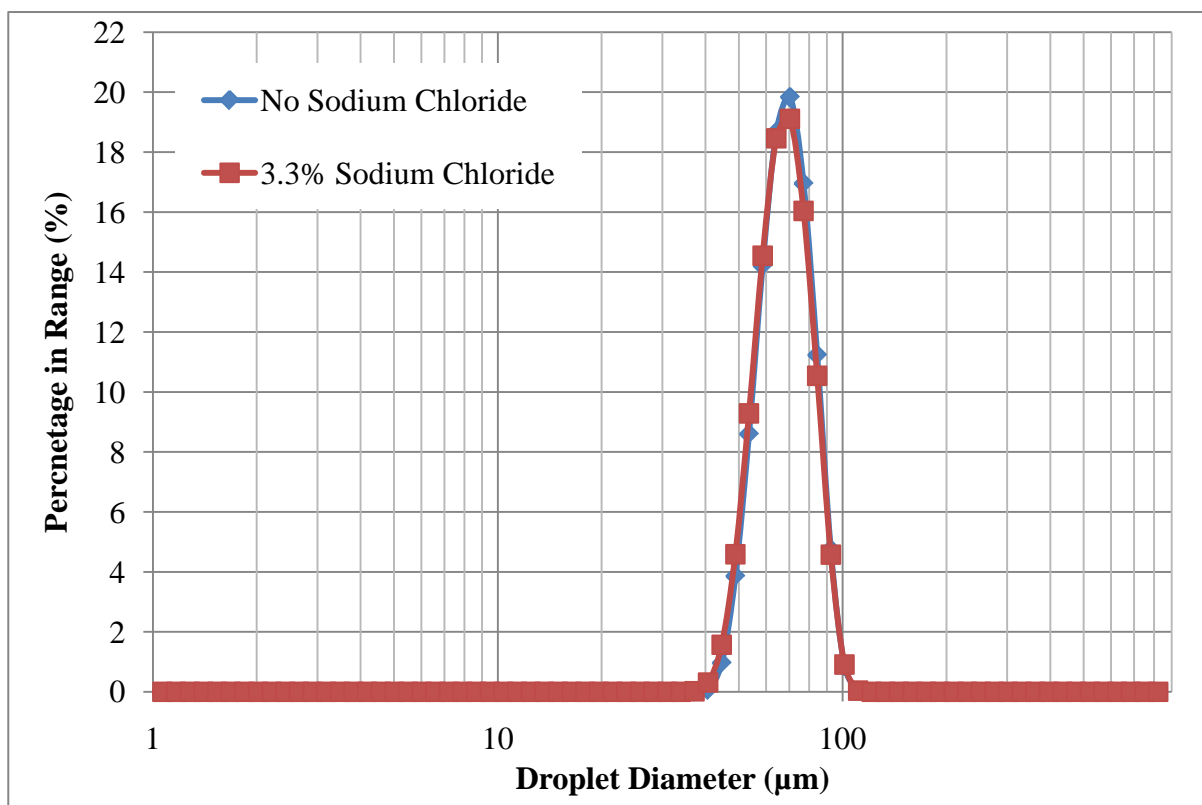


Figure 4.8: Toluene droplet size distributions, comparing the effect of adding sodium chloride to the continuous phase, generation conditions 1% PVA and 1010 rpm stirrer speed

The addition of NaCl is important to the research carried out here as it is required in the continuous phase to prevent the dissolution of the organic phase into the water phase. This experiment clearly shows that the addition of NaCl to the continuous phase has no impact on the droplet generated by the emulsification process and as such the work in section 4.2 can be used to determine droplet size when the continuous phase contains NaCl.

From this initial study it can be concluded that using a Micropore Technologies stirred cell will allow the generation of droplets of median size ranging from 30 to 190 µm using a 10 µm pore membrane the generation of droplets down to ~55 µm provide tight droplet size distributions, droplets can be generated below this level however droplet distribution suffers as a result.

Figure 4.7 while useful in determining a median droplet diameter does not however show the effect on droplet size distribution and as observed lower PVA concentrations and higher stirrer speeds (for smaller droplets) provide greater distribution control.

In terms of the overall research the use of a Mircropore Technologies membrane and stirred cell is an efficient method for generating droplets of tight size distribution and will be utilised for the control of particle size for all adsorbents generated for analysis.

4.3 Effect on Droplet/Particle Size During Polymerisation

To identify what happens to the droplet size and consequently the resulting particle size during polymerisation an emulsion was generated using as the discontinuous phase styrene, divinylbenzene and toluene, this was injected into a 2% solution of PVA and 3.3% sodium chloride with a stirrer speed of 335rpm, referring to Figure 4.7 we would expect a modal droplet size of 160-170 μm , the emulsion was then transferred to a suspension polymerisation reactor and polymerised at 80°C for 24 hours a sample was taken after 5 hours of polymerisation and again once the reaction had completed. Figure 4.9 shows the results from this experiment as expected the initial emulsion has a modal droplet size of 167 μm , after 5 hours we see a similar distribution however a larger volume of smaller (<100 μm) particles are recorded, after the reaction has completed we see an increase in particles of larger volume (>300 μm) these are aggregates and easily removed from the sample.

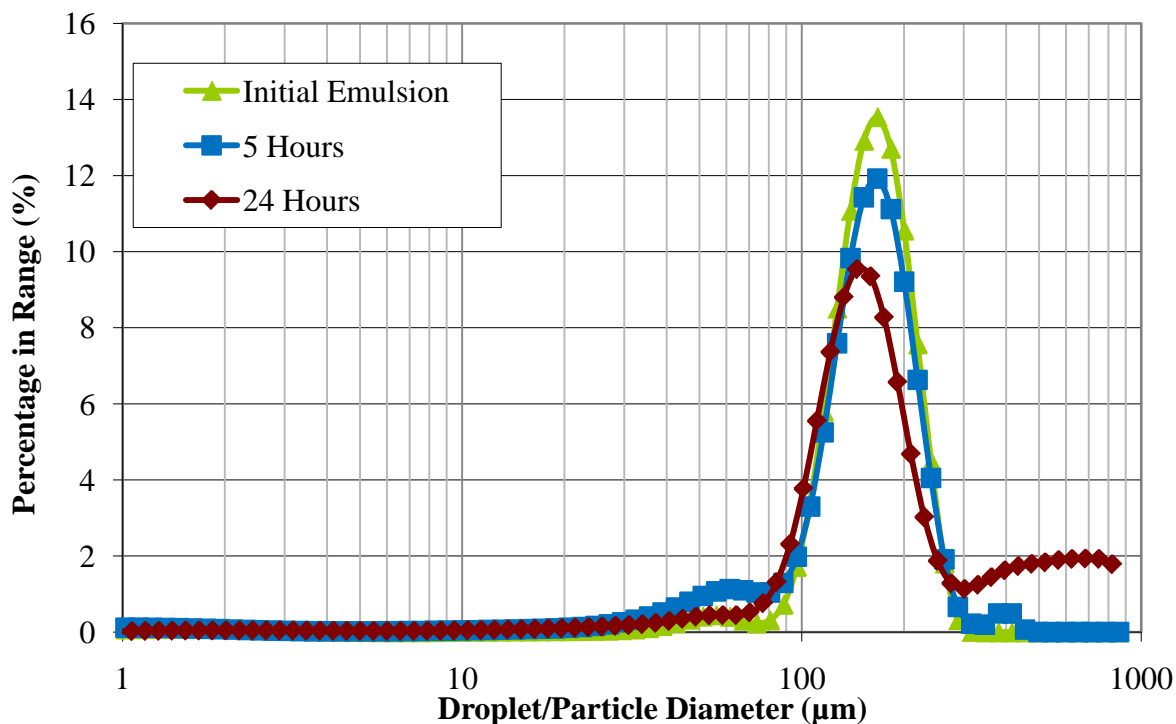


Figure 4.9: Polystyrene-divinylbenzene emulsion generation and droplet/particle size progression during polymerisation, 2% PVA, 3.3% sodium chloride and 335rpm stirring.

The use of a toluene analogue for the monomer mixture for determining the target values for stirrer speed and PVA concentration has been shown to be reasonable. Consequently if further work was required to determine a membrane/stirrer speed/stabiliser combination for the generation of a particular particle size toluene could be used in place of a polymerisation mixture.

As shown final particle size is not affected by the polymerisation process apart from the generation of some smaller particles due to break up in the main reactor and some aggregation. However in tailoring a final particle size using the initial droplet distribution as a good estimate can be considered a reasonable assumption.

4.4 Porous structure of polymer adsorbents

The most widely used method of analysing the internal pore structure of polymer adsorbents is gas adsorption. For determining the effects on pore structure generated through the varying of polymerisation conditions gas adsorption provides a reliable, repeatable and relatively quick analysis.

4.4.1 Effect of Porogen and Monomer Composition on Adsorbent Internal Pore Structure

Porogen – Solubility of Polystyrene

From Table 4.1 we observe that three porogens have been utilised during this work they are toluene, undecane and naphthalene. Mixtures of these porogens were used to change the internal pore structure of the polymer adsorbents. Figure 4.10 shows the effect of changing these porogens, with dramatic results. As is clearly evident large differences in pore structure can be achieved through the use of different porogens as expected the addition of a poor solvent for polystyrene, in this case undecane has increased the total pore volume as well as the maximum pore size. Interestingly the addition of naphthalene reduces maximum pore size over toluene, this would indicate a higher solubility affinity for the naphthalene toluene solution towards polystyrene than plain toluene.

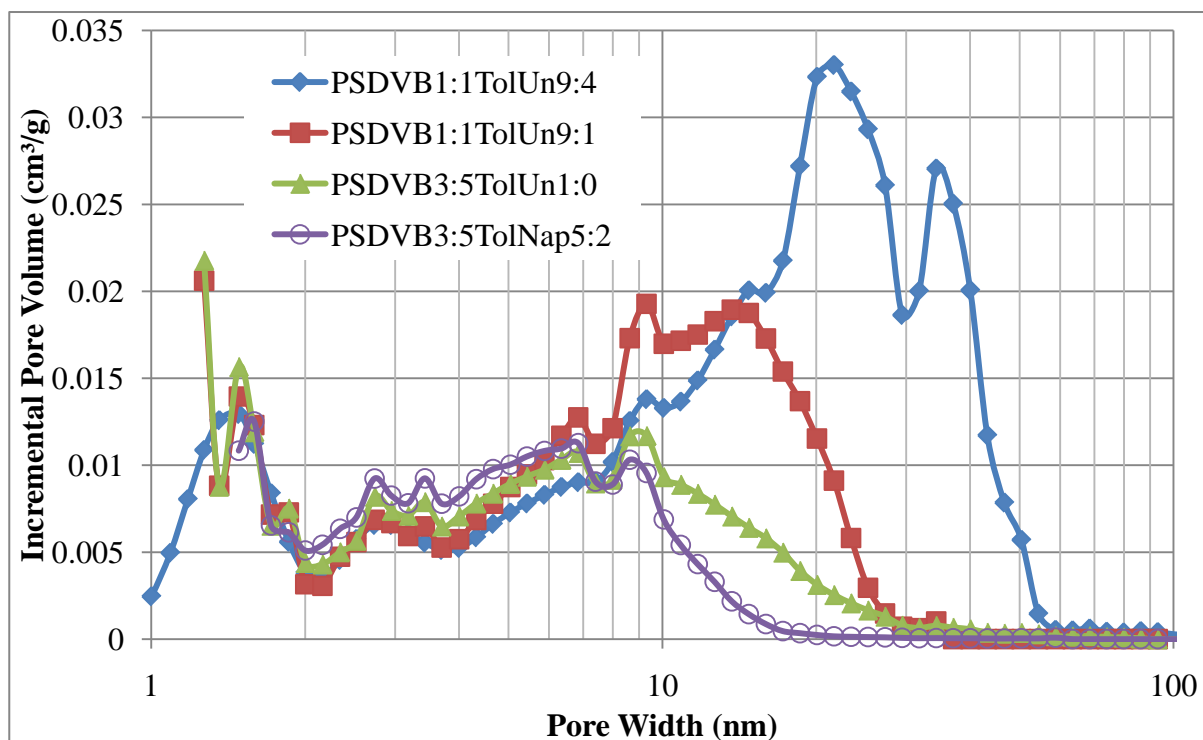


Figure 4.10: Effect of porogen on pore volume distribution of poly(styrene-divinylbenzene) copolymer adsorbent particles measured using nitrogen gas adsorption.

Monomer to Porogen Ratio

Another porogen related factor which can be investigated is the monomer to porogen ratio by increasing the percentage of porogen in each droplet the total pore volume should be increased changing the monomer to porogen ratio to 1:2 from an original figure of 1:1 increases the percentage of each droplet to 67% porogen. Figure 4.11 shows an increase in pore volume across the whole distribution, resulting in a slightly higher maximum pore width. Table 4.4 reports the numerical data and shows a total pore volume increase of 37% this is slightly higher than you would expect as the percentage of the droplet consisting of porogen only increased 33%.

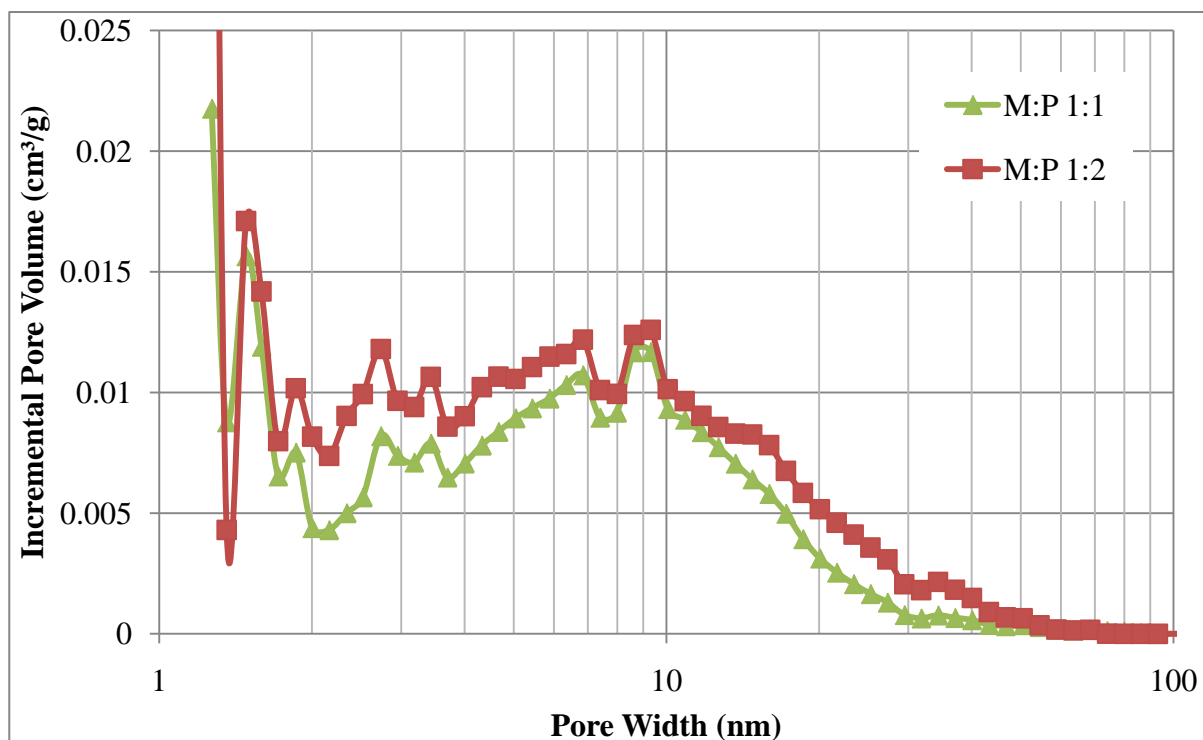


Figure 4.11: Effect of monomer to porogen ratio on pore volume distribution of a poly(styrene-divinylbenzene) copolymer adsorbent with a nominal 50% crosslinking degree and toluene as the porogen, analysed with nitrogen gas adsorption.

Crosslinking degree

Moving away from the porogens we can manipulate the monomers to influence porosity generation as well. The main parameter we can change here is the nominal degree of crosslinking, working with toluene as the porogen three levels of crosslinking were investigated 50%, 65% and 80% (the maximum possible crosslinking degree due to the purity of the monomers) Figure 4.12 presents the incremental pore volume distributions for each of these levels of crosslinking using toluene as the porogen a dramatic increase in pore volume and surface area is obtained, from Table 4.4 we can see an increase in total surface area of 120% moving from 50% to 80% nominal degree of crosslinking, this is echoed in the region 2 – 10

nm. Maximum pore size is increased again as an unavoidable side effect of increasing the pore volume.

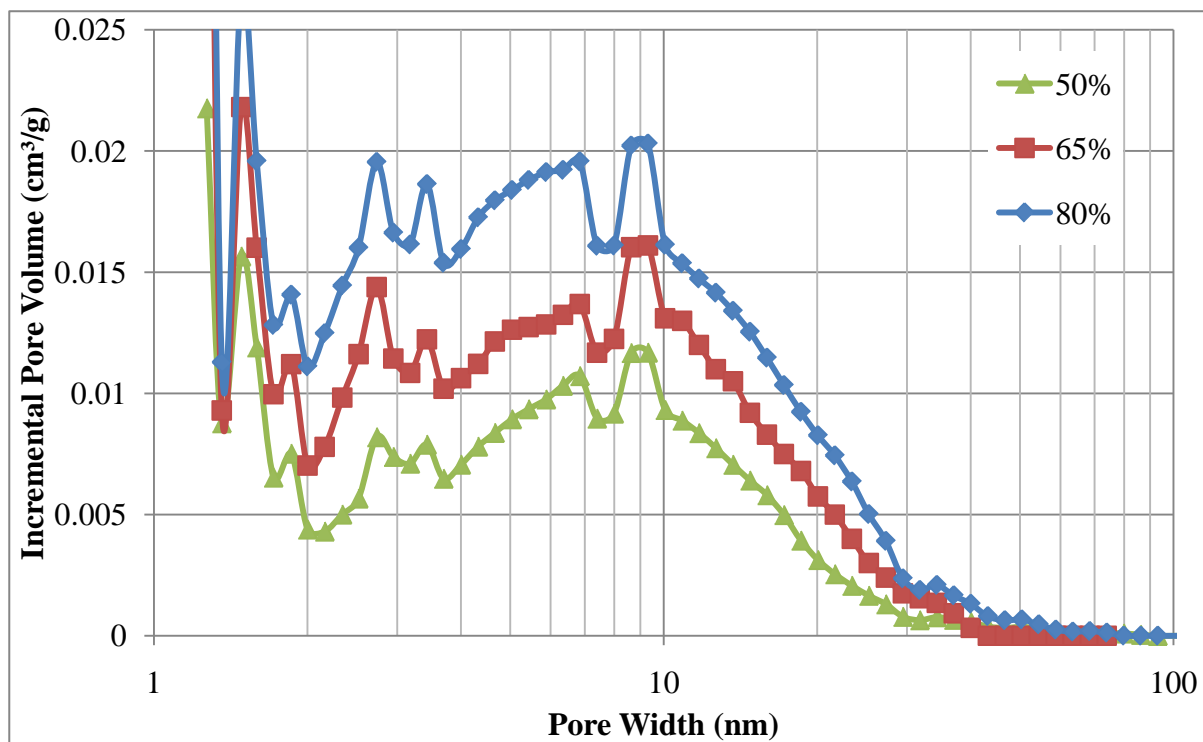


Figure 4.12: Effect of nominal crosslinking degree on poly(styrene-divinylbenzene) adsorbents utilising adsorbents generated using toluene as porogen and assessed using nitrogen gas adsorption.

Table 4.4: Nitrogen porosimetry results for polymer adsorbents, refer to Table 4.1 for compositional information.

Identifier	BET Surface Area (m ² /g)	Total Pore Volume (cm ³ /g)	DFT analysis			
			Surface area (m ² /g)		Pore Volume (cm ³ /g)	
			2-10 nm	10+ nm	2-10 nm	10+ nm
PSDVB1:1TolUn9:1	356	0.47	76	26	0.18	0.22
PSDVB1:1TolUn9:4	397	0.72	68	45	0.15	0.46
PSDVB3:5TolUn1:0	348	0.35	80	9.2	0.18	0.07
PSDVB3:5TolNap5:2	412	0.34	88	4.4	0.18	0.03
PSDVB0:1TolUn1:0	764	0.73	179	18.3	0.38	0.14
PSDVB3:13TolUn1:0	628	0.67	124	18.1	0.26	0.10
PSDVB3:5TolUn1:0P2	518	0.48	109	11.9	0.23	0.10
PSDVB0:1TolNap5:2	636	0.61	173	13.7	0.37	0.06

When assessing the effect of crosslinking degree we can look back to literature and compare the surface area values gained for similar materials Durie *et al* (2002) worked with poly(styrene-divinylbenzene) copolymers and using toluene as a porogen with 50% of the polymerisation mixture being porogen, this matches the conditions for this study. Table 4.5 shows a comparison between the results published here and those of Durie *et al* (2002) we can see that the figures are of similar magnitude with the 50% nominal crosslinking degree having the greatest disparity while at 80% the values are almost identical.

Table 4.5: Comparison of BET surface area for poly(styrene-divinylbenzene) adsorbents with varying nominal crosslinking degree and values obtained for similar materials reported by Durie *et al* (2002).

Nominal degree of Crosslinking	BET Surface Area (m ² /g)	BET Surface Area (m ² /g) (Durie <i>et al</i>)
50%	348	497
65%	628	562*
80%	764	756

*Durie *et al* (2002) material degree of crosslinking only 60%

In terms of the research problem presented here we see that pore size distributions, total pore volumes and surface areas can be varied considerably by the influence of a few parameters the most major influence is clearly the composition of the porogens and through this pore cut off can be controlled. Equally monomer variations as displayed by crosslinking degree have a large impact on volume of pores within a particular distribution. With the options available the generation of a material with the required properties for blood purification seems reasonable.

Droplet Size

With the membrane emulsion generation technology being utilised it is important to know if changing the droplet size has any effect on the final polymer's internal pore distribution to verify this PSDVB3:5ToIUn1:0 was produced in two distinct size fractions with median diameters of 37 and 120 μm these were compared via gas adsorption (Figure 4.13) as shown there are small differences in the pore volume distributions however these are more likely batch to batch variation rather than any effect caused by the droplet size.

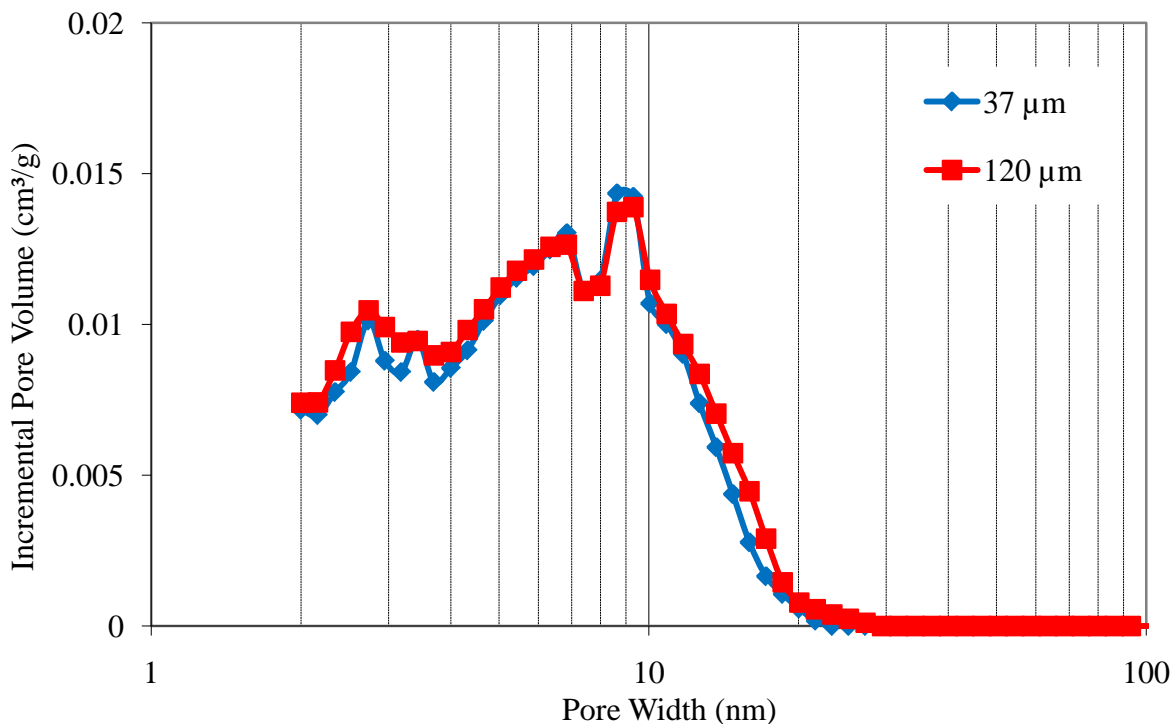


Figure 4.13: Comparison of pore volume size distributions using nitrogen gas adsorption for two identically specified polymer adsorbents of differing particle size

The fact that particle size has little to no effect on the generation of porous structure is of great importance to the overall problem being researched. If particle size had a significant effect on pore structure then assessing the pore structure of small particles using for example ISEC would be of no use if particles of significantly larger size were required for the final product. As we have shown there to be no effect of particle size on generated pore structure this concern can have been eliminated.

4.5 Influence of Swelling on Pore Structure

4.5.1 Inverse Size Exclusion Chromatography

Validating Inverse Size Exclusion Chromatography Methodology – Superdex 75

As a method for determining swollen state internal pore volume distributions inverse size exclusion chromatography (ISEC) appears to be a suitable method. To confirm that the processes and procedures developed for the packing of columns and running appropriate standards were suitable a standard material Superdex 75 was purchased and subjected to testing, Superdex 75 as discussed in Chapter 3 has a manufacturer's specification of a particle size of 22-45 μm and a pore structure suitable to separate dextrans in the range 3 – 70 kDa.

Initial testing on the particle size was carried out using the Coulter LS130 and the results can be seen in Figure 4.14 while the majority of the particles (83%) by volume are in the quoted size range 20 – 50 μm there is also a large number of smaller sub 10 μm particles present approximately 17% of the total volume.

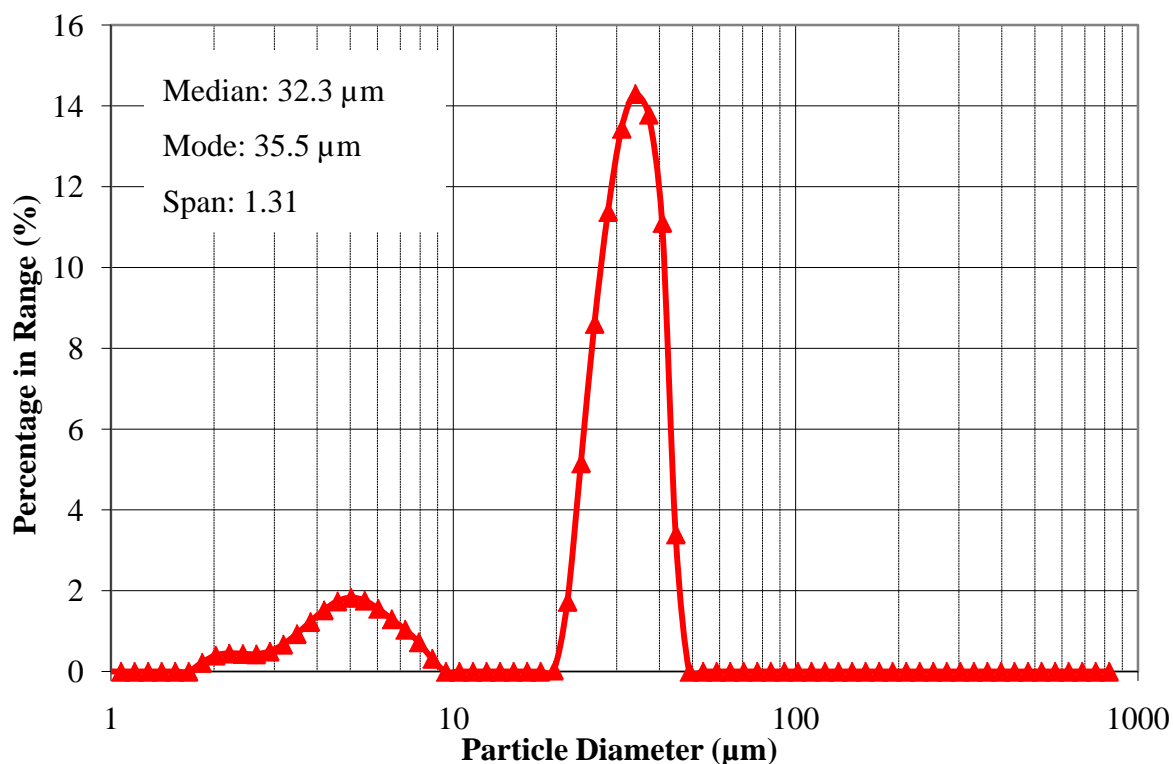


Figure 4.14: Particle size distribution for Superdex 75 Prep Grade.

The Superdex was then packed into two stainless steel liquid chromatography columns of differing diameter, 4.6mm and 10mm. Using ultra pure water as the eluent and a series of dextran standards (see Table 3.1) chromatograms were generated for each column, see Figures 4.15 and 4.16. On casual inspection we can see that the two columns perform similarly as you would expect from the identical packing material. When calculating the normalised cumulative pore distribution (pore size calculated as 2.5 times the viscosity diameter of the probe) (Figure 4.17) we can see that while not identical the two distributions are very close differing only a significant amount on one point. Plotting the dextran molecular weight against the solute elution volume generates a calibration curve (which

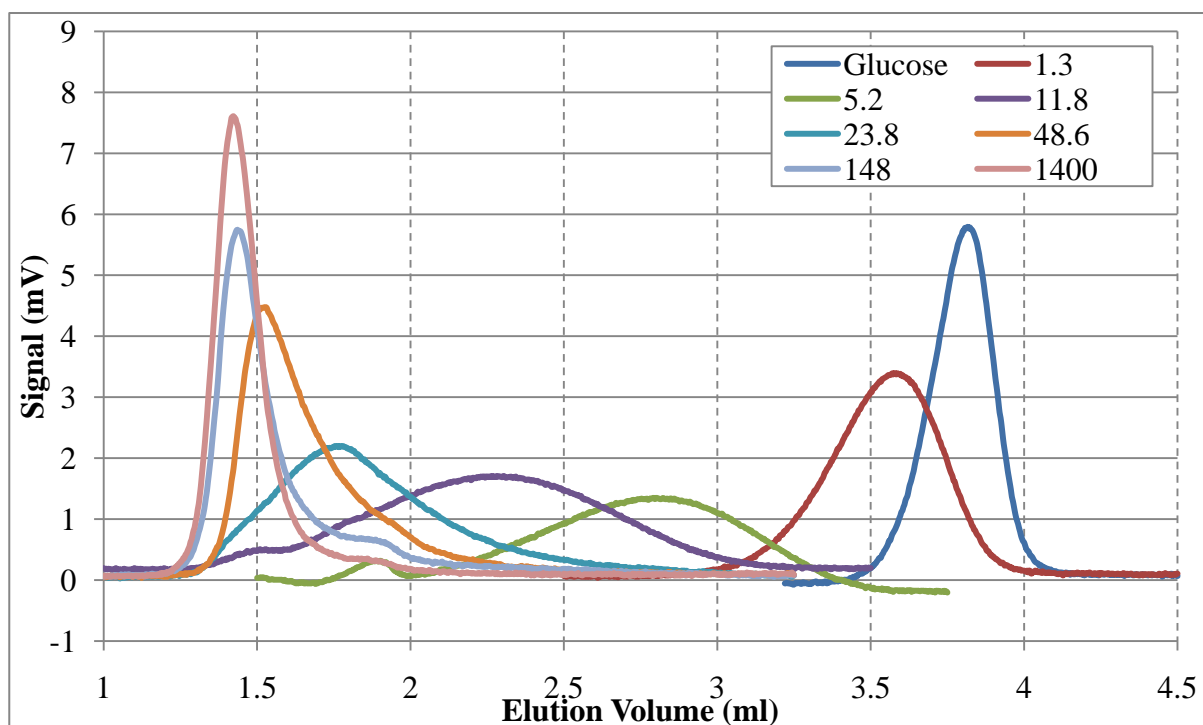


Figure 4.15: ISEC chromatogram for Superdex 75 packed in a 4.6 mm diameter column 250 mm in length, ultra pure water as the eluent, flow rate of 0.1 ml/min, probing with dextran standards size 180 Da – 1.4 MDa.

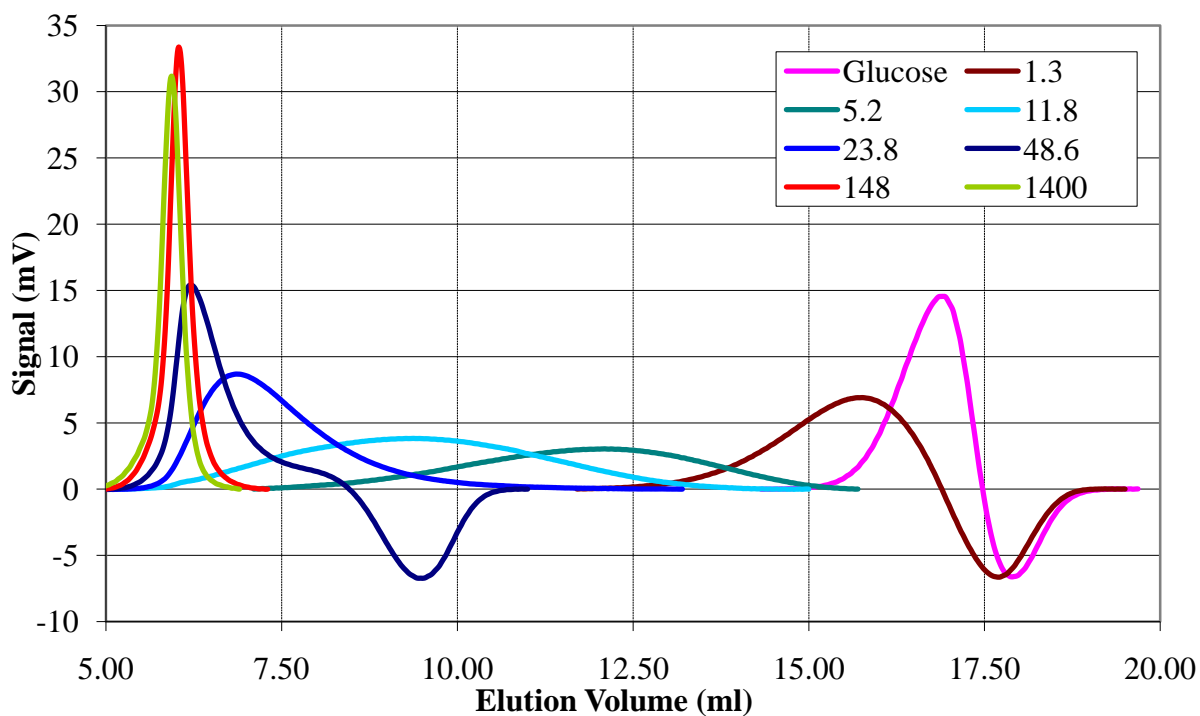


Figure 4.16: ISEC chromatogram for Superdex 75 packed in a 10 mm diameter column 250 mm in length, ultra pure water as the eluent, flow rate of 0.1 ml/min, probing with dextran standards size 180 Da – 1.4 MDa.

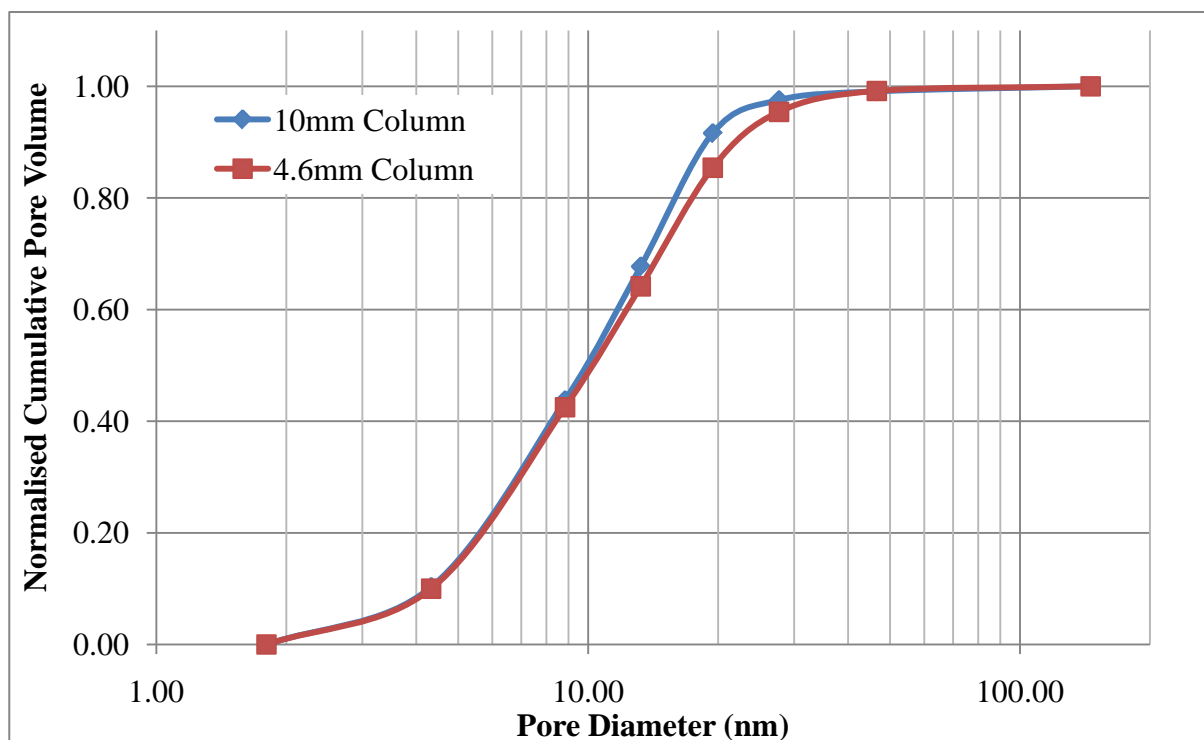


Figure 4.17: Normalised cumulative pore volume distributions for Superdex 75 comparing column size

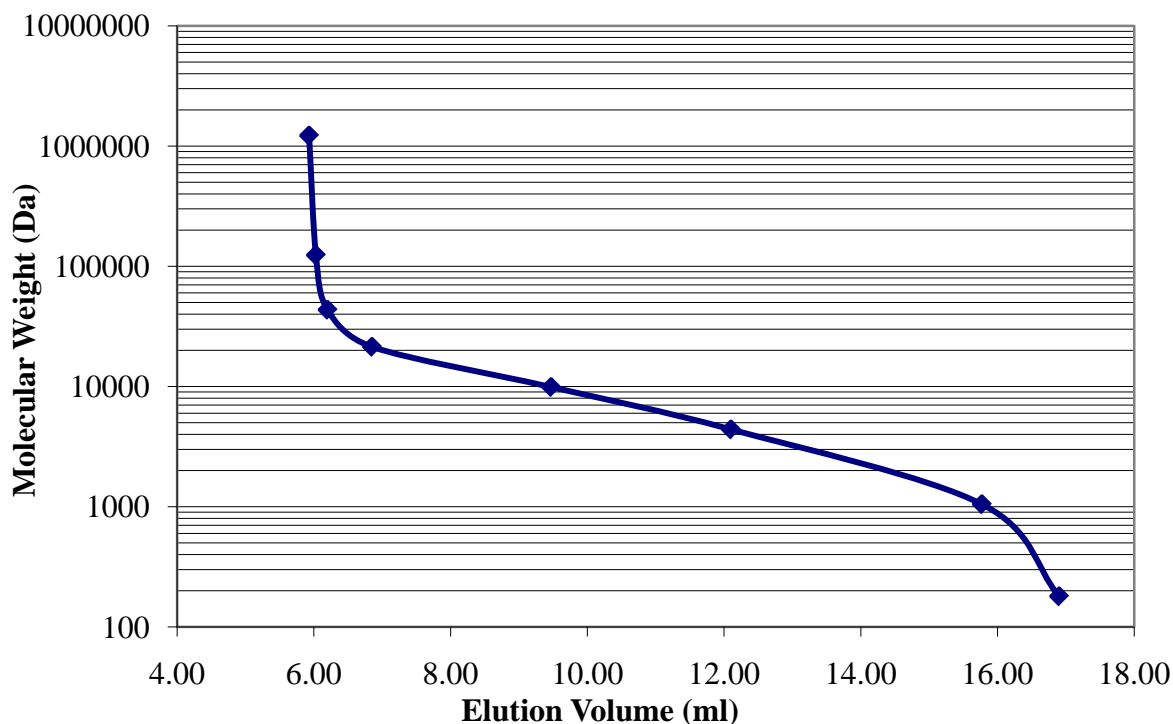


Figure 4.18: Dextran calibration curve for Superdex 75 (10mm diameter column)

could be used in traditional size exclusion chromatography for determining the molecular weight of an unknown sample) the linear section shows the area where separation can occur and this matches well with the manufactures claims for separation of 500 – 30000 Da while there are no standards exactly matching these values the linear section covers the majority of this area.

4.5.2 Protein Size Analysis – Superdex 75

With the usability of the columns now confirmed marker proteins albumin and lysozyme were injected using a phosphate buffer pH 7.2 with 0.1% SDS this resulted in elution volumes of 7.2 ml for albumin and 11.2 ml for lysozyme, using the calibration curve (Figure 4.18) we can determine the dextran equivalent molecular weight for each protein and subsequently the viscosity radius of the proteins. This is tabulated in Table 4.6

Table 4.6: Determination of lysozyme and human serum albumin viscosity radii by use of size exclusion chromatography, Superdex 75 and dextran standards

Protein	Elution Volume (ml)	Equivalent Dextran Molecular Weight (Da)	Viscosity Radius (nm) ^a
Albumin	7.20	20484	3.80
Lysozyme	11.20	5310	1.94

a – Calculated using values from Hagel, 1988

Knowing the size of the protein that is to be excluded (in this case human serum albumin) is very important for this research as it identifies a target cut off for the internal pore structure of the designed adsorbent. The value obtained for HSA from this size exclusion work (Table 4.6) was a viscosity radius of 3.8nm, referring to the literature Glynne *et al* (2002) report this at 3.6nm. These values are obviously within experimental error and add confidence to the method of analysis. Knowing the size of lysozyme is also important as it will be used to determine potential capacity of any adsorbent in this situation the fraction of the pore structure which is accessible to the protein will be of importance in determining the adsorbents effectiveness.

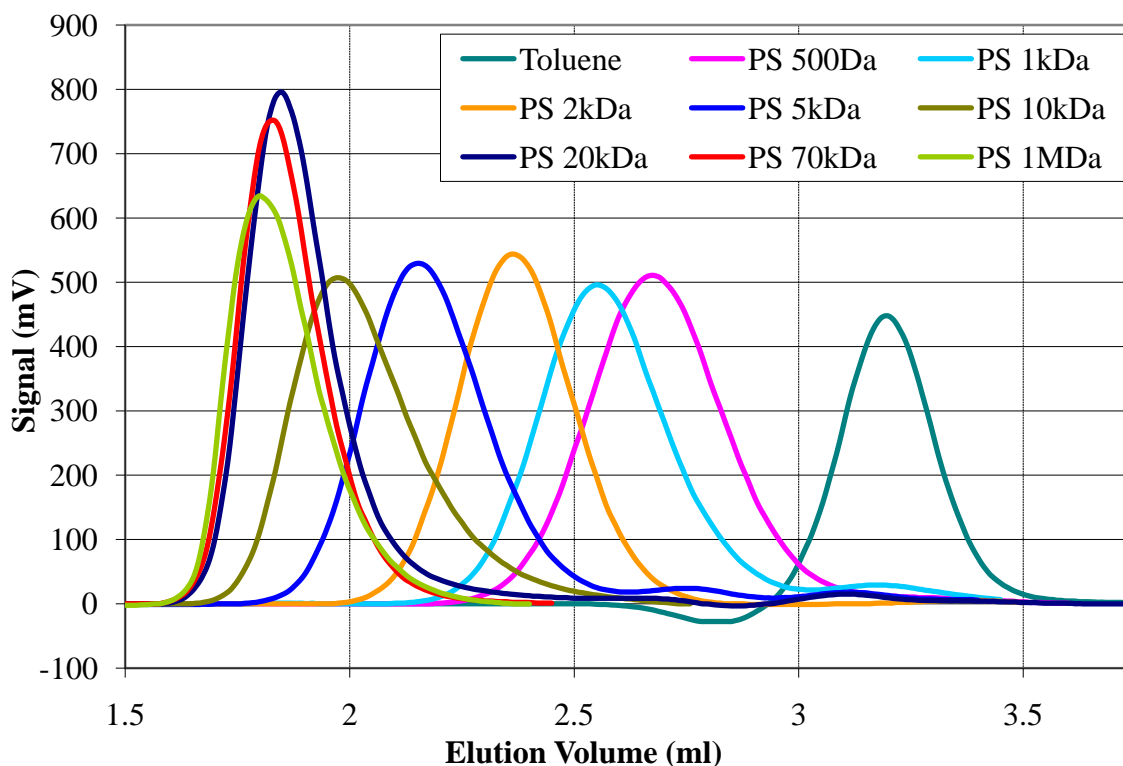
4.5.3 Inverse Size Exclusion Chromatography of Polystyrene Adsorbents

With the size of the protein to be excluded identified and verified through size exclusion chromatography sample adsorbents can be tested using tetrahydrofuran (THF) and polystyrene standards. While working in a aqueous solution would have been preferable the stipulations of ISEC mean that this is impossible.

Table 4.7: Inverse size exclusion chromatography adsorbents particle size distribution data

Adsorbent	Particle Diameter (μm)		Span
	Median	Mode	
PSDVB1:1ToIUn1:0	36.62	38.91	0.876
PSDVB1:1ToIUn9:1	29.64	35.52	1.276
PSDVB3:5ToINap5:2	28.16	29.61	1.529

Three adsorbents were generated using varying combinations of porogens and monomers, the Micropore Technologies stirred cell was used to generate particles as small as possible to improve the resolution of the ISEC. The pertinent particle size data can be seen in Table 4.7

**Figure 4.19:** ISEC chromatogram for adsorbent PSDVB3:5ToIUn1:0, polystyrene standards in THF

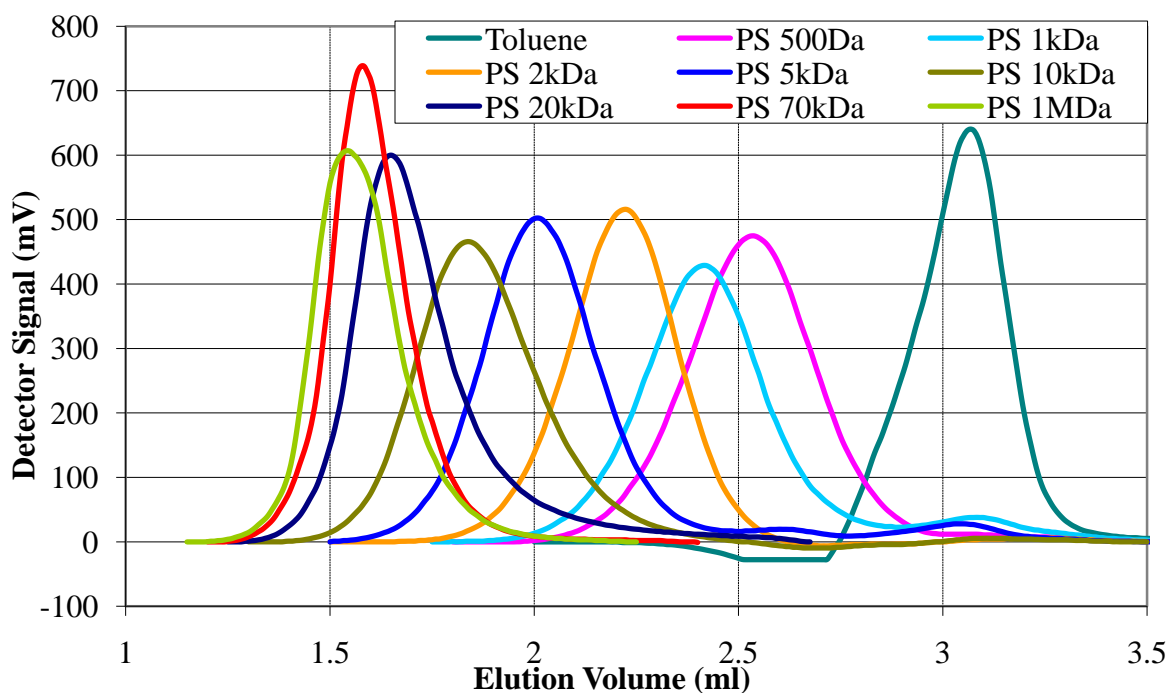


Figure 4.20: ISEC chromatogram for adsorbent PSDVB1:1TolUn9:1, polystyrene standards in THF

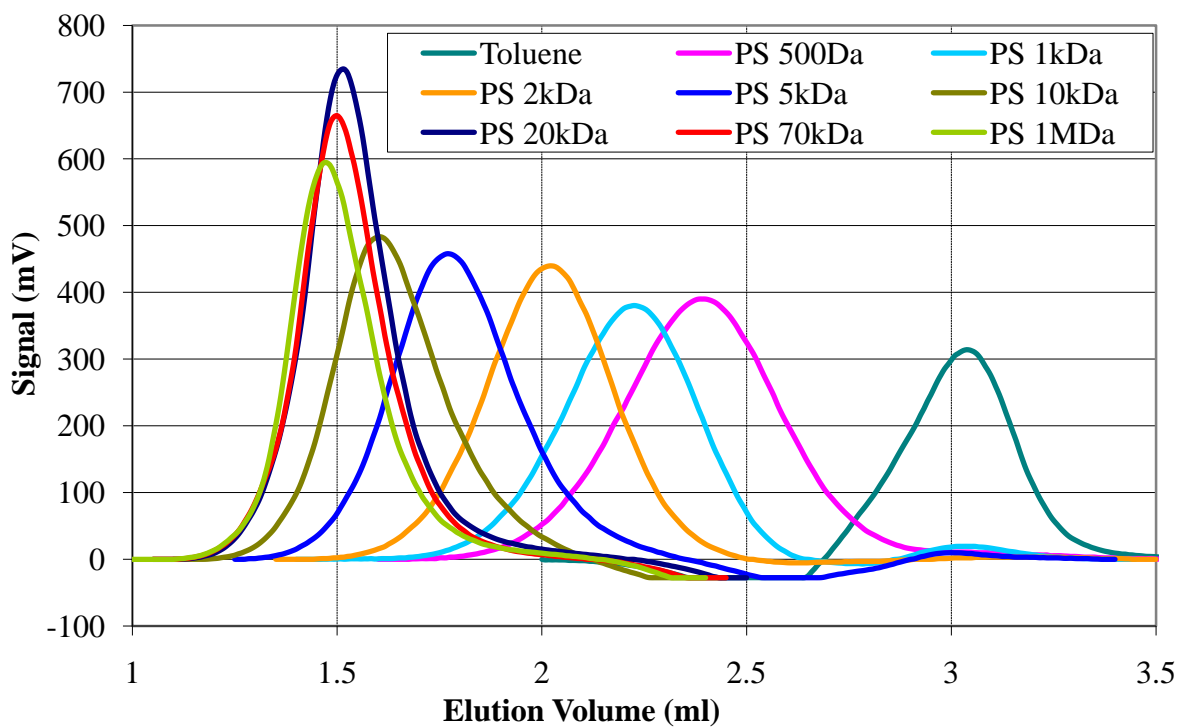


Figure 4.21: ISEC chromatogram for adsorbent PSDVB3:5TolNap5:2, polystyrene standards in THF

PVA concentrations were increased to 4.5% when generating these droplets in an attempt to generate the smallest possible particles at the expense of a monosize particle distribution (as discussed earlier in section 4.2). The particles were packed into 4.6 mm diameter columns and probed using polystyrene probes as reported in Table 3.2.

Starting with the chromatogram for PSDVB3:5Tolun1:0 (Figure 4.19) we observe the successful separation of polystyrene standards up to 10 kDa however the three largest standards while separated were very close together meaning separation at those sizes was minimal. Changing the porogen mixture to include undecane and lowering the crosslinking degree (PSDVB1:1TolUn9:1) from the nitrogen porosimetry data (Figure 4.10) we would expect greater separation of the larger standards. As expected the chromatogram Figure 4.20 shows good separation for standards up to 20 kDa with only the two largest standards being less easily separated. Moving onto the chromatogram for PSDVB3:5TolNap5:2 (Figure 4.21) we see that again the standards up to 10 kDa have been well separated and while the largest standards are very bunched together showing limited access to the internal pore structure of the substrate.

Converting the chromatograms into calibration curves to compare elution volume against polystyrene molecular weight (Figure 4.22) the gradient between two points determines the effectiveness of the material to separate the standards with greater gradients showing less separation. It is important to note that comparing multiple columns looking solely at elution volume is of little importance as this is affected by column packing and pore volume. As previously stated all three tested materials show good separation for the standards up to 10 kDa we see that the gradient increases faster between 10 kDa and 20 kDa for PSDVB3:5TolUn1:0 and PSDVB3:5TolNap5:2 than PSDVB1:1TolUn9:1 showing as expected the wider distribution and larger

pores in this material. Calculating K_d for each material and then converting this into a value of accessible pore volume (i.e. the volume of pores to which a probe of a particular size has access) we come to figure 4.23 this more clearly shows the differences in pore cut off than the chromatograms and calibration curves. The larger pore structure of PSDVB1:1ToIUn9:1 is clearly highlighted with ~6% of the pore structure being accessible to probes >10 nm while the other materials had ~2% available to probes of the same size. PSDVB3:5ToINap5:2 also shows a tighter distribution than that of PSDVB3:5ToIUn1:0.

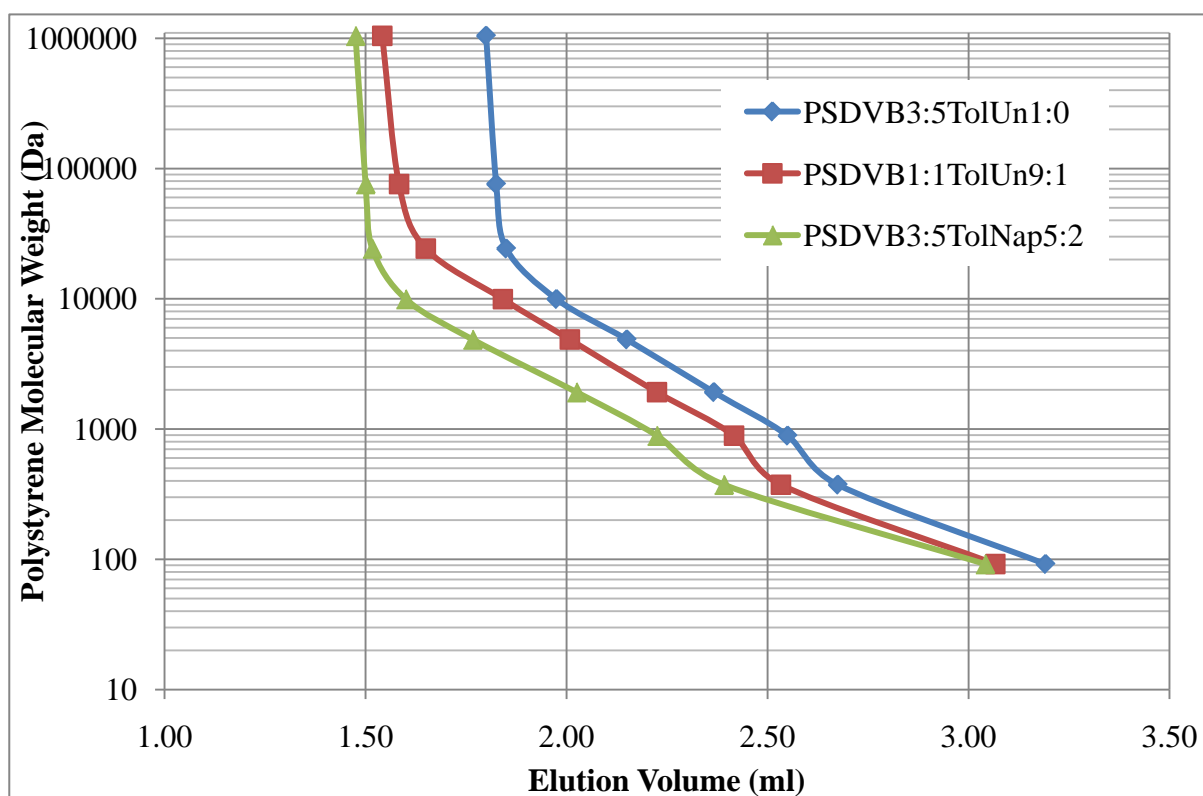


Figure 4.22: Molecular weight calibration curves for polystyrene in THF for three polymer adsorbents

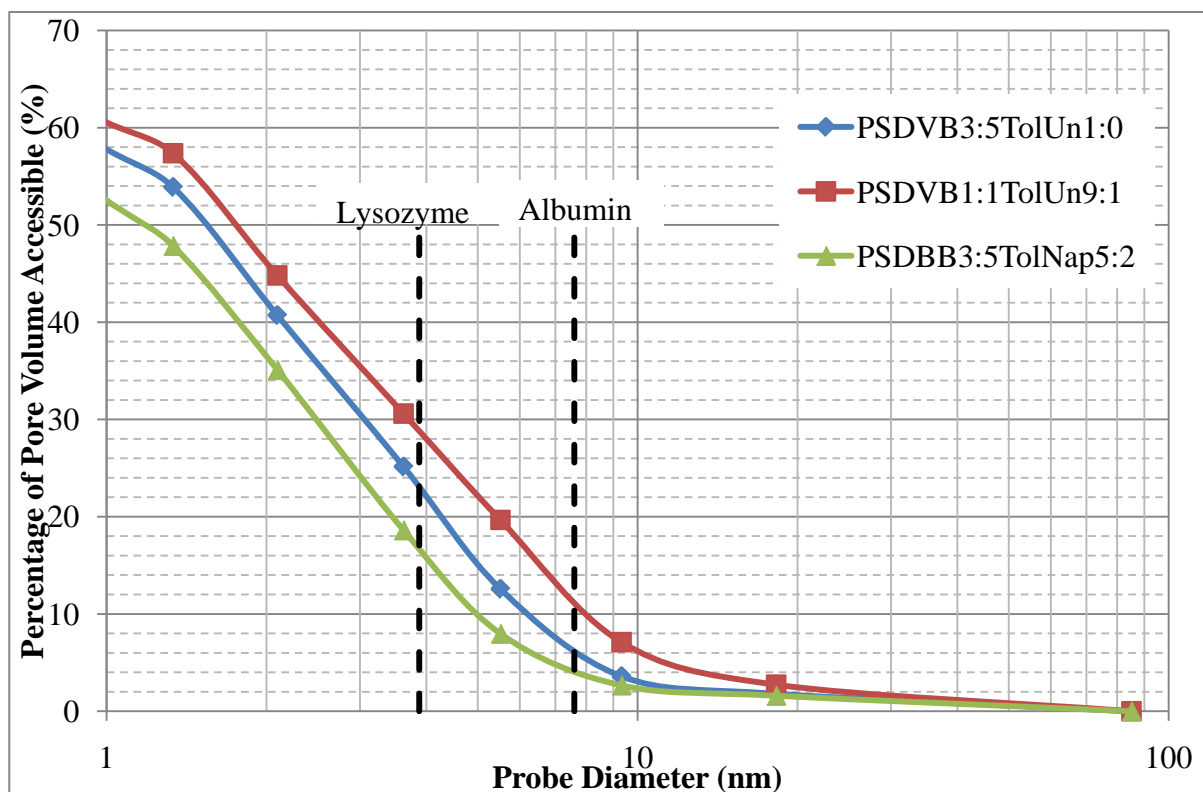


Figure 4.23: Percentage accessible pore volume distributions for three polymer adsorbents generated from ISEC with polystyrene standards in THF, with indicators for the size of albumin and lysozyme.

From the work using Superdex we have estimated the diameters of both albumin and lysozyme to be 7.8 and 3.86 nm respectively these are marked on Figure 4.23 from this we can determine that for the greatest exclusion of albumin from the pore structure PSDVB3:5TolNap5:2 is the superior material with only 4% of its pore volume accessible while PSDVB1:1TolUn9:1 has 11% of its pore volume accessible.

In terms of the research problem the ability to assess the adsorbents in a swollen state is important. Comparing the three materials we clearly see that by altering the porogen and crosslinking degree we affect the porous structure as expected from the nitrogen porosimetry data. By utilising this method we can confirm that PSDVB3:5TolNap5:2 appears to be the best

adsorbent for the size exclusion of human serum albumin as it possesses the smallest percentage of its pore volume accessible to a protein of albumins size.

4.5.4 Vacuum Drying of Polymer Adsorbents

While ISEC provides a good picture of swollen pore distributions it is limited by the constraints of the required solvent, in the case of polystyrene adsorbents THF. To investigate the effect of swelling the material in different solvents and provide insight into how the pore structure could be expected to change a process of swelling the adsorbent in a number of different solvents and then drying under vacuum at low temperatures, essentially fixing the pore structure. Samples prepared in this manner could then be subjected to gas adsorption to determine the pore size distributions.

4.5.5 Drying at Ambient Temperature

To test the effect different solvents have on the pore structure PSDVB3:5TolNap5:2 was swollen in three different solvents toluene, acetone and methanol. Each was then dried under vacuum and assessed for pore size distribution. Table 4.8 shows the results with a clear increase in pore volume (15%) and surface area (16%) as the swelling solvent has a lower affinity towards the polymer (methanol having the lowest affinity and toluene the highest). Interestingly while the pore size distributions vary in total pore volume when the cumulative distributions are normalised (Figure 4.24) the three samples overlay each other showing that while the pore volumes may have changed the overall distribution of that pore volume remains the same.

Table 4.8: Nitrogen gas adsorption porosity data for a poly(styrene-divinylbenzene) adsorbent (PSDVB3:5TolNap5:2) dried under vacuum at ambient temperature or freeze dried at -20°C from different solvents.

Solvent Sample Pre-swollen In	BET Surface Area (m ² /g)	Total Pore Volume (cm ³ /g)	DFT analysis			
			Surface area (m ² /g)		Pore Volume (cm ³ /g)	
			2-10 nm	10+ nm	2-10 nm	10+ nm
Toluene	488	0.40	104	4.5	0.22	0.03
Acetone	528	0.43	115	4.6	0.24	0.03
Methanol	567	0.46	126	4.8	0.26	0.03
Benzene*	510	0.37	97	3.8	0.19	0.04
Cyclohexane*	539	0.41	113	4.2	0.22	0.03

*Sample freeze dried

4.5.6 Freeze Drying of Polymer Adsorbents

Freeze drying the sample will theoretically reduce any solvent interactions with the polymer matrix during the drying process. Due to the requirements of freeze drying benzene and cyclohexane were chosen as suitable solvents, due to their relatively high freezing points and the ease by which they are sublimed. Table 4.8 shows the pore distribution results and with total pore volumes and surface areas remain comparable between comparative samples benzene/toluene and cyclohexane/acetone. Figure 4.25 shows the normalised cumulative pore volume distributions for the freeze dried samples and toluene (dried at ambient temperature) the two freeze dried while not overlaying exactly are still in close agreement, the toluene sample dried at ambient temperatures it slightly further away highlighting the effects of solvent interaction during the drying process it is notable however, that the maximum pore size remains unchanged at ~20 nm

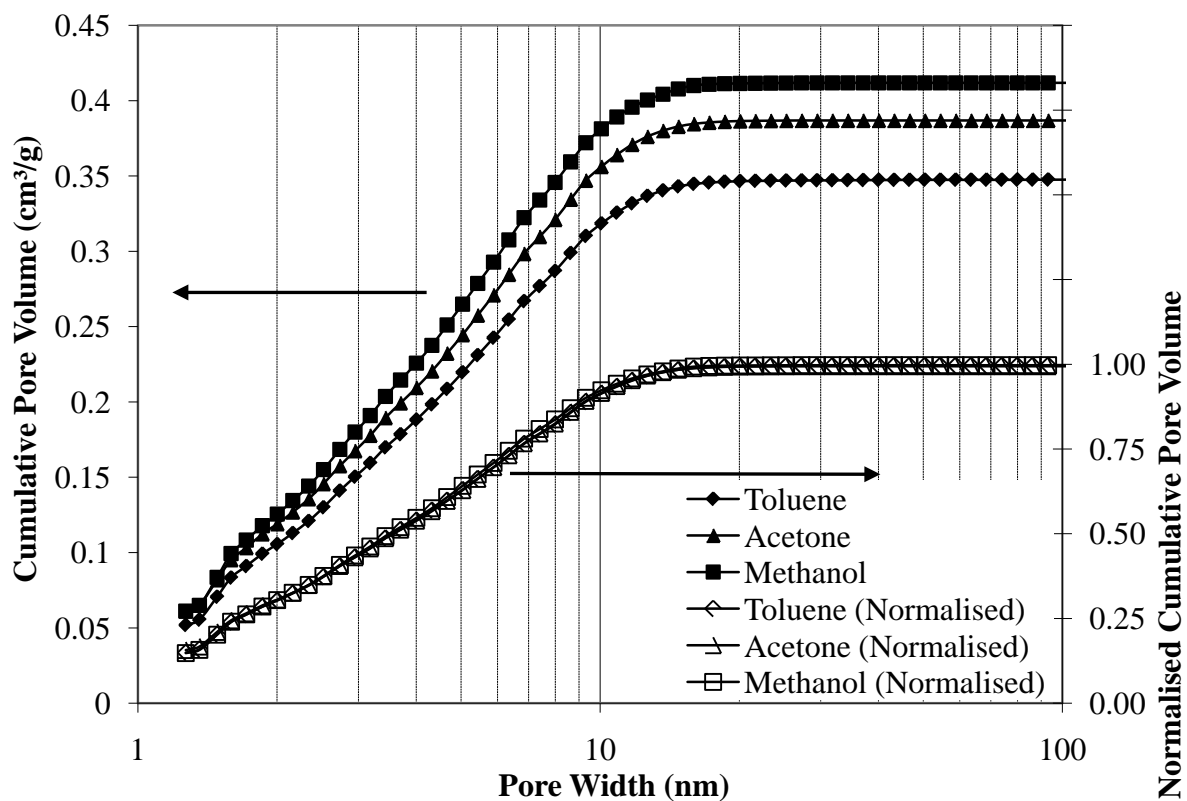


Figure 4.24: Nitrogen gas adsorption cumulative pore volume distributions for PSDVB3:5TolNap5:2 dried under vacuum from different solvents, and normalised cumulative pore volume distributions for the same samples. Arrows indicate which axis for each set of results.

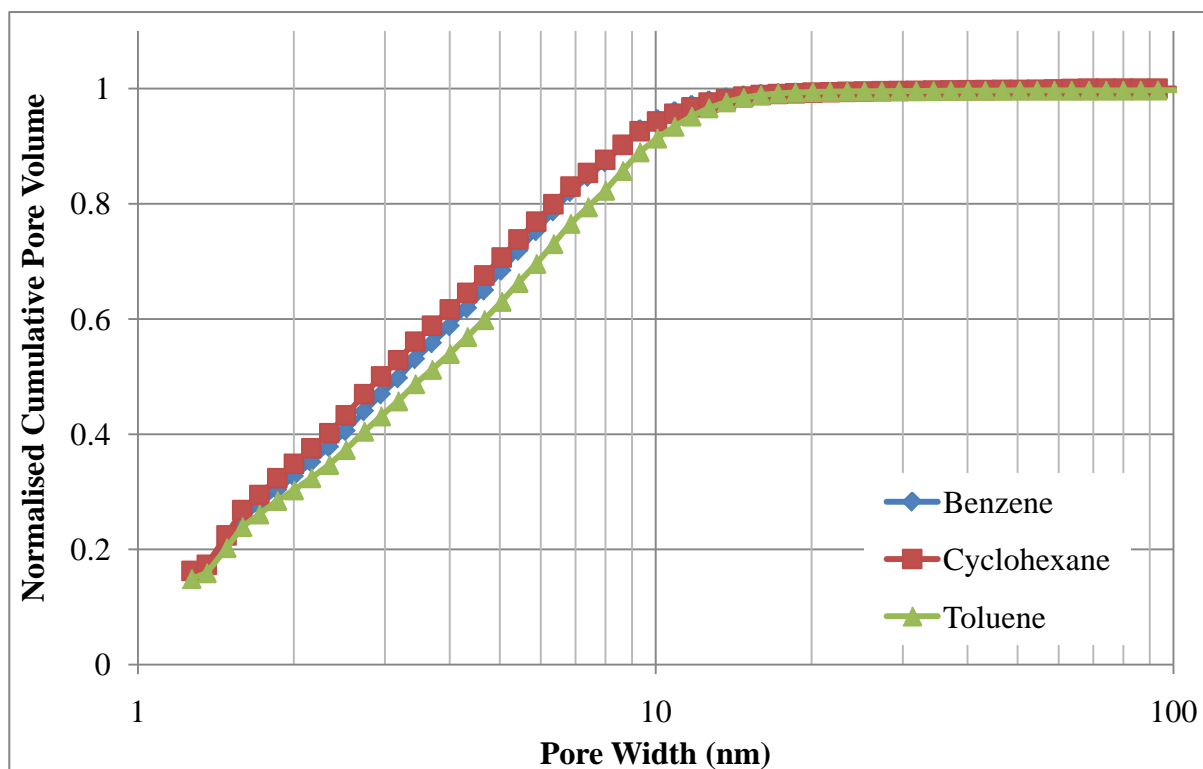


Figure 4.25: Normalised nitrogen gas adsorption cumulative pore volume distributions for PSDVB3:5ToINap5:2 freeze dried from benzene and cyclohexane with toluene thermally dried as a comparison.

From this we can expect that while swollen in THF during ISEC the pore volume will be similar to that as reported when dried from toluene, and even when utilised in an aqueous system the pore distribution will remain relatively unchanged maintaining the same pore cut off.

This series of analyses comparing thermally dried, freeze dried and swollen samples has shown that while swelling in different solvents will impact upon the porous structure of an adsorbent pore cut off remains unchanged, this means that analysis of future adsorbents could be made by any of the above outlined methods and reasonable assumptions as to the performance in terms of protein exclusion could be made.

4.6 Choosing the most suitable adsorbent

Having determined that a polystyrene-divinylbenzene adsorbent generated using a porogen mixture of toluene and naphthalene will generate the lowest pore size cut off as determined by both gas adsorption and ISEC it would seem sensible to attempt to maximise surface area without compromising pore cut off. Figure 4.26 compares incremental pore volume distributions showing that by increasing crosslinking degree to 80% from 50% we can achieve a 97% increase in surface area in the 2 – 10 nm range (Table 4.4) while not increasing maximum pore size.

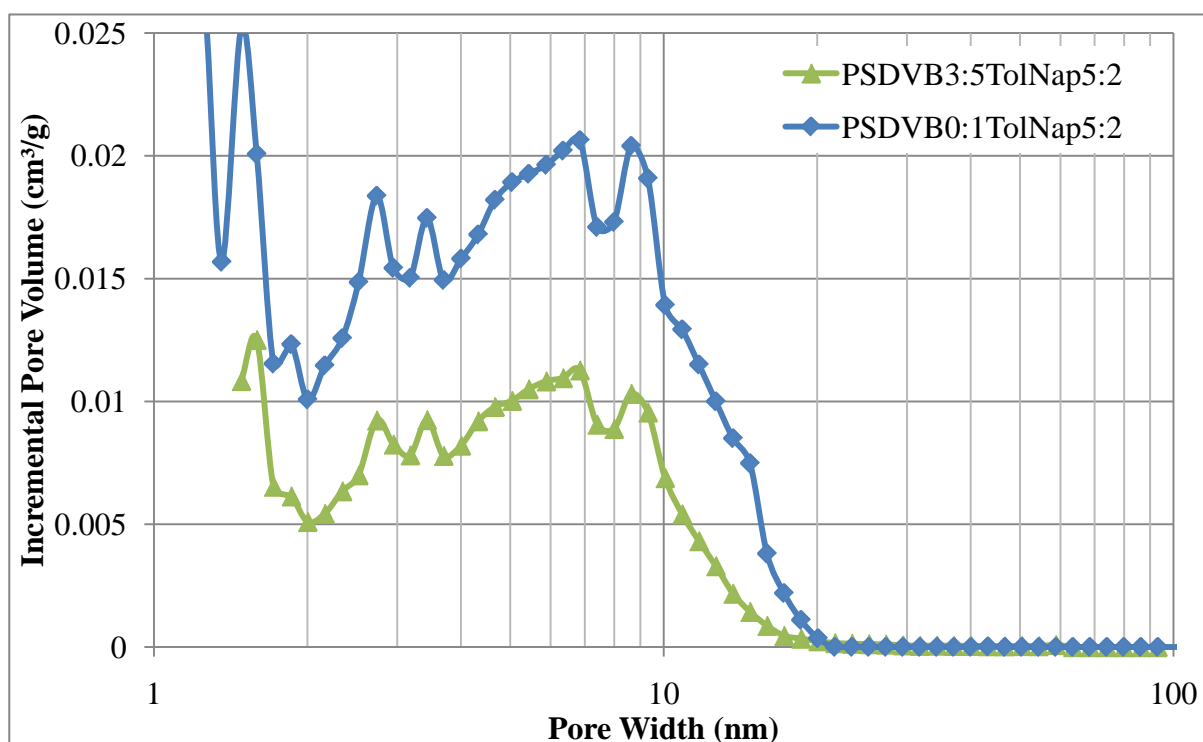


Figure 4.26: Comparison between 50% and 80% crosslinking for an adsorbent using toluene and naphthalene for a porogen.

4.7 Conclusions

A polymer adsorbent with a tailored pore structure to exclude albumin can be manufactured with an optimised pore cut off and surface area for the removal

of middle molecular weight molecules. The two major factors affecting the pore size distribution of the adsorbent are the composition of the diluents/porogen and the crosslinking degree. For the exclusion of albumin the pore size cut off was required to be at as low a level as possible from the experimental work a combination of toluene and naphthalene (5:2 by weight) provided the tightest pore distribution at ~20 nm. Crosslinking degree increases total surface area and pore volume significantly while leaving maximum pore size largely unchanged. The other parameters which were investigated the monomer to porogen ratio and particle size had differing results. Increasing the porogen to monomer ratio increased pore volume and surface area in the 2-10 nm range by 28% and 35% respectively however maximum pore size also increased significantly from 30 nm to 50nm this makes increasing the porogen to monomer ratio less appealing in the context of this work. Particle size had little to no effect on the generation of pore structure and so is of no concern when considering this aspect of the project.

Particle size control through use of the Micropore Technologies stirred cell was excellent, allowing droplets ranging from 50 – 200 μm to be generated with good selectivity. Pushing the technology to its limits droplets of 30 μm were generated however the particle size distributions suffered as a result. From the two parameters investigated stabiliser (PVA) concentration and stirrer speed increasing stirrer speed seems to be the optimum method for generating smaller droplets with tight droplet distributions. Increasing PVA concentrations past 2% has a detrimental effect on droplet size distribution however it is the only method available to generate very small droplets <50 μm .

For the analysis of pore structure it is important to remember that changes occur with the solvent used. However, as has been shown through the use of vacuum drying the polymer samples maximum pore size and the overall

distribution of pores do not vary significantly. The pore volume and surface area however can alter significantly however for comparative purposes a choice of a single solvent and drying method would be required.. As pore cut off and distribution is largely unaffected by solvent ISEC can be used to determine pore accessibility to molecules of a particular size in the swollen state is a valuable method of analysis, this is enhanced by the relatively fast analysis times that can be achieved compared to the nitrogen porosimetry alternative.

5 *In Vitro* Evaluation of Size Exclusion Principle: Adsorption Studies

In vitro evaluation of the adsorbents was undertaken to verify whether the tailored pore structure of the synthesised adsorbents was suitable in: (i) removing surrogate middle molecules (adsorption capacity); (ii) preventing access to human serum albumin (size exclusion) and (iii) effective in providing rapid adsorption rates for solutes able to access the internal pore structure (kinetics).

5.1 Analysis of Protein Uptake Data

Adsorption data for single solute buffered systems was obtained for PSDVB3:5ToINap5:2, PSDVB0:1ToINap5:2 and XAD4. The objective of the tailored pore structure was to minimise removal of human serum albumin (MW 69kDa, size ~7nm) by preventing access to the internal pore structure of the adsorbent particles by size exclusion. Lysozyme (hen egg white, MW 14.4 kDa, size ~4nm) was selected as a low cost surrogate middle molecular weight protein.

Table 5.1: Lysozyme and human serum albumin (HSA) total adsorption capacity q^* and Γ values for selected adsorbent materials.

Material	Lysozyme		
	q^* (mg g ⁻¹)	Γ^a (mg m ⁻²)	Area accessible (m ² g ⁻¹)
XAD4	330 ± 60	2.8	120
PSDVB3:5TolNap5:2	59 ± 7	2.7	22
PSDVB0:1TolNap5:2	572		
Material	Human Serum Albumin		
	q^* (mg g ⁻¹)	Γ^b (mg m ⁻²)	Area accessible (m ² g ⁻¹)
XAD4	95 ± 5	2.4	40
PSDVB3:5TolNap5:2	2 ± 1	2.4	0.9
PSDVB0:1TolNap5:2	51		

^a Approximate footprint of lysozyme, 9 nm²

^b Approximate footprint of albumin, 49 nm²

Table 5.1 shows the q^* (saturation capacity) values for the three materials for both HSA and lysozyme. The saturation capacity (q^*) values for lysozyme were 59 mg g⁻¹, 572 mg g⁻¹ and 330 mg g⁻¹ for PSDVB3:5TolNap5:2, PSDVB0:1TolNap5:2 and XAD4 respectively. The saturation capacity (q^*) values for HSA were 2 mg g⁻¹, 51 mg g⁻¹ and 95 mg g⁻¹ for PSDVB3:5TolNap5:2, PSDVB0:1TolNap5:2 and XAD4 respectively. The saturation capacity values (q^*) were found to be concentration-independent (irreversible adsorption). This is fairly common for single protein adsorption studies, where surface coverage has been found in many cases to equate to quasi-monolayer adsorption (Ramsden, 1997 and 2002). The protein saturation capacity values were found to correlate with the surface area accessible to lysozyme (22 m² g⁻¹) and albumin (0.9 m² g⁻¹) for PSDVB3:5TolNap5:2 (nitrogen porosimetry data) determined on the basis of

size exclusion from pores smaller than 6 nm for lysozyme and 14 nm from albumin. This corresponds to surface coverage Γ of 2.7 mg m⁻² for lysozyme and 2.4 mg m⁻² for albumin. Analysis of protein saturation data for XAD4 using a similar basis as for PSDVB3:5ToINap5:2 yields the surface areas accessible to lysozyme (120 m² g⁻¹) and albumin (40 m² g⁻¹). This corresponds to $\Gamma = 2.8$ mg m⁻² for lysozyme and 2.4 mg m⁻² for albumin. These values are comparable to jammed, randomly adsorbed monolayer coverages reported previously (Ball and Ramsden, 2000; Kurrat *et al*, 1997).

XAD4 showed considerable adsorption of the smaller protein lysozyme however, a significant quantity of HSA was also adsorbed. PSDVB3:5ToINap5:2 with its tight pore structure excluded the vast majority of HSA in solution resulting in a maximum capacity of only 2mg/g. This data supports those obtained from the inverse size exclusion chromatography work (see section 4.5.3). However, PSDVB3:5ToINap5:2 displayed a significantly reduced adsorption capacity for lysozyme (59 mg/g) thereby requiring greater amounts of adsorbent to remove similar quantities of lysozyme from solution (~6 times the amount of adsorbent compared to XAD4). However, with ~6 times the adsorbent HSA removal would still be significantly less using the adsorbent PSDVB3:5ToINap5:2 resulting in 12 mg of HSA uptake for 330mg of lysozyme removed. Increasing the overall pore volume and surface area per gram of adsorbent while maintaining a similar pore distribution as PSDVB3:5ToINap5:2, PSDVB0:1ToINap5:2 showed an increase in HSA uptake but also a significant increase in the removal of lysozyme. From these findings PSDVB0:1ToINap5:2 would appear to balance the higher adsorption capacity requirement for lysozyme whilst minimising removal of HSA in significant quantities, comparing again to XAD4 to remove 330mg of lysozyme you would require 0.6g of PSDVB0:1ToINap5:2 which would remove 30mg of HSA.

Table 5.2: Mass of adsorbent required for the removal of 1g of lysozyme and the mass of the consequential removal of human serum albumin (HSA).

Adsorbent	Mass of adsorbent (g)	Mass of HSA removed (mg)
XAD4	3.03	288
PSDVB3:5ToINap5:2	16.95	34
PSDVB0:1ToINap5:2	1.75	89

Table 5.2 clearly shows how the three investigated materials compare to each other depending on the requirements for the final solution (for example pressure drop over the column, particle size, cost, maximum HSA removal) each of the materials has merits XAD4 is a well characterised and widely available adsorbent which could be purchased and then treated for use in haemoperfusion (surface treatments, cleaning and particle size grading) however the removal of large quantities of HSA would be a major disadvantage as would waste from grading the adsorbent for the desired particle size. PSDVB3:5ToINap5:2 would remove the least HSA but would have the largest cost and pressure drop due to the large quantity of adsorbent required, generating the material in house using the droplet generation methods covered in this work would ensure less waste from particle size grading. PSDVB0:1ToINap5:2 would appear to be the best choice with the least material required and in house production limiting wastage. The one down side would be HSA removal which is ~3 times that of PSDVB3:5ToINap5:2 if this would be a significant enough problem would require further research.

Comparing adsorption data for the materials above with those reported in literature is rather difficult as most relevant work uses adsorbents in column mode in contact with patient blood. Thus, reported clinical data in literature is for a more complex system which has not been investigated during the

present work. Davankov et al (2000) for example studied cleansing of blood using a hypercrosslinked polymer in a packed column over a 4 hour period. The adsorbent was shown to remove 95% of the β_2 -microglobulin (initial concentration 63.5 mg/l) and with it ~5% of all other proteins which were monitored (initial concentration 6.2 g/l). Thus a substantial quantity of other proteins including albumin were removed as well.

5.2 Single Solute *Batch Adsorption Dynamics*

In addition to total capacity data the kinetics of adsorption were investigated for XAD4 and PSDVB3:5ToINap5:2. As both adsorbents are based on poly(styrene-divinylbenzene) their affinities for the proteins are assumed to be similar leaving pore structure as the major variable. Nitrogen porosimetry data suggested that XAD4 with a more open mesoporous structure should display faster adsorption kinetics in comparison with PSDVB3:5ToINap5:2.

Dynamic adsorption experiments were carried out using 15g of material and a starting concentration of 100mg/l of lysozyme. The effect of diffusion path length was investigated by measuring protein adsorption rates for particles of different particle sizes. Figures 5.1 and 5.2 show the kinetics for XAD4 and PSDVB3:5ToINap5:2 respectively.

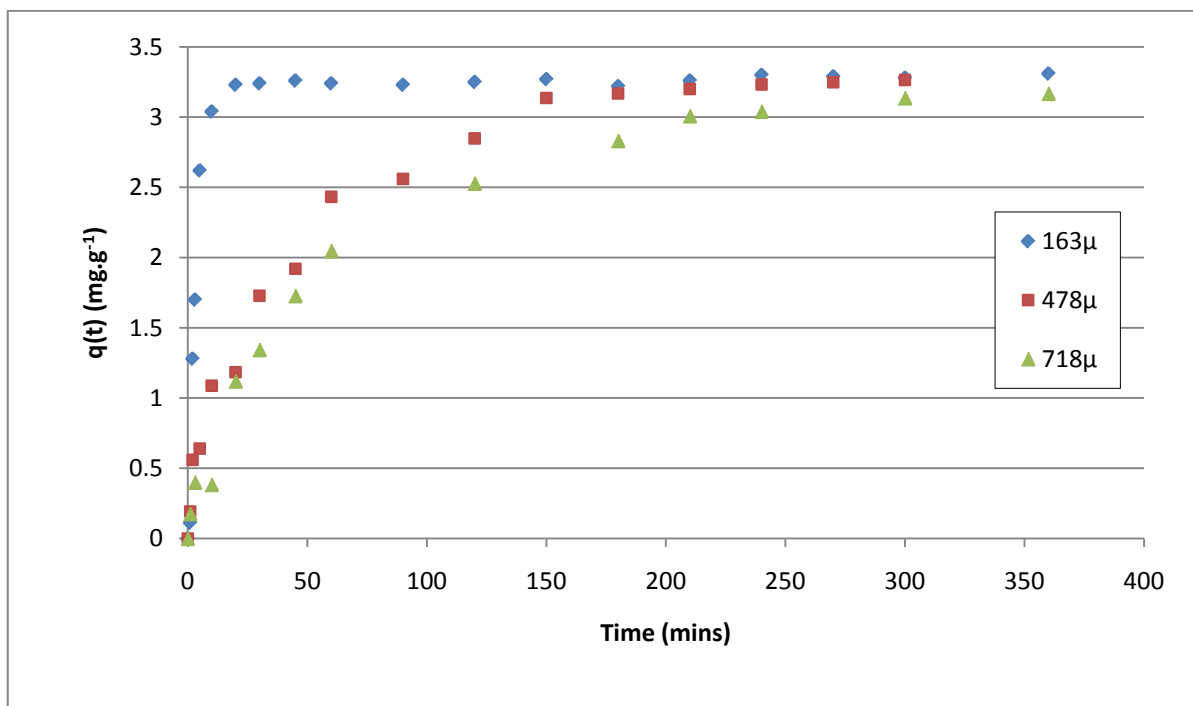


Figure 5.1: Lysozyme adsorption kinetics for XAD4, varying particle diameter (sauter mean) at stirrer speed 826 rpm to minimise external film diffusion effects.

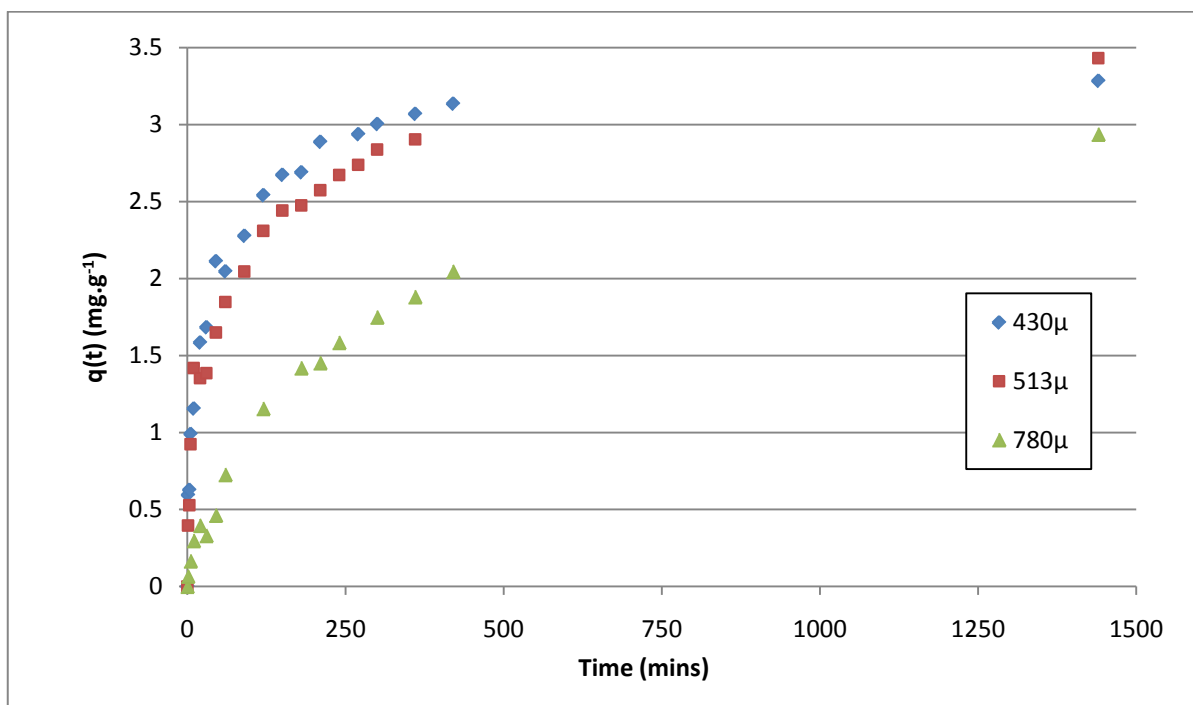


Figure 5.2: Lysozyme adsorption kinetics for PSDVB3:5ToINap5:2, varying particle diameter (sauter mean) at stirrer speed 826 rpm to minimise external film diffusion effects.

Immediate comparisons of the two materials indicate that as expected XAD4 exhibits faster kinetics with even the largest material removing all available protein within 400 minutes. Conversely the largest PSDVB3:5ToINap5:2 fraction is only ~2/3 of the way to complete removal within this time frame. To ensure that the differences in uptake kinetics seen between particle size fractions were due to simply the sizes of the particles and not internal pore structure, the data was re-plotted y-axis re-scaled as normalised uptake values $q(t)/q(f)$ (where $q(f)$ is the reading at 24 hours) and plotted against dimensionless time to rescale time and path length disparities. Figures 5.3 and 5.4 show that the observed differences in the uptake kinetics between different particle size fractions is due to the diffusion path length with the different curves falling on top of one another. These data support earlier results (e.g. those shown previously in Figure 4.13) that adsorbent particles of different sizes produced from the same batch have similar pore size distribution.

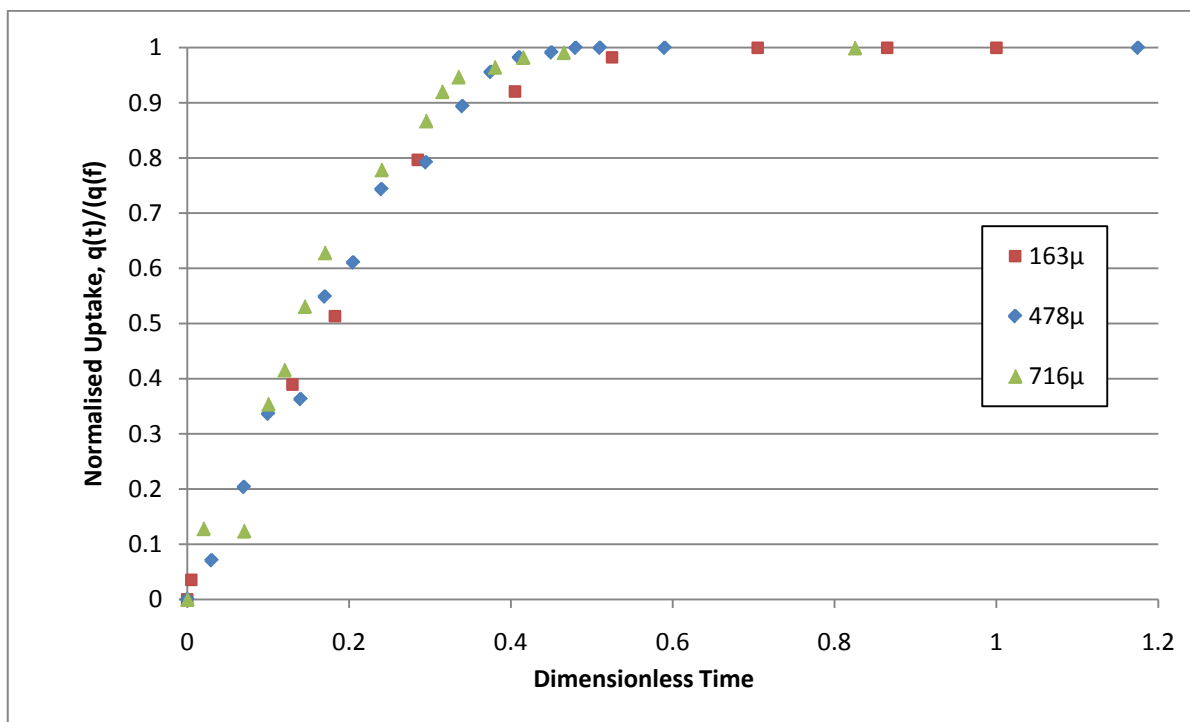


Figure 5.3: Lysozyme adsorption kinetics for XAD4, y-axis plotted as $q(t)/q(f)$ (normalised uptake) against dimensionless time.

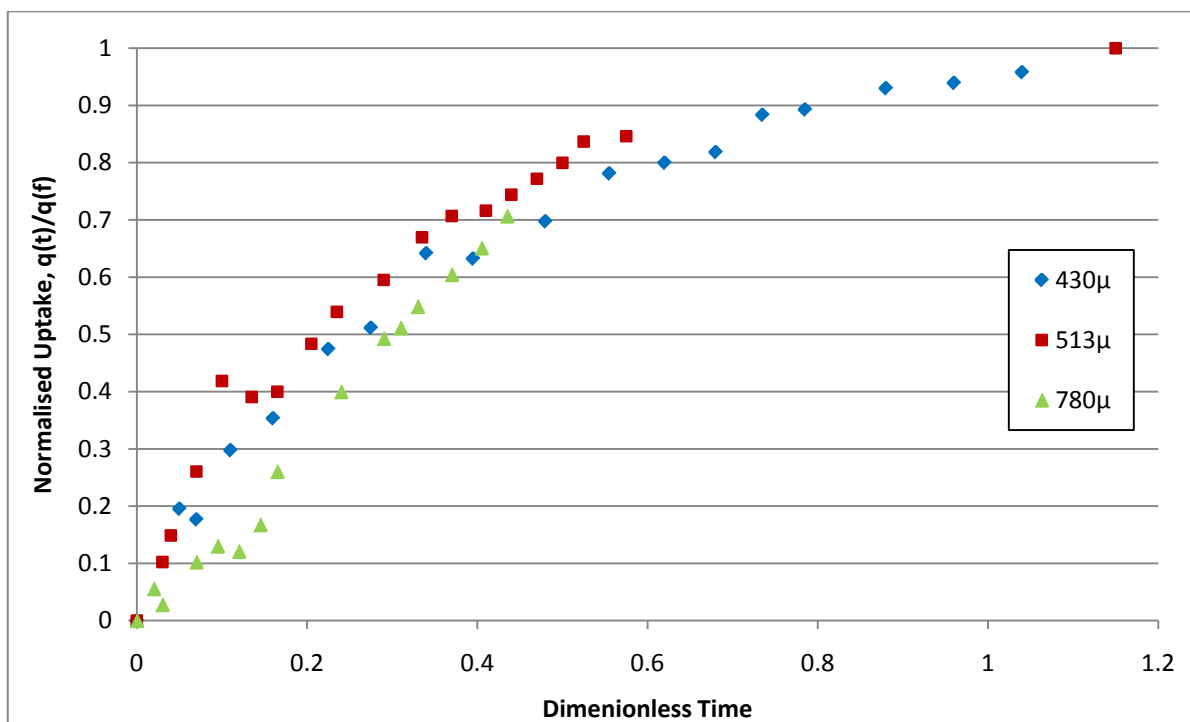


Figure 5.4: Lysozyme adsorption kinetics for PSDVB3:5ToINap5:2, y-axis plotted as $q(t)/q(f)$ (normalised uptake) against dimensionless time.

Lysozyme adsorption onto both XAD4 and PSDVB3:5ToINap5:2 has been shown to be significant within the time frame of a standard dialysis treatment 3-5 hours while XAD4 is undoubtedly the faster of the two adsorbents this is due to the presence of transport pores as well as the much higher number of possible adsorption sites reducing the required diffusion distance within the particle.

To record the uptake kinetics of HSA the concentration of HSA in solution was increased to 200mg/l. In addition, the very smallest particle size fraction was excluded from the studies.

Figures 5.5 and 5.6 show the uptake kinetics for XAD4 and PSDVB3:5ToINap5:2. From Figure 5.5 we can see clearly that the larger size of albumin and its consequential slower rate of diffusion has a more significant effect on the kinetics of adsorption. After 24 hours the final uptake value $q(f)$ for XAD4 were for the 400 μ m fraction was ~3 mg/g and for the 716 μ m fraction was ~2mg/g showing that even after this length of time the larger material had not reached equilibrium/saturation.

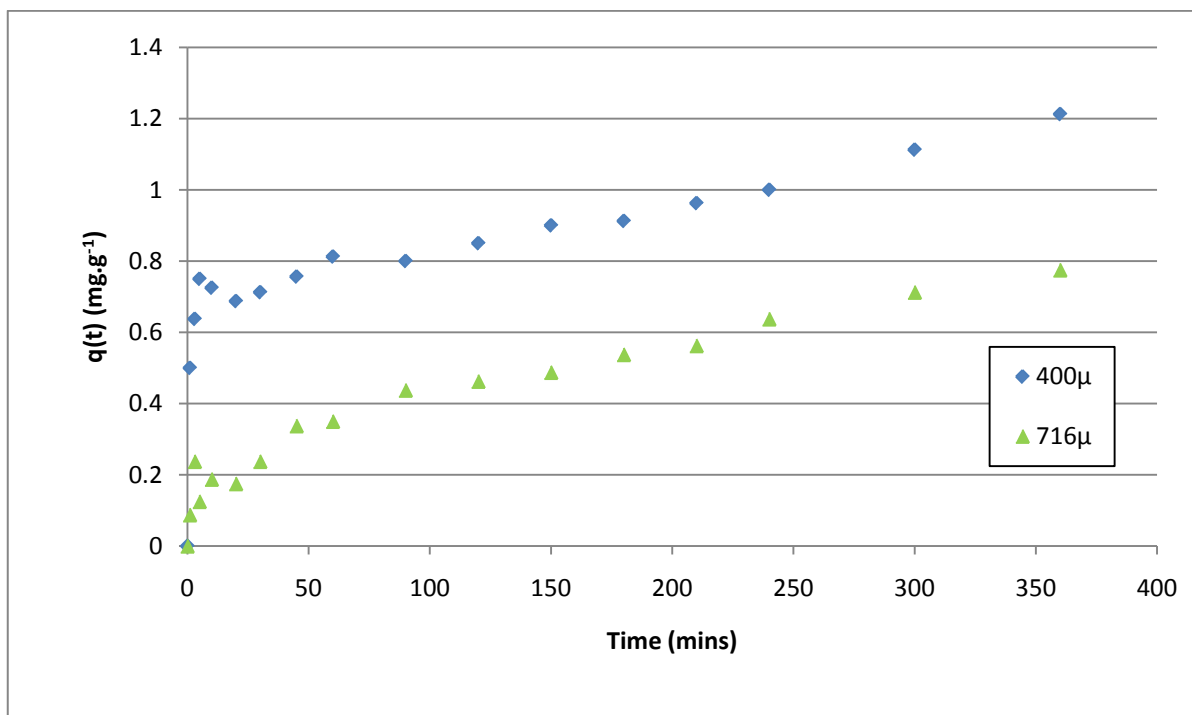


Figure 5.5: HSA adsorption kinetics for XAD4, varying particle diameter (sauter mean) at stirrer speed 826 rpm to minimise external film diffusion effects.

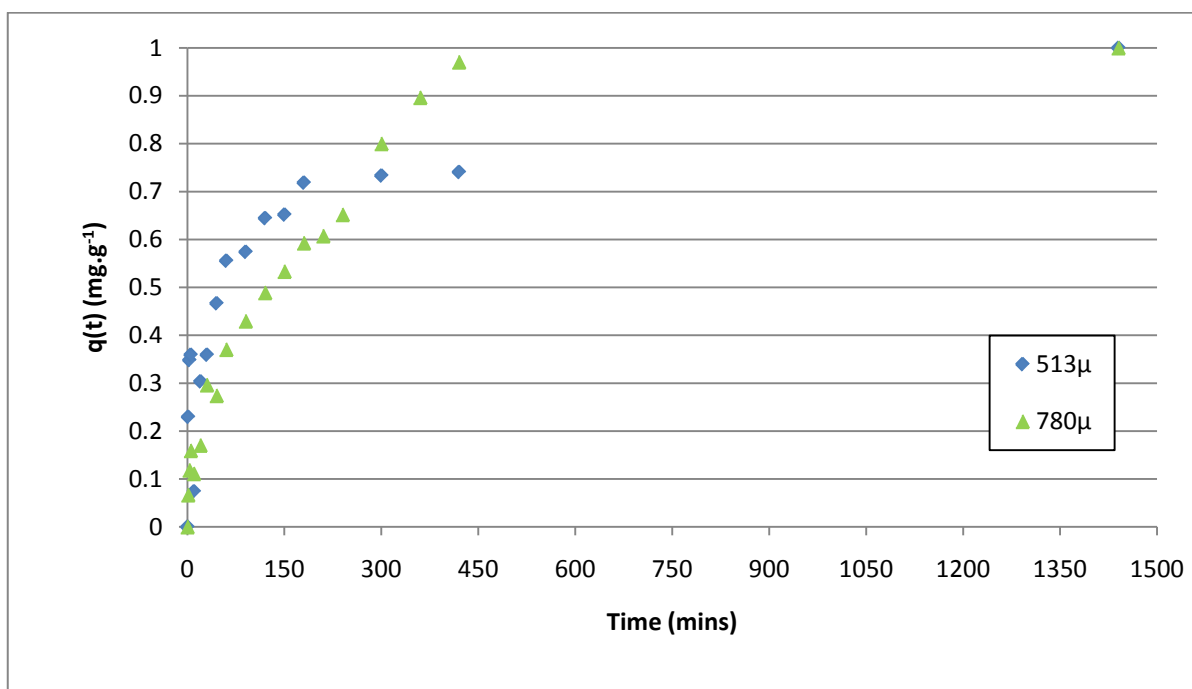


Figure 5.6: HSA adsorption kinetics for PSDVB3:5ToINap5:2, varying particle diameter (sauter mean) at stirrer speed 826 rpm to minimise external film diffusion effects.

Figure 5.6 showing the uptake of HSA onto PSDVB3:5ToINap5:2 does not display the same trend as with XAD4 the change in particle size appears to have a small if not negligible effect on the uptake kinetics. One possible explanation of this is that the adsorption of albumin takes place almost solely on the external surface of the particle due to the designed pore size cut off and so diffusion through the particle does not hinder the kinetics in any appreciable fashion.

In relation to the research problem posed as relates to the adsorption of lysozyme uptake is hindered by the reduction/elimination of transport pores in PSDVB3:5ToINap5:2 however this is counteracted by the significant reduction in HSA removal.

5.3 Multiple Solute *Batch Adsorption Dynamics*

To assess the suitability of size exclusion as a method to exclude large blood proteins (ie HSA) while still removing middle molecular weight toxins we have investigated the uptake of HSA and Lysozyme using single solute systems (Section 5.2) while this has shown the effectiveness of PSDVB3:5ToINap5:2 as a material to remove lysozyme and exclude HSA it does not show how the material will perform in a more complex system.

If we consider a more complex multi-solute system of lysozyme and HSA we would expect to see competitive adsorption between the two proteins. This competitive adsorption will result in a reduced capacity for both lysozyme and HSA additionally the kinetics of protein adsorption will be affected. Depending on the adsorbents structure and diffusivities of the proteins we can expect to experience a number of possible outcomes, we are concerned with the uptake of lysozyme and so will concentrate on the effect we may see

to its uptake capacity and kinetics. The following two possibilities have been identified

- No change in kinetics and capacity
- Reduced capacity, slower kinetics

If we observe no change in the capacity and kinetics of the uptake of lysozyme then again there are two possibilities that could account for this firstly the HSA has been effectively size excluded from the adsorbent and as such the reduction of available adsorption sites is minimal. Secondly the diffusivity of lysozyme is greater than that of HSA so it reaches the available adsorption sites first preventing HSA adsorption. The reduced capacity and slower kinetics will obviously mean competitive adsorption has occurred be that due to a more open pore structure or comparable diffusivities.

Iain Roche, a fellow member of my research group has investigated the effects of a binary system of lysozyme and HSA on the uptake of lysozyme on PSDVB3:5ToINap5:2. His thesis “Nanoporous polymeric adsorbents for blood purification” (2008) investigates this binary system referring to PSDVB3:5ToINap5:2 as CW1. Three experiments were conducted in all cases 15g of adsorbent with a particle size of 430 μ m (saunter mean) was used, the concentration of lysozyme was 100mg/l and a stirrer speed of 826rpm to minimise external film diffusion effects was maintained. The three experimental conditions where no HSA, 200 mg/l HSA and 1000 mg/l HSA.

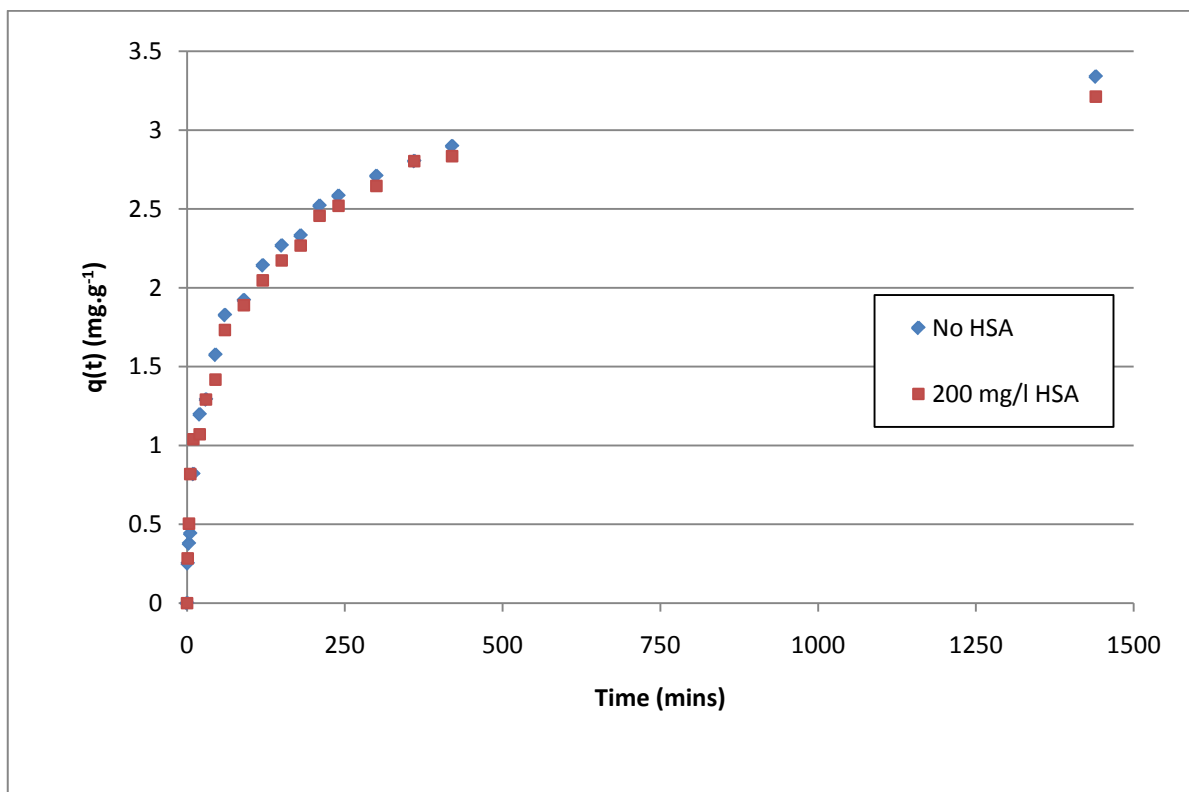


Figure 5.7: Lysozyme adsorption kinetics for 15g of PSDVB3:5ToINap5:2, 420 μm particle diameter (sauter mean), comparing the uptake kinetics in the presence of 200 mg/l HSA. At a stirrer speed of 826 rpm to minimise external film diffusion effects.

Figure 5.7 compares the uptake data for lysozyme onto PSDVB3:5ToINap5:2 with no HSA and in the presence of 200mg/l HSA and Figure 5.8 the comparison between the control and 1000mg/l HSA. Examining first Figure 5.7 we see that there is no change in uptake kinetics when a relatively low concentration of HSA is in solution this means that we could be in one of two situations size exclusion of HSA or the higher diffusivity of lysozyme flooding all available HSA adsorption sites before significant HSA adsorption can occur.

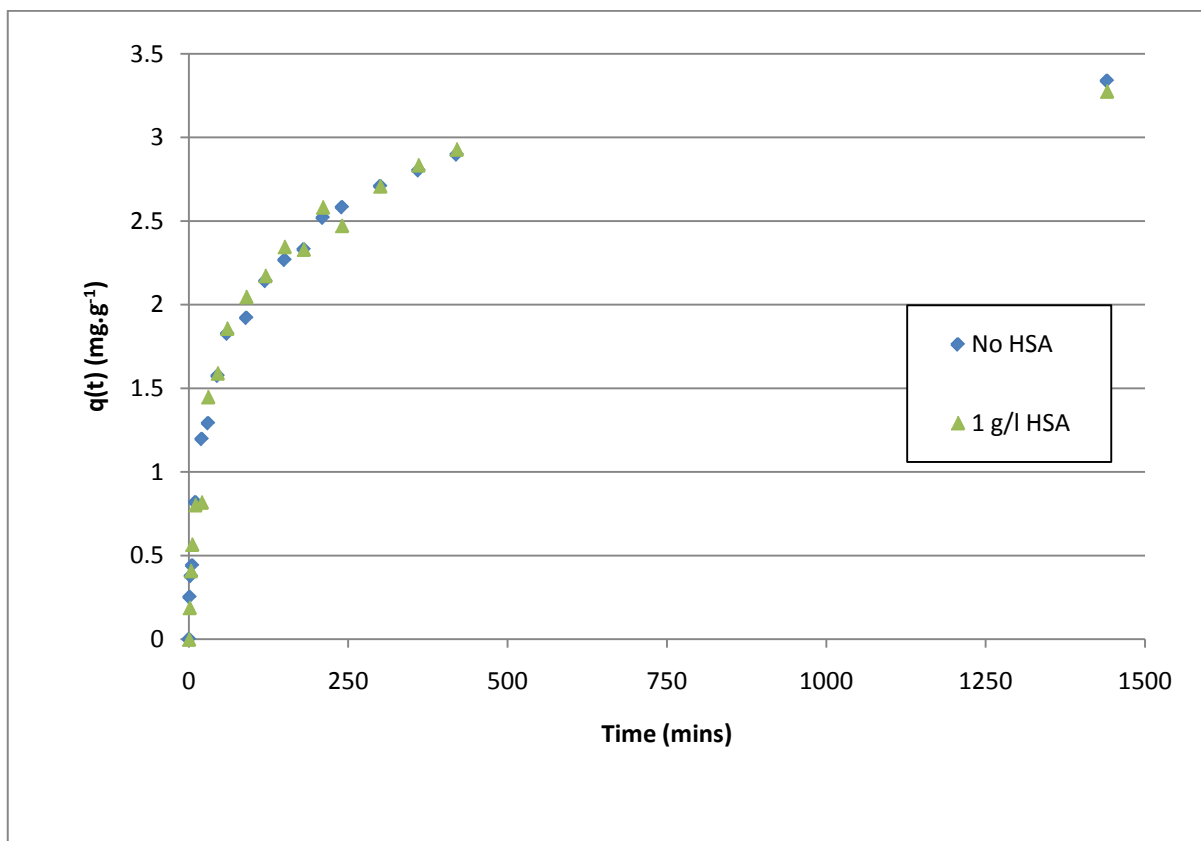


Figure 5.8: Lysozyme adsorption kinetics for 15g of PSDVB3:5ToINap5:2, 420 µm particle diameter (sauter mean), comparing the uptake kinetics in the presence of 1000 mg/l HSA. At a stirrer speed of 826 rpm to minimise external film diffusion effects.

To test this we look to Figure 5.8 the increased HSA concentration will go some way to eliminating the diffusivity disparity. Again we observe no difference in uptake kinetics this strongly suggests that HSA is size excluded and any external surface adsorption does not unduly affect access to the internal pore structure where the majority of the adsorption surface area is located.

In relation to the problem being investigated in this research the binary system has demonstrated that the presence of large blood proteins (HSA) in solution even in relatively concentrated solutions of 1000mg/l does not

impact on the kinetics of middle molecular weight toxin (lysozyme) uptake when the adsorbents internal pore structure excludes these larger proteins.

5.4 Modelling Batch Adsorption Dynamics Data

Time series data were modelled using the irreversible adsorption model proposed by Suzuki and Kawazoe (1974) to extract solute intraparticle diffusivities (De). Adsorbent samples used were sieved to obtain tight particle size fractions. Experiments were performed using a single dissolved protein in 0.1M Hepes buffer solution. A summary of the values of the experimental variables used for the batch adsorption experiments are provided in Table 5.3. The stirrer speed was set to 726rpm as this was found to minimize external film mass transfer resistance to solute diffusion permitting evaluation of the intraparticle diffusional resistance to mass transfer.

Suzuki and Kawazoe (1974) derived a 1st order differential equation by relating the change in solute concentration in the solution to uptake by the adsorbent. This relationship was solved using Matlab software (version 7). The effective solute diffusivity De was fitted by minimizing the sum of the squares of the errors (the difference between the predicted value (model) and the experimental data). The intraparticle diffusivity values De evaluated for lysozyme and HSA adsorption on PSDVB3:5ToINap5:2 and XAD 4 are presented in Table 5.3. Figure 5.9 shows the experimental kinetic data plotted as fractional uptake $F(t)$ (symbols), the predictions made by the model are represented by solid curves. The fitted intraparticle diffusivity values De obtained from this data for the adsorption of lysozyme suggest that uptake kinetics for PSDVB3:5ToINap5:2 ($De = 4 \times 10^{-13} \text{m}^2 \text{s}^{-1}$) are in an order of magnitude slower when compared with XAD4 ($De = 4 \times 10^{-12} \text{m}^2 \text{s}^{-1}$).

The data in Figure 5.9., shows slower lysozyme uptake by XAD4 this is caused by the larger particles size used in the experimental work for XAD4 ($d_p = 576\mu\text{m}$) compared with PSDVB3:5TolNap5:2 ($d_p = 28\mu\text{m}$). The reduced adsorption kinetics in PSDVB3:5TolNap5:2 can be attributed to the designed tighter mesopore structure within compared to XAD4's wider structure including larger transport pores.

PSDVB3:5TolNap5:2, manifested in a reduction in the magnitude of the effective diffusivity of the solute within the adsorbent particle. HSA ($De = 5 \times 10^{-11} \text{m}^2 \text{s}^{-1}$) adsorption kinetics for XAD4 was found to be faster in comparison with lysozyme ($De = 4 \times 10^{-12} \text{m}^2 \text{s}^{-1}$) removal. HSA is able to access only a fraction of the adsorbent pore structure, which appears to provide little hindrance to the diffusion of the solute, this is supported by the multi-solute work carried out by Iain Roche (2008) and discussed in section 5.3. For HSA the effective diffusivity and free solution diffusivities are similar in magnitude ($6.1 \times 10^{-11} \text{m}^2 \text{s}^{-1}$). The adsorption capacity for HSA on PSDVB3:5TolNap5:2 is small suggesting predominantly adsorption on the external bead surface, as would be expected by the tailored pore structure. The fitted intraparticle diffusivity was similar in magnitude to the free solution diffusivity for HSA ($6.1 \times 10^{-11} \text{m}^2 \text{s}^{-1}$).

The model was compiled by Dr Danish Malik and a copy of the Modelling parameters and equations are located in appendix III

Table 5.3: Summary of experimental variables used for measuring lysozyme (LYZ) and HSA batch adsorption dynamics

	TN_5:2	TN_5:2	XAD4	XAD4
Solute	*LYZ	^HSA	*LYZ	^HSA
Particle size, $d_{3,2} \times 10^6$ (m)	28	197	576	163
Mass of sorbent, (g)	2.5	22	5	0.5
C_o , (mg/l)	402	204	5361	200
C_f , (mg/l)	107	106	2058	105
Saturation uptake, q^* (g/g)	0.059	0.0022	0.330	0.095
Stirrer speed, rpm (min^{-1})	726	726	726	726
Porosity, ε (-)	0.29	0.29	0.55	0.55
Solid density, ρ (kg/m^3)	1040	1040	1120	1120
Intraparticle Diffusivity, $D_e \times 10^{12}$ (m^2s^{-1})	0.4	40	4	50

* Diffusivity in solution (1×10^{-10} , m^2s^{-1}) ^ Diffusivity in solution (6.1×10^{-11} , m^2s^{-1})

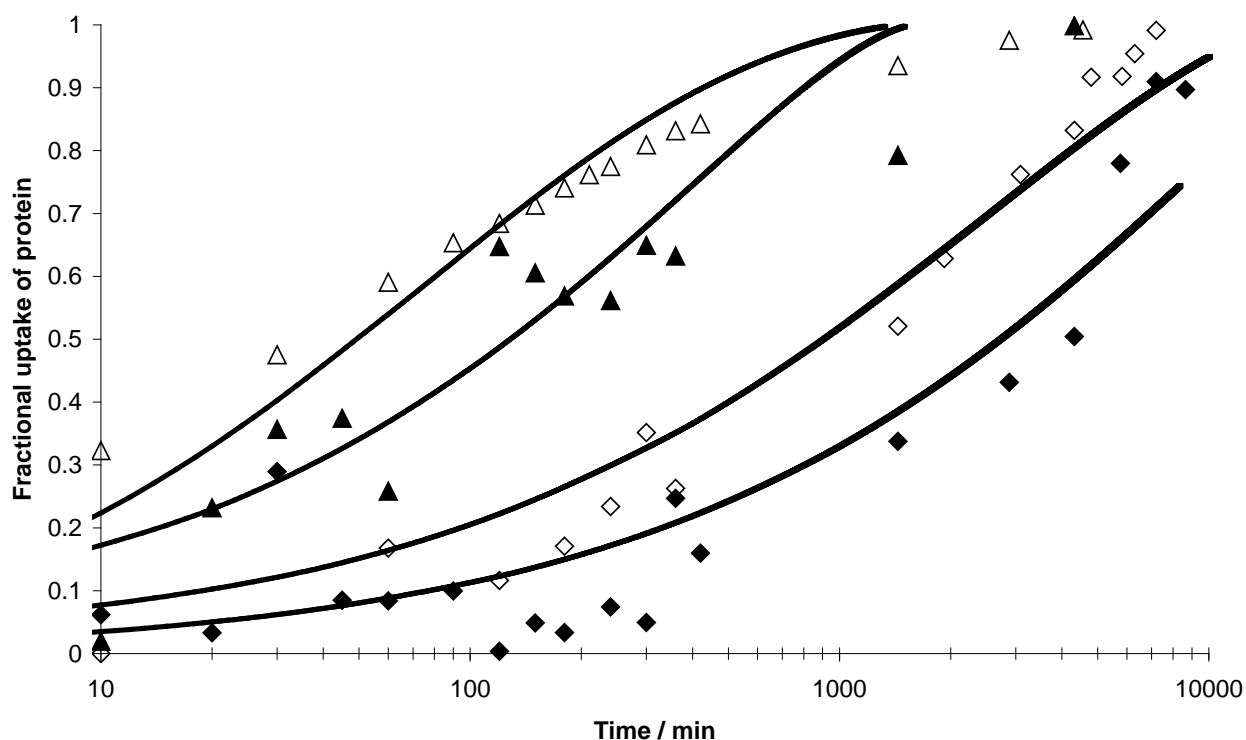


Figure 5.9: Fractional uptake ($q(t)/q^*$) versus adsorption time, comparison of PSDVB3:5ToINap5:2 (open triangles – lysozyme data; solid triangles – HSA data) and XAD4 (open diamonds – lysozyme data; solid diamonds – HSA data). Solid lines are the irreversible isotherm model predictions for the data.

5.5 Conclusions

From the batch adsorption uptake studies carried out it is clear that the controlled pore structure developed for PSDVB3:5ToINap5:2 has successfully size excluded human serum albumin with an available surface area $<1 \text{ m}^2 \text{ g}^{-1}$ resulting in an uptake of 2 mg g^{-1} . Lysozyme was still removed (59 mg g^{-1}) showing that access to the porous structure was still possible for the smaller molecule. XAD4 provided significantly more available surface area for both lysozyme and human serum albumin uptake and this is reflected in the higher protein uptake values 330 mg g^{-1} and 95 mg g^{-1} respectively. The final material tested was PSDVB0:1ToINap5:2 this adsorbent offered significantly higher surface area for the removal of proteins

than PSDVB3:5ToINap5:2 while maintaining the pore cut off. The removal of human serum albumin was greater than for the previous material however still only ~50% of that for XAD4. Lysozyme uptake was also greatly improved with an almost 10x increase compared to PSDVB3:5ToINap5:2. It becomes apparent from this data that there is a trade off to be made between the two in house adsorbents the greater surface area of PSDVB0:1ToINap5:2 would result in less material being required in a haemoperfusion device however human serum albumin uptake would be significantly impacted.

The batch adsorption dynamics studies exposed that the removal of transport pores present in XAD4 by reducing maximum pore cut off in PSDVB3:5ToINap5:2 have a large impact on the uptake kinetics for lysozyme and this may need to be addressed for use in a haemoperfusion device where treatment time is limited to 3-5 hours. Additionally the multi-solute work carried out by Iain Roche (2008) shows that during competitive adsorption the kinetics of lysozyme adsorption are not impacted for PSDVB3:5ToINap5:2 due to the exclusion of HSA from the internal pore structure, and no apparent pore blockage as a result of external surface coverage.

6 Conclusions and Recommendations for Further Work

The objectives of the research were as follows:

1. Control the internal pore structure of the adsorbent to exclude human serum albumin
2. Optimise the adsorbent pore structure and accessible surface area in the region 2-10nm relevant for the removal of middle molecular weight uremic toxins
3. Develop a method to increase the useful yield of adsorbent particles through control of particle size distribution
4. Determine whether dry state (gas adsorption) porosimetry is a suitable method for characterising the pore structure of the adsorbents
5. Verify (*in vitro*) through protein adsorption studies that the adsorbents remove middle molecular weight molecules e.g. using lysozyme as a surrogate middle molecular weight solute whilst excluding human serum albumin.

6.1 Control of Internal Porous Structure of Polymeric Adsorbents

6.1.1 Exclusion of human serum albumin

Methods used for the control of the internal porous structure of poly(styrene-divinylbenzene) adsorbents have previously been reviewed by Okay (2000), Sherrington (1998), Guyot (1988) and Davankov et al (2002). Consulting the open literature yielded general principles for generating and controlling porosity within polymeric beads, however most sources tend not to focus on generating small mesopores in the range 2-10nm. Focus in literature is on adsorbents designed to have large surface areas in the micropore domain

such as the hyper-crosslinked polymers of Davankov et al (2002) whilst large transport pores were sought after to help in accessing the internal pore structure more efficiently. The primary target of the research was to develop an adsorbent which would non-selectively remove middle molecular weight proteins while size excluding larger proteins including human serum albumin. This approach required tailoring the adsorbent structure so that a substantial surface area is present due to pores in the 2-10nm range while micropores (<2nm) were of little interest. Presence of large transport pores may only serve to increase serum albumin uptake and were therefore not sought after. Limited literature was found on the subject of controlling pores in the relevant 2-10nm size range. Experimental work proved that the use of a high degree of crosslinking and a good solvent (toluene) produced an adsorbent with the pore size cut-off around ~30nm however, this was still significantly larger than was the target region (~ 10nm) if albumin was to be excluded. The use of other solvents such as undecane increased the pore volume however this also led to larger pores. The solution to the problem was found through the addition of naphthalene as part of the porogenic mixture (toluene was still required to dissolve the naphthalene for use at room temperature), this pulled the maximum pore size down to 20nm. 20nm was as low as the maximum pore size could be lowered to using the methods available and as the inverse size exclusion and protein adsorption studies undertaken during the research show, the pore structure is adequate for the exclusion of human serum albumin whilst permitting the removal of middle molecules.

6.1.2 Optimisation of pore structure

From the literature it was apparent that there were a number of methods available to increase the pore volume and surface area of polymeric adsorbents over the entire range of pores of interest (2-10nm). These methods focused on the polymer network and the porogens being utilised.

The first option was to increase the degree of crosslinking whilst employing good solvents for the polymer (e.g. toluene). A high degree of crosslinking (nominally 50%) was required to generate a porous resin retaining porosity in the dry state. Lower degrees of crosslinking resulted in gel-type polymers which are porous when swollen in suitable solvents but do not show porosity in the dry state. Increasing the nominal crosslinking degree from 50% to 65% and finally 80% (the maximum possible using the available technical grade divinylbenzene) showed a significant increase in the surface area and pore volume of the adsorbents when using pure toluene as the solvent. Changing from 50% DVB to 80% DVB increased the surface area in the range 2-10nm from $80 \text{ m}^2 \text{ g}^{-1}$ to $179 \text{ m}^2 \text{ g}^{-1}$. With naphthalene included as a porogen a similar increase was also observed with surface area increasing from 88 to $173 \text{ m}^2 \text{ g}^{-1}$. Thus it would appear that through increasing the crosslinking degree, a material with almost double the surface area in the mesoporous range may be synthesised. The downside was that pores greater than 10nm also increased. Fortunately the maximum pore size for the adsorbent prepared using a mixture of toluene:naphthalene still did not exceed 20nm. The other alternative was changing the ratio of monomers to porogens. Increasing the porogen ratio increases the solubility of the growing polymer chains resulting in the formation of more nuclei which in turn when joined together in the final matrix provide a greater yield of pores in the >2nm range. A disadvantage of increasing porogen concentration is mechanically weaker particles, this is due to the reactivity ratio of the comonomers divinylbenzene is more reactive than styrene and so reacts first in the nucleus of the polymerisation reaction (see Figure 2.4) the more dilute the polymerisation mixture the less likely that crosslinks will form between the nuclei as the divinylbenzene has been already utilised this results in the mechanically weaker particles. In an extreme case a microgel powder is formed when insufficient crosslinking monomer remains in solution to join the nuclei together. In terms of surface area in the 2-10nm region changing from

a 1:1 porogen to monomer ratio to a 2:1 porogen to monomer ratio resulted in an increase in the adsorbent surface area by 24% while the surface area in the range greater than 10nm increased by 30%. In addition to this increased surface area in the >10nm range, the pore cut off was increased. Informed by these the method of choice for generating greater mesoporous surface area (< 10nm range) and therefore increasing middle molecule adsorption capacity without sacrificing size exclusion was to increase the crosslinking degree to the highest possible level.

6.2 Increasing the yield of particles of the required size range during suspension polymerisation

Using the Micropore Technologies stirred cell it has been possible to generate droplets with a tight size distribution in the range 30-300 μ m. This was achieved using a 10 μ m membrane however, the droplet sizes could easily be increased (if required) by using a larger pore membrane. The ability to generate a size exclusion adsorbent with a controlled particle size was important for two reasons. Firstly, the ability to generate small average particle size material <50 μ m was essential for use in inverse size exclusion chromatography where the smaller particles were essential to achieve the resolution required for separating the polystyrene standards. Additionally, control of the particle size through membrane emulsification has advantages for the commercial manufacture of these adsorbent materials such as the removal of the downstream particle classification process and would potentially cut down on product loss. XAD4 (an example of a commercially generated polymer adsorbent) is supplied with particles in the size range (90% or more of the material in the sample) within 350-1180 μ m (Rohm and Hass product data sheet). The wide particle size range would result in a low yield of product (thus high cost) if the desired particle size is near the high or low end of the particle size range. Droplet size and subsequently particle size was controlled through altering the shear rate at the membrane surface

(by adjusting the speed of the paddle stirrer) and the quantity of the suspension stabiliser polyvinyl alcohol (PVA) which also affects the solution viscosity. Higher PVA concentrations and stirrer speeds allowed control of the shear stress at the membrane surface however, the quantity of stabiliser was found to be an important variable, having a high concentration (>3%) encouraged smaller droplets to form and become stable. This meant that as the stabiliser concentration increased, the mono-disperse nature of the droplets generated decreased.

The generation of the droplets is only one stage in the manufacture of the particles. The droplets produced at the membrane surface must remain unchanged during the polymerisation process. Although some droplet breakup was observed following emulsion generation which resulted in smaller sized material and conversely some droplets were observed to coalesce or became loose aggregates, overall, this was not found to be a serious problem. Looking at Figure 4.9 we see that approximately 96% of droplets generated during membrane emulsification were between 80 - 300 μm , after 5 hours in the polymerisation reactor this range represents 88% of the droplets and after 24 hours this has reduced to 76%. After 5 hours we see a small amount of break up as shown by the increase in slightly smaller droplets/particles after 24 hours the majority of the change in particle size is due to aggregation. The aggregates were either broken up using a sonic bath or removed for use during size critical work.

It is envisaged that in a haemoperfusion clinical device the average particle size range would be between 300-500 μm , a compromise between the path length for diffusion (smaller resulting in faster kinetics) and the pressure drop (lower external surface area per unit volume of the column resulting in a lower pressure drop across the column). With this size range in mind a membrane with a larger pore size will be required as shown by the

experimental data particle sizes using a 10 μm pore size are limited to $\sim 200\mu\text{m}$ Kosvintsev et al (2005) show scaling with membrane pore size using a stirred cell with a 40 μm membrane (producing droplets of sunflower oil in water with 1% Tween 20) in the appropriate range 150-400 μm under the same conditions a 9 μm pore membrane generated 50-200 μm droplets.

6.3 Analysis of Porous Structure

The conventional method of analysing the pore structure of nanostructured polymer adsorbents is by nitrogen porosimetry. This method works well for adsorbents with a fixed pore structure e.g. inorganic materials such as clays and zeolites etc., or polymeric adsorbents that will be used in the dry state. However, polymeric adsorbent materials wetted by a solvent show changes in the porous structure this is apparent in materials generated using high and low levels of crosslinking, it is however, more apparent in low crosslinking degree polymers where porosity varies significantly in the presence of solvents. Take the example of Superdex 75 which was used in the ISEC work it has negligible surface area when dry however is highly porous when wetted. With size exclusion the objective of the work here, it was important to evaluate whether the maximum pore size of adsorbents prepared during the study change when wetted by different solvents. To determine if this is the case, a number of methods have been proposed by Okay (2000). Literature suggests that by drying the adsorbent from different solvents the porosity in the dry state would change. To evaluate these effects, a sample from the same adsorbent material was vacuum dried following swelling in three different solvents: toluene, acetone and methanol. This process allowed changes in porosity due to swelling in different solvents to be observed. Material dried following contact with methanol (the poorest solvent for the matrix) displayed the largest surface area and pore volume however, the distribution of the pores did not change appreciably and the maximum

pore cut off remained the same. As an alternative to the thermal drying process, freeze drying of the materials was considered. The difficulty here was finding solvents with sufficiently high freezing points such that the pore solvent could be easily sublimed. Benzene (T_m 5.5°C) and cyclohexane (T_m 6.5°C) were settled on as examples of a good and a poor solvent respectively. Water was dismissed as a suitable candidate due to its expansion during freezing. As with the thermally dried samples, the freeze dried samples showed increase in total pore volume and surface area when dried from poorer solvents. However the pore distribution did not alter significantly. Thus, although swelling in different solvents was found to change the total pore volume, no significant affect on the distribution of pores supports the conclusion that a wet method of analysis may be employed to probe the pore structure of adsorbents.

Inverse size exclusion chromatography (ISEC) allows for the physical probing of a polymer matrix using probes of known physical size. The major disadvantage of this application is that the probe and solvent have to meet certain stringent criteria, in particular that there are minimal interactions between the probe and the adsorbent's surface. In the case of polystyrene based polymers this meant using polystyrene standards in tetrahydrofuran (THF). This solvent isn't an ideal analogue for water however the nitrogen porosimetry data suggests that changing solvents has little affect on the pore distribution. ISEC chromatograms generated by the probing of the adsorbents were found to be a valuable tool in determining the extent of size exclusion of probe solutes within the porous structure of the adsorbent. Thus, used in combination with nitrogen porosimetry a more complete picture of the adsorbent pore structure and size exclusion characteristics were obtained.

ISEC was found to be useful for the determination of an adsorbent material's pore size cut off and accessibility of suitably sized probes to the internal pore structure. The presence of larger pores within the structure but those that may be inaccessible to the specific probe due to narrow pore entrances may be detected using a combination of ISEC and nitrogen porosimetry. These features would not be apparent in the data obtained from nitrogen porosimetry alone. This may explain some of the disparity in the accessible pore volume values between ISEC and nitrogen porosimetry for a probe the size of albumin. In this case for PSDVB3:5ToINap5:2 ISEC data suggest around ~5% of the pore volume would not be accessible to albumin whilst the nitrogen porosimetry data suggests a value closer to 15%.

6.4 Adsorption of Marker Proteins

The adsorption capacity studies for the proteins human serum albumin (HSA) and lysozyme for the adsorbent PSDVB3:5ToINap5:2 suggest that the adsorbent has good potential as a size selective adsorbent for blood purification. HSA adsorption on PSDVB3:5ToINap5:2 was measured as 2 mg g⁻¹ compared with around 60 mg g⁻¹ for lysozyme. The commercial adsorbent XAD4 displayed significantly higher surface area in the mesopore domain and was found to adsorb significantly more lysozyme from buffered solution (415 mg g⁻¹). XAD4 also displayed higher HSA uptake (100 mg g⁻¹) compared with PSDVB3:5ToINap5:2. To counter the low lysozyme uptake by PSDVB3:5ToINap5:2, PSDVB0:1ToINap5:2 was tested and found to have significantly higher lysozyme capacity (579 mg g⁻¹). However, this increase in adsorption capacity also applied to HSA which was recorded as 51mg g⁻¹. The adsorption data suggests that XAD4 is not the preferred adsorbent for haemoperfusion due to the potential removal of blood serum albumin. The choice between PSDVB3:5ToINap5:2 and PSDVB0:1ToINap5:2 is less clear. Although a high lysozyme adsorption capacity is desirable, it comes at the

expense of increase has removal. The decision will depend on how much adsorbent material is required for the clinical treatment, i.e. the size of the haemoperfusion column (capacity) and the length of the clinical treatment session (kinetics).

The kinetic studies of XAD4 and PSDVB3:5ToINap5:2 shed further light on the situation. The faster kinetics afforded by the transport pores in XAD4 mean that in a clinical situation where a patient is treated for example for a limited period of 4 hours a material with transport pores will be more effective unless significantly more of the alternative adsorbent is utilised to increase the uptake rate.

6.5 Conclusions

All of the research objectives originally identified at the beginning of the research have been met. A nanostructured adsorbent material (PSDVB3:5ToINap5:2) with a controlled pore structure (2-10nm region) has been synthesised and has shown to size exclude HSA whilst removing a surrogate middle molecular weight protein lysozyme. Analysis of the internal pore structure has been assessed using two methods: nitrogen porosimetry, which is well established and provides a wealth of pore structure and area information and ISEC which provided information regarding accessibility of the internal pore structure to solutes of sizes relevant for evaluating the influence of pore structure on size exclusion of blood proteins. Particle size control through the use of membrane emulsification has allowed manufacture of material yielding pseudo mono-sized particles. While the stirred cell may not be suitable for industrial scale manufacture, scaling-up of the process, e.g. using crossflow systems following the same principle is quite feasible.

6.6 Further Work

To continue the work that has been undertaken during the present project the following avenues need exploration:

1. Improving adsorption kinetics through the introduction of transport pores, these should be sufficiently large that they could be potentially treated to minimise protein adsorption.
2. Biocompatibility of the external surface of the adsorbent
3. Multi-solute / complex fluid (blood plasma) adsorption studies
4. Packed column testing of the adsorbents

Objectives 1 and 2 are at first seemingly connected however they will have potentially very different solutions. The generation of transport pores can be easily achieved as was shown by the introduction of undecane (Chapter 4) to the porogen mixture, or through the use of commercially available adsorbents (e.g. XAD4). The ideal porous structure would however be a bimodal pore distribution where the introduction of transport pores >100 nm would be accomplished while maintaining minimal pore surface area in the >10 nm range, this could not be achieved with the introduction of undecane however, as has been shown in Chapter 4 as the transport pores generated through the introduction of alkanes are not solely in the macroporous region and add significantly to the pore surface area in the region (>10 nm) this work has sought to eliminate. One possible option would be the introduction of an oligomeric porogen as put forward by Macintyre and Sherrington (2004) although their work was not focussed on the effect these porogens had on the mesoporous range so further study would be required. The surface of any transport pores ideally need to be treated/altered to reduce or prevent adsorption, this process would have to be a subsequent treatment and potentially be accomplished as part objective 2.

Biocompatibility of the external surface (objective 2) can be achieved through a number of methods including a treatment post generation to chemically bond a biocompatible molecule to the surface of the adsorbent, one possible way to achieve this would be using a plasma to create reactive sites on the external surface. The alternative would be a one-pot method, to include during the polymerisation stage an agent in the aqueous phase (potentially the stabilising agent) which would react with the polymerising droplet and impart a biocompatibility to the surface, an example of a one pot method has been covered by Albright (2005) in his patent (US Patent # 6884829).

Objectives 3 and 4 the packed column testing and multi solute or complex systems are more application specific as opposed to the synthesis of the material however, they will be vital in ensuring that any adsorbent produced is fit for purpose. Column testing will ensure that materials are of suitable size to provide low pressure drop over the system (important to prevent damage to the patient's blood) while still maintaining the required protein uptake kinetics and ensuring their mechanical properties. The testing of more complex systems specifically full blood is of vital importance to assess the suitability of the material for its ultimate purpose and equally to ascertain the quantity of material needed to remove the required toxins. Additionally the biocompatibility of the final product will need to be checked using full blood.

7 References

Ahmed, M., Malik, M. A., Pervez, S. and Raffiq M. *Effect of porosity on sulfonation of macroporous styrene-divinylbenzene beads*, European Polymer Journal, 40, 2004, 1609–1613.

Albright, R., *Hemocompatible Coated Polymer and Related One-Step Methods*, United States Patent, Number 6884829, 2005.

Ball, V. and Ramsden, J.J., *Analysis of hen egg white lysozyme adsorption on Si(Ti)O₂-aqueous solution interfaces at low ionic strength: a biphasic reaction related to solution self-association*, Colloids Surfaces B 17 (2000) 81–94.

Beldie, C., poinescu, c. and Cotan, V., *Synthesis of macroporous bifunctional ion exchangers containing sulfo and carboxyl groups*, Journal of Applied Polymer Science, 29 1984,13-22

Caro, E., Marce, R.M., Borrull, F., Cormack, P.A.G. and Sherington, D.C., *Application of molecularly imprinted polymers to solid-phase extraction of compounds from environmental and biological samples*, Trends in Analytical Chemistry, 25(2), 2006, 143-154.

Carothers, W. H., *Studies on Polymerisation and Ring Formation. I. An Introduction to the General Theory of Condensation Polymers*, Journal American Chemical Society, 51, 1929, 2548.

Coutinho, F. M. B. and Rabelo, D., *Scanning electron microscopy study of styrene-divinylbenzene copolymers*, European Polymer Journal, 28, Issue 12, 1992, 1553-1557.

Davankov, V.A., Pavlova, L.A., Tsyurupa, M.P. and Tur, D.R., *Novel polymeric solid-phase extraction material for complex biological matrices portable and disposable artificial kidney*, Journal of Chromatography B, 689, 1997, 117-122

Davankov, V.A., Pavlova, L.A., Tsyurupa, M.P., Brady, J. Balsamo, M. and Yousha E., *Polymeric adsorbent for removing toxic proteins from blood of patients with kidney failure*, Journal of Chromatography B, 739, 2000, 73-80.

Davankov, V., Tsyurupa, M., et al, *Hypercross-linked Polystyrene and its Potential for Liquid Chromatography: A Mini Review*, Journal of Chromatography A 965, 2002, 65-73

Dember, L.M., and Jaber, B.L., *Dialysis-Related Amyloidosis: Late Finding or Hidden Epidemic?*, Seminars in Dialysis, 19, 2006, 105-109

Dephillips, Peter and Lenhoff, Abraham. M., *Pore Size Distributions of Cation-Exchange Adsorbents Determined by Inverse Size-Exclusion Chromatography*, Journal of Chromatography A, 883, 2000, 39-54.

Depner, T., Daugirdas, J., et al, *Dialysis Dose and the Effect of Gender and Body Size on Outcome in the HEMO Study*, Kidney International, 65:4, 2004, 1386-1394.

Dowding, P. J., Goodwin, J. W. and Vincent, B., *production of porous suspension polymer beads with a narrow size distribution using a crossflow*

membrane and a continuous tubular reactor, Colloids and surfaces, 180, 2001, 301-309.

Dowding, P.J. and Vincent, B., *Suspension polymerisation to form polymer beads*, Colloids and surfaces, 161, 2000, 259-269.

Durie, S., Jerabek, K., mason, C., and Sherrington, D. C., *One-pot synthesis of branched poly(styrene-divinylbenzene) suspension polymerised resins*, Macromolecules, 35, 2002, 9665-9672.

Erbay, E. And Okay, O., *Macroporous Styrene-Divinylbenzene copolymers: Formation of Stable Porous Structures During the Copolymerisation*, Polymer Bulletin, 41, 1998, 379-385.

Erbay, E. And Okay, O., *Pore Memory of Macroporous Styrene-Divinylbenzene Copolymers*, Journal of Applied Polymer Science, 71, 1999, 1055-1062.

Feinfeld, D.A., Rosenberg, J.W., Winchester, J.F., *Three Controversial Issues in Extracorporeal Toxin Removal*, Seminars in Dialysis, 19, 2006, 358-362

Fernandez, A., Ramsden J.J., *On Adsorption-Induced Denaturation of Folded Proteins*, Journal of Biological Physics and Chemistry, 1, 2001, 81-84

Flory, P. J. (1953) *Principles of Polymer Chemistry*, New York, Cornell University Press.

Gejyo, F., Kawaguchi, Y., et al, *Arresting Dialysis Related Amyloidosis: A Prospective Multi-Centre Controlled Trial of Direct Haemoperfusion with a*

Beta(2)-Microglobulin Adsorption Column, *Artificial Organs*, 28, 2004, 371-380

Gejyo, F., Teramura, T., et al, *Long Term Clinical Evaluation of an Adsorbent Column (BM-01) of Direct Haemoperfusion Type for Beta-2-Microglobulin on the Treatment of Dialysis-Related Amyloidosis*, *Artificial Organs*, 12, 1995, 1222-1226

Glynn, P., Allen, A. and Pusey C. (2002) *Acute Renal Failure in Practice*, London, Imperial College Press.

Gomez, C. G., Igarzabal, C. I. A. and Strumia, M. C., *Effect of the crosslinking agent on porous networks formation of hema-based copolymers*, *Polymer*, 45, 2004, 3189-6194.

Grassman, A., Gioberge, S., et al, *ESRD Patients in 2004: Global Overview of Patient Numbers, Treatment Modalities and Associated Trends*, *Nephrology Dialysis Transplantation*, 20, 2005, 2587-2593.

Grovender, E.A., Kellogg, B., et al, *Single Chain Antibody Fragment-Based Adsorbent for the Extra-Corporeal Removal of Beta(2)-Microglobulin*, *Kidney International*, 65, 2004, 310-322

Hagel L. *Pore Size Distributions*. In: Dubin PL, editor. *Journal of Chromatography Library – Volume 40, Aqueous Size-exclusion Chromatography*. Netherlands: Elsevier, 1988. p. 119-155

Hiyama, E., Hyodo, T., et al., *Performance of the Newer Type (Lixelle Type S-15) on Direct Haemoperfusion Beta-2-Microglobulin Adsorption Column for Dialysis-Related Amyloidosis*, *Nephron*, 92:2, 2002, 501-502

Horak, D., Lednicky, F. and Bleha, M., *Effect of Inert Components on the Porous Structure of 2-Hydroxyethyl Methacrylate-ethylene Dimethacrylate Copolymers*, Polymer, 37, 1996, 4243-4249.

Humes, H.D., Fissell, W.H. and Tiranathanagul, K., *The Future of Haemodialysis membranes*, Kidney International, 69, 2006, 1115-1119

Kellum, J.A., Song, M.C., et al, *Haemoadsorption Removes Tumor Necrosis Factor, Interleukin-6, and Interleukin-10, Reduces Nuclear Factor-Kappa B DNA Binding, and Improves Short-Term Survival in Lethal Endotoxemia*, Critical Care Medicine, 32:3, 2004, 801-805

Kurrat, R., Prenosil, J.E. and Ramsden, J.J., *Kinetics of human and bovine serum albumin adsorption at silica-titania surfaces*, Journal of Colloid Interface Science 185 (1997) 1–8.

Kutsuki, H., *Beta(2)-Microglobulin-Selective Direct haemoperfusion Column for the Treatment of Dialysis Related Amyloidosis*, Biochemica et Biophysica Acta-Proteins and Proteomics, 1753, 2005, 141-145

Lornoy, W., Beaus, I., et al, *On-Line Haemodiafiltration. Remarkable Removal of Beta(2)-Microglobulin. Long-Term Clinical Observations*, Nephrology Dialysis Transplantation, 15, 2000, 49-54

Lysaght, M., *Maintenance Dialysis Population Dynamics: Current Trends and Long-Term implications*, Journal Am Soc Nephrol, 13, 2002, 37-40.

Macintyre, F. and Sherrington, D., *Control of Porous Morphology in Suspension Polymerised Poly(divinylbenzene) Resins Using Oligomeric Porogens*, *Macromolecules*, 37, 2004, 7628 – 7636.

Malik, D. J., Warwick, G. L., Mathieson, I., Hoenich, N.A. and Streat, M., *Structured carbon haemoadsorbents for the removal of middle molecular weight toxins*, *Carbon*, 43, 2005, 2317-2329.

Malik, M. A., Ahmed, M. and Ikram M., *A new method to estimate pore volume of porous styrene-divinylbenzene copolymers*, *polymer Testing*, 23, 2004, 835-838.

McCaffery, Edward M. (1970) *Laboratory Preparation for Macromolecular Chemistry*, New York, McGraw-Hill.

Mogi, M., Harada, M., Kojima, K., Adachi, T. and Nakamura, S., *Selective removal of beta 2-microglobulin from plasma specimens of long-term haemodialysis patients by high-performance immunoaffinity chromatography*, *Clinical Chemistry*, 39, 1993, 277-280.

Nicholson, John W. (1997) *The Chemistry of Polymers*, Second Edition, Cambridge, RSC Paperbacks.

Odian, George (1991) *Principles of Polymerisation*, Third Edition, New York, Wiley Interscience.

Okay, O., *Phase Separation in Free Radical Crosslinking Copolymerisation: Formation of Heterogeneous Polymer Networks*, *Polymer*, 40, 1999, 4117-4129

Okay, O. *Macroporous copolymer networks*, Progress in Polymer Science, 25, 2000, 711-779.

Patrick, John W. (Ed) (1995) *Porosity in Carbons: Characterization and Applications*, London, Edward Arnold.

Peng, S.J. and Williams R.A., *Controlled production of emulsions using a crossflow membrane part I: droplet formation from a single pore*, Trans IChemE, 76 1998, 894-901.

Perry, Robert, H. (1997) *Perry's Chemical Engineers' Handbook*, Seventh Edition, Auckland, McGraw-Hill.

Poinescu, C. Beldie, C. and Vlad, C., *Styrene-divinylbenzene copolymers: influence of the diluent on network porosity*, Journal of applied polymer science, 29, 1984, 23-34.

Poinescu, C. and Vlad, C., *Effect of polymeric porogens on the properties of poly(styrene-co-divinylbenzene)*, European polymer journal, 33, 1997, 1515-1521.

Ramsden, J.J., *Dynamics of protein adsorption at the solid/liquid interface*, Recent Res. Dev. Phys. Chem. 1, 1997, 133–142.

Ramsden, J.J., *Adsorption kinetics of proteins*, in: A. Hubbard (Ed.), Encyclopaedia of Surface and Colloid Science, Dekker, New York, 2002, 240–261.

Roche, I., *Nanoporous Polymeric Adsorbents for Blood Purification*, Loughborough University, PhD Thesis, 2008.

Santora, B. And Gagne, M., *Porogen and Crosslinking Effects on the Surface Area, Pore Volume Distribution, and Morphology of Macroporous Polymers Obtained by Bulk Polymerisation*, *Macromolecules*, 34, 2001, 658 – 661.

Schildknecht, Calvin E. and Skeist, Irving (Eds) (1977) *High Polymers Vol. XXIX Polymerisation Processes*, New York, Wiley Interscience.

Sherrington, D.C., *Preperation, structure and morphology of polymer supports*, *Chemical communications*, 21, 1998, 2275-2286.

Sherrington, D.C. and Hodge, P. (Eds) (1988) *Synthesis and Separations Using Functional Polymers*, Tiptree, John Wiley & Sons.

Stepto, R. F. T. (ed) (1998) *Polymer Networks Principles of Their Formation Structure and Properties*, London, Blackie academic & professional.

Strelko, V. (1999) *Selective removal of heavy metals using novel active carbons*, Loughborough University Thesis.

Suzuki, M. and Kawazoe, K., *Batch measurement of adsorption rate in an agitated tank – pore diffusion kinetics with irreversible isotherm*, *Journal of Chemical Engineering of Japan* 7 (1974) 346–350.

Trochimczuk, A.W., Streat, M. and Kolarz B. N. *Highly Polar Polymeric Sorbents Characterisation and Sorptive Properties Towards Phenol and its Derivatives*, *Reactive and Functional Polymers*, 46, 2001, 259-271.

Tsuchida, K., Takemoto, Y., et al, *Lixelle Adsorbent to remove Inflammatory Cytokines*, *Artificial Organs*, 22, 1998, 1064-1067

Tsuchida, K., Yoshimura, R., et al, *Blood Purification for Critical Illness: Cytokines Adsorption Therapy*, Therapeutic Apheresis and Dialysis, 10, 2006, 25-31

Vanholder, R., *Replacement of Renal Function by Dialysis*, Replacement of Renal Function by Dialysis, C. J. e. al, Kluwer Academic Publishers Inc, 1996, 1-31.

Vanholder, R., De Smet, R., et al. *Redesigning The Map of Uremic Toxins*. Dialysis, Dialyzers and Sorbents: Where Are We Going? 133, 2001, 42-70

Vanholder, R., Schepers, E., et al, *What is Uremia? Retention Verses Oxidation*, Blood Purification, 24, 2006, 33-38

Vraetz, T., Ittel, T.H., et al, *Regulation of Beta(2)-Microglobulin Expression in Different Human Cell Lines by Proinflammatory Cytokines*, Nephrology Dialysis Transplantation, 14:9, 1999, 2137-2143.

Wall, Leo A. (Ed) (1972) *The Mechanisms of Pyrolysis, Oxidation, and Burning of Organic Materials*, U.S. Government Printing Office.

Winchester JF, Audia PF., *Extracorporeal strategies for the removal of middle molecules*. Seminars in Dialysis, 19(2), 2006, 110-114.

Winchester, J.F., Amerling, R., et al, *The Potential Application of Sorbents in Peritoneal Dialysis*. Peritoneal Dialysis: A Clinical Update, 150, 2006, 336-343.

Winchester JF, Kellum J, Ronco C, Brady JA, Quartararo PJ, Salsberg JA, Levin NW. *Sorbents in acute renal failure and the systemic inflammatory response syndrome*. Blood Purification, 21(1), 2003, 79-84.

Winchester, J.F., Ronco, C., et al, History of Sorbents in Uremia, Dialysis, Dialyzers and Sorbents: Where Are We Going? 133, 2001, 131-139

Winchester, J.F., Ronco, C., et al, *Sorbent Augmented Dialysis: Minor Addition or Major Advance in Therapy?*, Blood Purification, 19:2, 2001, 255-259

Winchester, J.F., Ronco, C., et al, *Sorbent Augmented Dialysis Systems*, Haemodialysis Technology, 137, 2002, 170-180.

Winchester, J.F., Ronco, C., *Sorbent Haemoperfusion in End-Stage Renal Disease: An In Depth Review*, Advances in Renal Replacement Therapy, 9:1, 2002, 19-25

Winchester, James F., Salsberg, Jamie and Yousha, Eric. *Removal of Middle Molecules with Sorbents*, Artificial Cells, Blood Substitutes, and Immobilization Biotechnology, 30, 2002, 547-554.

Winslow, F. H., Matreyek, W. and Yager, W. A. (1958) *Carbonisation of Vinyl Polymers, Industrial Carbon and Graphite (Conference) Proceedings London 1957*, London, Society of Chemical Industry.

8. Appendices

8.1 Appendix I Standard operating procedures

Standard Operating Procedure: SOP-01		
Description: Continuous Phase Generation		
Chemicals:	General Apparatus:	Specific Apparatus
Ultra Pure Water Poly-Vinyl Alcohol (PVA), molecular weight 205 kDa degree of hydrolysis 88% Sodium Chloride	Balance Hot Plate & Magnetic Stirrer	Glass/Pyrex Beaker Weighing Boats x2 Spatula/Spoon Foil Thermometer Magnetic Stirrer Flea
Hazards and Risks:		Precautions:
Near Boiling Liquid		Handle with care using heat proof gloves
Procedure:		
<ol style="list-style-type: none"> 1. Weigh the beaker and record the empty weight 2. Using the first weighing boat, weigh the required quantity of NaCl 3. Using the second weighing boat, weigh the required quantity of PVA 4. Weigh approximately the required water into the beaker 5. Place the beaker on the hot plate/stirrer and add the magnetic flea 6. Loosely cover the beaker with foil to prevent contamination from dust etc. 7. Turn on stirrer to vigorously agitate the water 8. Heat the water to ~80°C 9. Add the NaCl to the hot water and recover 10. Allow the NaCl to completely dissolve 11. Slowly add the PVA a spatula at a time to the solution allowing each spoonful to become well mixed before adding the next. 12. Recover and allow to mix at 80°C for 2 hours or until no particles of PVA are evident 13. Turn the temperature down to 35°C and allow to mix for a further 2 hours. 14. Turn off the heat. 15. Weigh the beaker/solution and add additional water to achieve the desired weight. 16. If particles of PVA remain reheat to 80°C and then turn off the hot plate and allow to mix over night. 17. Reweigh the solution and add additional water if required 		

18. Maintain mixing after production to prevent skin formation

Standard Operating Procedure: SOP-02		
Description: Organic Phase Preparation		
Chemicals:	General Apparatus:	Specific Apparatus
Monomers 1. Styrene 2. Divinylbenzene (DVB) Porogens/Diluents 1. Toluene 2. Undecane 3. Naphthalene Benzoyl Peroxide (BPO)	Magnetic Stirrer Plate Balance	Glass/Pyrex Beakers for Liquids Weighing Boats for solids Magnetic Stirrer Flea Spatula/Spoon Foil
Hazards and Risks:		Precautions:
Toxic Oxidising agent Flammable liquids		Wear appropriate PPE, work inside a fume cupboard at all times.
Procedure:		
<ol style="list-style-type: none"> Using the beakers weigh the liquid components of the porogens and cover with foil to prevent evaporation. Using a weighing boat, measure the required quantity of Naphthalene if applicable Using a second weighing boat measure the required (BPO), cover with foil. Mix the liquid porogens together add the magnetic stirrer flea, recover with foil and stir until homogenous If using naphthalene then spoon this slowly into the mixing solvents, allowing each spoonful to dissolve before adding the next, cover during dissolution. Using more beakers weigh the monomers and cover with foil, in the case of DVB cover the entire beaker to prevent reaction with UV light. Mix the monomers with the porogens and allow to become a homogeneous mixture. When ready to proceed with the polymerisation add the BPO and allow to dissolve completely. <p>NB – If high concentrations of naphthalene are to be used it may be required to combine the liquid porogens and monomers before the dissolution of naphthalene can be completed, in this case ensure the beaker is covered in foil to minimise reaction to UV light.</p>		

Standard Operating Procedure: SOP-03		
Description: Membrane Emulsification		
Chemicals:	General Apparatus:	Specific Apparatus
Continuous Phase, solution of PVA and NaCl in ultra pure water Organic Phase 1. Toluene 2. Monomers and Porogens	Syringe Pump DC Power Supply 3-12v Ultrasonic Bath	Micropore Technologies Membrane Emulsification Cell 1. PTFE Base 2. Glass Cell 3. PTFE Coated Rubber Seal 4. Paddle Stirrer and Motor 5. Membrane Disc Glass Syringe Plastic Syringe Tubing Tubing Clamp Stopwatch Glass/Pyrex Beaker
Hazards and Risks:		Precautions:
Toxic Flammable Liquid		Wear appropriate PPE Work in a fume cupboard
Procedure:		
<ol style="list-style-type: none"> 1. Submerge the membrane in the continuous phase and place in an ultrasonic bath for 5 minutes to ensure the pores are wetted. 2. Connect the tubing to the base of the membrane cell. 3. Using the plastic syringe fill the tubing and base full of continuous phase 4. Place the wetted membrane into the base, place the seal on top and screw the glass cell hand tight. 5. Add 50ml of continuous phase to the cell 6. Tilt the cell so the tubing outlet is as high as can be without allowing the membrane to be exposed to the air 7. Using the Plastic syringe pull ~10ml through the membrane to ensure no air bubbles 		

are trapped beneath the membrane, ensuring during this process the membrane remains submerged

8. Place the cell on the bench and push the 10ml back through the membrane, no bubbles should appear from the membrane
9. Fill the cell to the required volume and position the stirrer and motor unit
10. Power the stirrer motor ensuring the paddle is spinning freely, adjust the voltage to achieve the required speed
11. Fill the glass syringe with the organic phase, remember to fill the syringe with an excess of at least 10ml due to the dead volume of the cell and tubing
12. Clamp the tubing and remove the plastic syringe and attach the glass syringe containing the discontinuous phase
13. Remove the tubing clamp and push the discontinuous phase from the glass syringe until the tubing is nearly full
14. Place the glass syringe into the syringe pump, set the pumping rate and start the pump.
15. Watch the cell for the first sign of an emulsion being formed, start the stopwatch
16. Once the required volume of discontinuous phase has been injected stop the syringe pump, and stirrer, remove the stirrer motor assembly and pore the emulsion into the beaker.

Standard Operating Procedure: SOP-04		
Description: Cleaning of Membrane Emulsion Cell		
Chemicals:	General Apparatus:	Specific Apparatus
Deionised Water	Ultrasonic Bath	Glass/Pyrex Beaker (Large)
Acetone	Compressed Air Source	Glass/Pyrex Beaker
Detergent	Small Soft Cleaning Brush	(Medium) x2
Continuous and Discontinuous Phases from Emulsification		Tweezers
Hazards and Risks:		Precautions:
Flammable		Wear appropriate PPE
Toxic		Work in a fume cupboard while dealing with discontinuous phase from emulsification
Procedure:		
<ol style="list-style-type: none"> 1. Rinse cell with deionised water, ensure waste is collected in large beaker 2. Fill the cell to approximately half with deionised water, tip the cell so the tubing is as high as possible while the membrane remains submerged 3. Using the syringe pull the water back through the membrane, this should flush the majority of the discontinuous phase from the cell and tubing 4. Pour the remaining water from the cell into the waste beaker, remove the syringe and place the end of the tubing in the beaker, unscrew the glass cell from the base, all residual water/discontinuous phase should run into the waste beaker. 5. Remove the seal and set aside for cleaning 6. Lift the Membrane from the cell, rinse with copious amounts of deionised water. 7. Using a soft brush and detergent clean the membrane and then rinse with deionised water. 8. Place the membrane in the medium sized beaker cover with deionised water and place in the Ultrasonic bath for 5 minutes. 9. Remove the membrane from the deionised water and rinse with fresh deionised water to remove any residual detergent. 10. Place the membrane in the second medium sized beaker and cover with acetone, place in the ultrasonic bath for 1 minute 11. Remove the membrane from the acetone with the tweezers and dry using a 		

compressed air source.

12. Check the membrane is clean by inspecting it under a bright light.
13. Place membrane in protective bag for storage until next use
14. Clean remaining items following normal laboratory practice

Standard Operating Procedure: SOP-05		
Description: Suspension Polymerisation		
Chemicals:	General Apparatus:	Specific Apparatus
Continuous Phase – Solution of PVA, NaCl and Water Discontinuous Phase – Mixture of Monomers and Porogens	Thermally Controlled Water Bath with Pump and Anti-evaporation Precautions Variable Speed Overhead Stirrer Motor Silicon Grease	Jacketed Reactor 1. Reactor 2. Lid with Central Opening for Overhead Stirrer, 2x Side Ports for Condenser and Filling/Sampling 3. PTFE Sealing Ring 4. Stirrer Gland 5. Condenser 6. Glass stoppers 7. Wire Clamp PTFE Shaft Stirrer (Propeller) Glass Funnel Thermometer
Hazards and Risks:		Precautions:
High Temperatures Toxic Flammable		Wear appropriate PPE Work in a fume cupboard
Procedure:		
<ol style="list-style-type: none"> 1. Ensure the reactor is clean and that no contaminants are present 2. Connect the jacket of the reactor to the inlet and outlet hoses of the water bath 3. Using silicon grease ensure all ground glass joints are greased to ensure good seals 4. Fix the Stirrer shaft through the lid and gland to ensure an air tight seal 5. Place the PTFE seal on the reactor and then lid/gland stirrer assembly, fix in place using the wire clamp 6. Position the stirrer ~1/3 from the bottom of the reactor and secure in the gland and stirrer motor 7. Turn on the stirrer motor to ensure the stirrer will rotate freely, once confirmed turn 		

off

8. Attach the condenser to one of the side ports and ensure that cold water will flow freely
9. Using the alternate side port and the glass funnel fill the reactor with the required volume of continuous phase.
10. Remove the funnel, use a glass stopper to seal the port.
11. Start the stirrer motor and set the required speed.
12. Power on the water bath and set the temperature to 83°C
13. Once the water temperature reaches ~50°C add the discontinuous phase to the reactor via the side port using the funnel, reseal the reactor
14. Monitor temperatures to ensure the reaction mixture achieves 80°C
15. Leave for 24 hours for the reaction to complete

Standard Operating Procedure: SOP-06		
Description: Separation of Polymer Particles from Reaction Mixture		
Chemicals:	General Apparatus:	Specific Apparatus
Deionised Water Acetone	Vacuum Pump Magnetic Stirrer Hot Plate	Glass/Pyrex Beaker Buchner Funnel and Filter Paper, 90mm Sintered Glass funnel Magnetic Stirrer Flea Spatula/Spoon
Hazards and Risks:		Precautions:
Procedure:		
<ol style="list-style-type: none"> 1. Turn off Overhead stirrer, and water bath and allow the reaction mixture to cool and particles to separate out. 2. Once cool enough to handle open the reactor and use a spoon/spatula to remove the particles from the reaction vessel and place them in a beaker of ample volume 3. Add water to the particles place them on the magnetic stirrer at the flea and mix vigorously 4. Using either a sintered glass funnel or Buchner funnel and filter paper separate the particles from the water, return the particles to the beaker and repeat steps 3 and 4 an additional 4 times 5. After the fifth filtering heat some water (10 bed volumes) on the hotplate to $\sim 50^{\circ}\text{C}$ and allow this to percolate through the particles. 6. Finally wash the particles with acetone to remove any residual water from between the particles. 7. The Particles are now ready for Soxhlet extraction 		

Standard Operating Procedure: SOP-07		
Description: Soxhlet Extraction		
Chemicals:	General Apparatus:	Specific Apparatus
Toluene	Soxhlet Extractor Heating Mantle Vacuum Oven	Glass/Pyrex Beaker Spatula/Spoon Extraction Thimble Crucible Foil
Hazards and Risks:		Precautions:
Flammable Toxic		Use appropriate PPE Work in fume cupboard
Procedure:		
<ol style="list-style-type: none"> 1. Place the polymer particles in a beaker and cover with toluene and allow them to swell for at least 1 hour 2. Once swollen, spoon the particles into the extraction thimble fill each thimble to approximately three quarters 3. Fill the solvent evaporation section of the extractor approximately half full of toluene ensuring there is sufficient to fill the extractor without boiling dry 4. Place the thimble in the extractor and connect the condenser 5. Turn on both the cold water supply to the condenser and the heating mantle 6. Monitor the system to ensure the solvent is gently boiling and the condenser is working leave for 8 hours, checking at regular intervals 7. Once the extraction is completed turn off the heating mantle and allow the extractor to cool 8. Once cooled turn off the water supply to the condenser 9. Remove the thimble from the extractor and spoon the polymer particles into a crucible 10. Loosely cover the crucible with foil and place in the vacuum oven, gradually increase the vacuum allowing the particles time to equilibrate 11. Once maximum vacuum has been reached allow the particles to dry overnight at ambient temperature 		

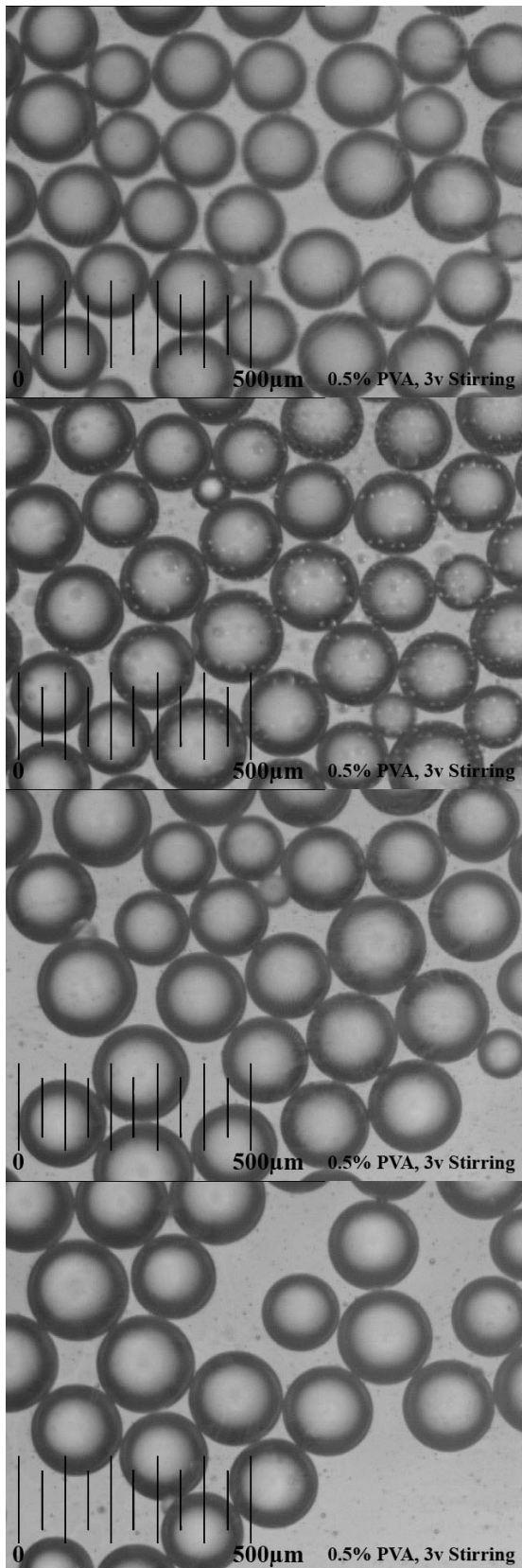
Standard Operating Procedure: SOP-08		
Description: Column Packing		
Chemicals:	General Apparatus:	Specific Apparatus
Tetrahydrofuran (THF)		<p>Column packer</p> <ol style="list-style-type: none"> 1. Pump/Control Unit 2. Compressed Air Source 3. Solvent Reservoir 4. Packing Reservoir 5. Column couplings 6. Safety Screen <p>Column Glass/Pyrex Beaker Measuring cylinder</p>
Hazards and Risks:		Precautions:
<p>Toxic</p> <p>Flammable</p> <p>High Pressure Liquids</p>		<p>Use appropriate PPE – Latex gloves, THF attacks nitrile.</p> <p>Work in a fume cupboard when possible</p> <p>Ensure all safety screens are in place before starting the column packer.</p>
Procedure:		
<ol style="list-style-type: none"> 1. Using a measuring cylinder measure the out the particles based on the volume of the column to be packed, allow 120% of the columns volume. Tap the measuring cylinder gently to ensure there are no large air pockets trapped in between the particles. 2. Transfer the particles to a beaker and generously cover with THF, leave for at least an hour to swell 3. Transfer the slurry to the packing reservoir 4. Attach the column couplings and column 5. Ensure the column is being packed upwards 6. Position the safety screens 7. Turn on the column packer ensure the pressure of the packing solvent is ~200 bar 8. Leave for 15 minutes 		

9. Reduce the pressure to 100 bar and continue to pack for a further 10 minutes
10. Reduce the pressure to 50 bar and pack for 5 minutes
11. Turn off the pump and rotate the column so that the backed column is now below the packing reservoir.
12. Leave the column for 15 minutes, then remove the column
13. Detach the reservoir from the column using the edge of the spatula remove any excess material from the end of the column.
14. Place the frit on the end of the column and attach its end cap.
15. Ensure the ends are sealed with column plugs to prevent the particles drying out.

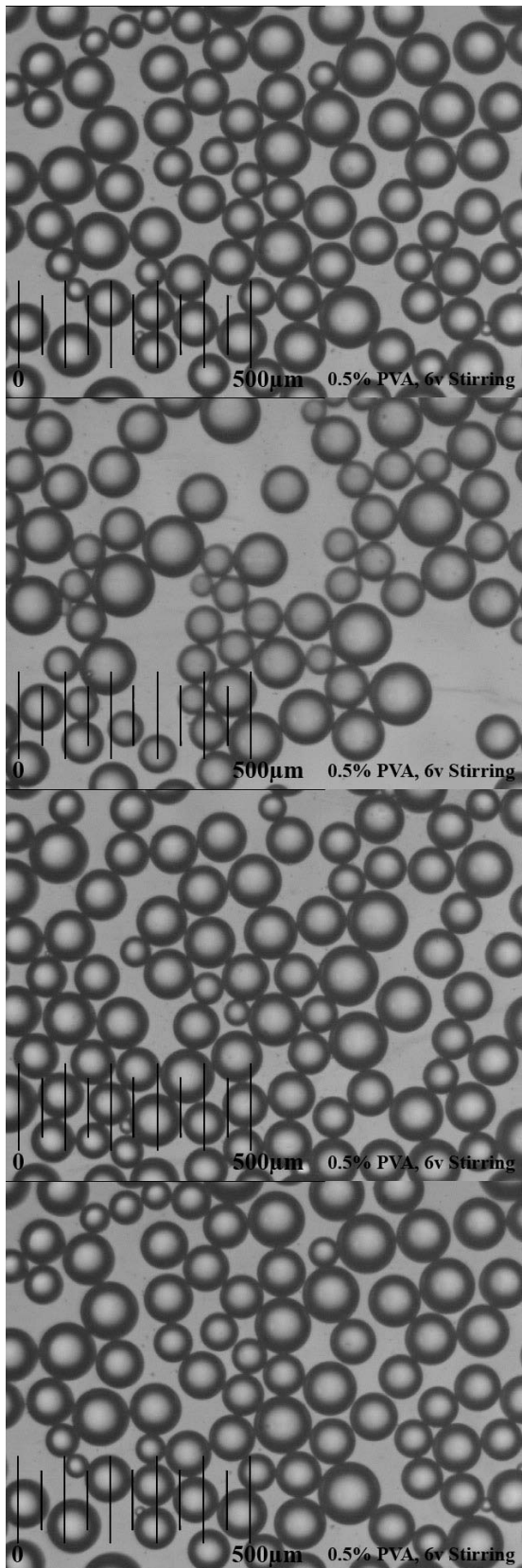
Standard Operating Procedure: SOP-09		
Description: Preparation of Size Exclusion Standards		
Chemicals:	General Apparatus:	Specific Apparatus
Tetrahydrofuran (THF) Toluene Polystyrene Standards Ultra Pure Water Dextran Standards	Balance	Sample Bottle Spatula Weighing Boat / Foil Volumetric Flask Glass/Pyrex Beaker Pipette
Hazards and Risks:		Precautions:
THF and Toluene Toxic Flammable		Use appropriate PPE Work in fume cupboard (when using THF) THF requires the use of Latex gloves
Procedure:		
<ol style="list-style-type: none"> 1. Clean all glassware thoroughly, and dry. 2. Using a weighing boat or piece of foil weigh the required amount of standard. 3. Weigh the volumetric flask 4. Transfer the weighed standard to the volumetric flask 5. Reweigh the volumetric flask, calculate the amount of standard contained within the flask 6. Add solvent to the volumetric flask, approximately half the required volume 7. Mix the flask to dissolve the standard 8. Once the standard is dissolved fill the flask to the required volume using a pipette to ensure accuracy 9. Mix the solution well 10. Transfer to the sample bottle, seal and label with the standards name and concentration. 		
NOTES:		
<ol style="list-style-type: none"> 1. If making polystyrene standards use THF as your solvent , for dextrans use ultra pure water. 2. When using THF ensure sample bottles are fitted with PTFE seals 		

8.2 Appendix II Toluene droplet micrographs

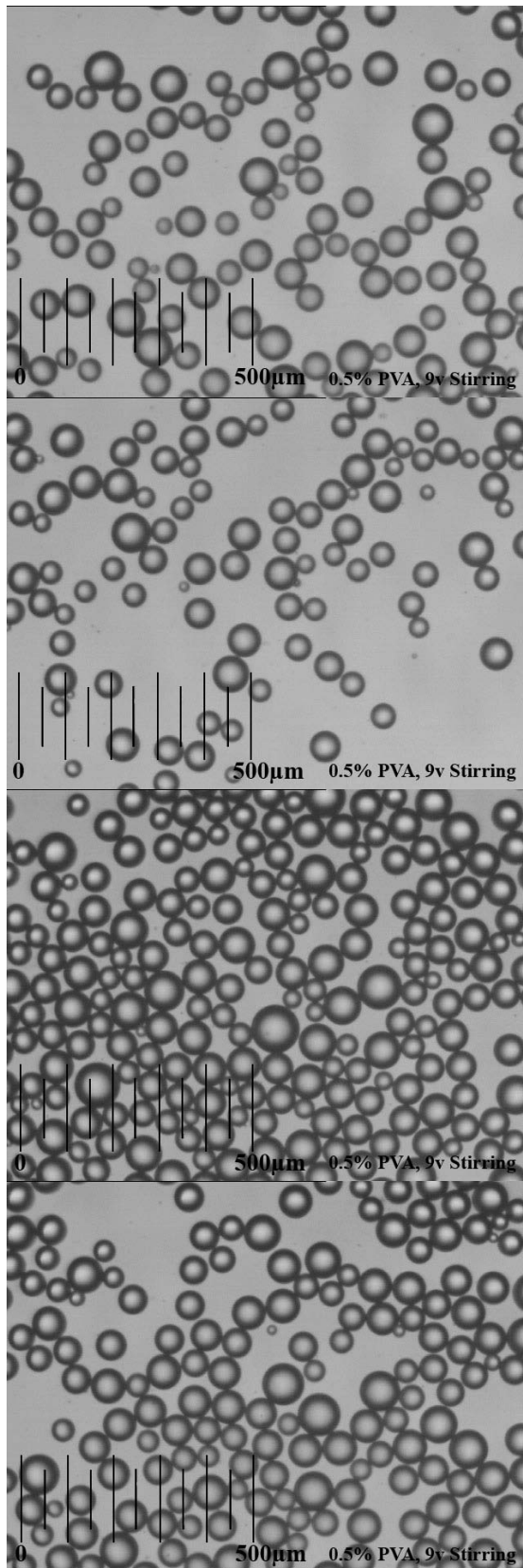
PVA Concentration 0.5%, Stirrer Voltage 3v



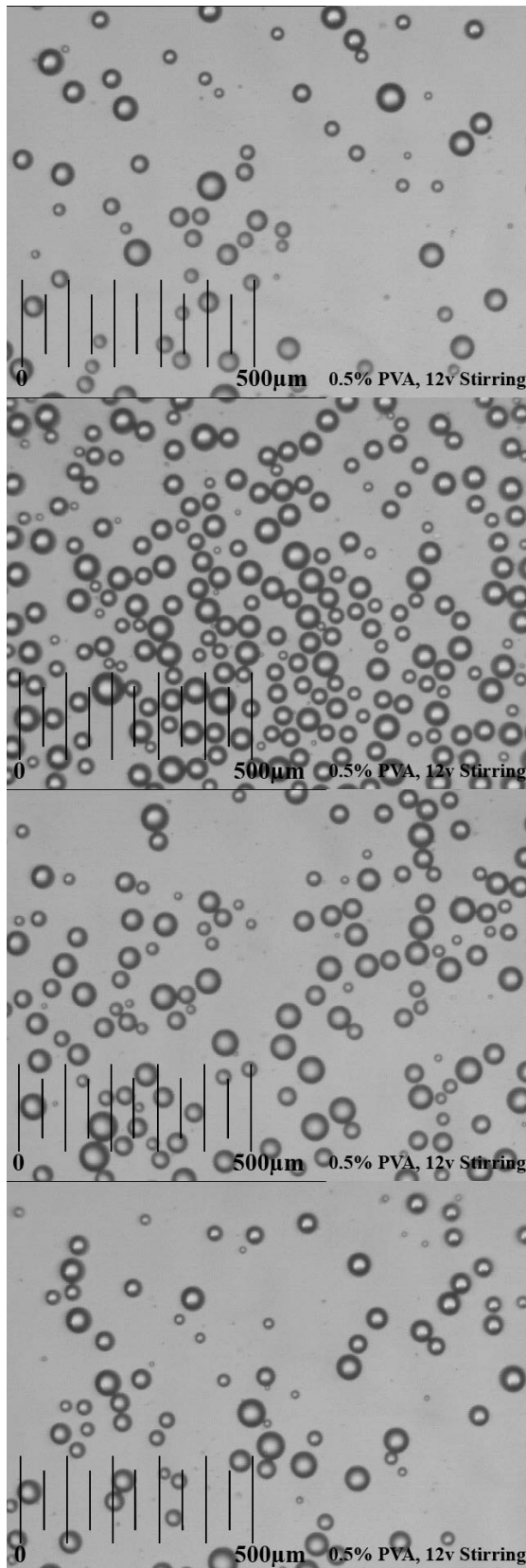
PVA Concentration 0.5%, Stirrer Voltage 6v



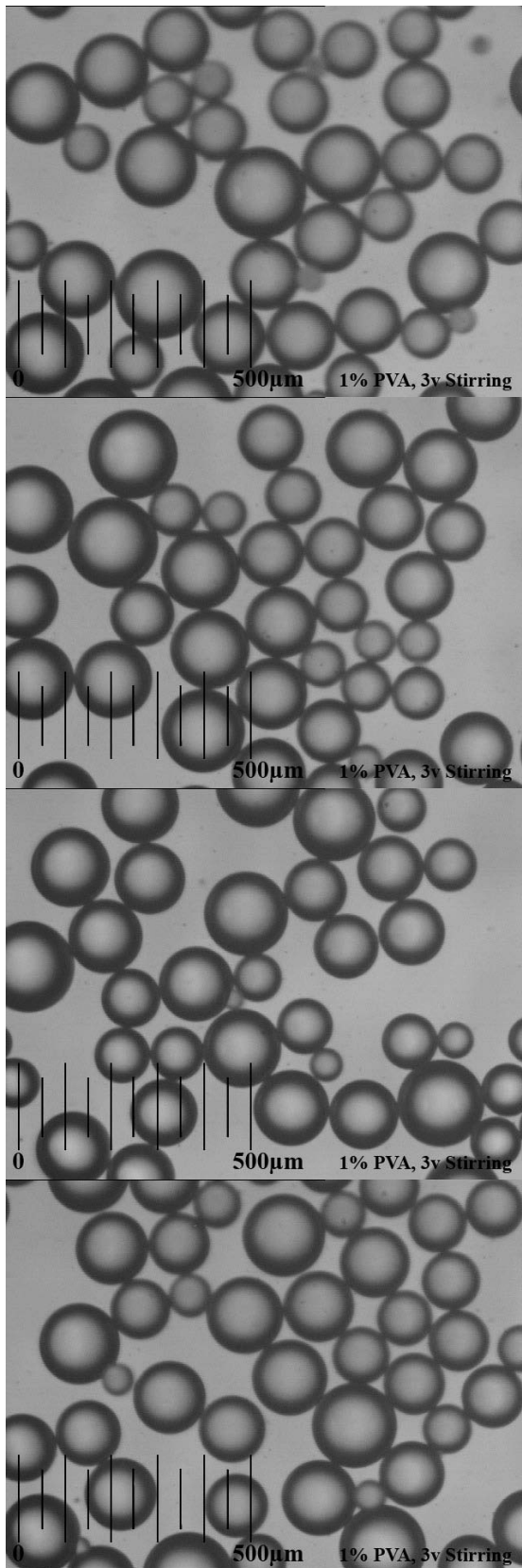
PVA Concentration 0.5%, Stirrer Voltage 9v



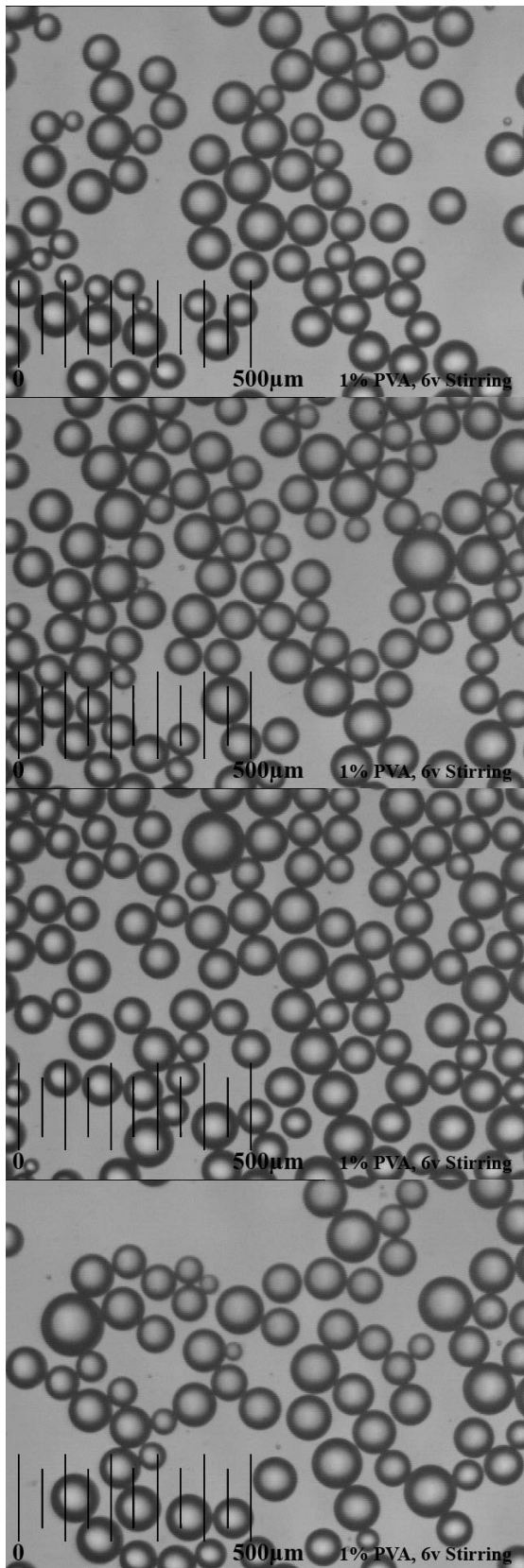
PVA Concentration 0.5%, Stirrer Voltage 12v



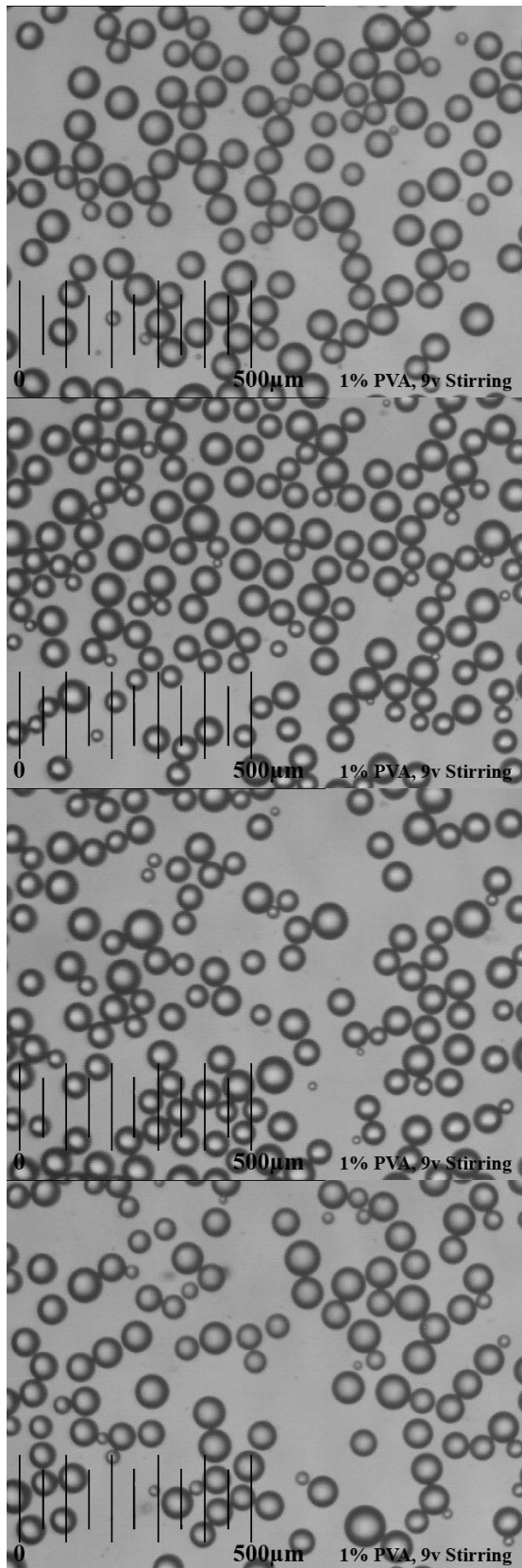
PVA Concentration 1%, Stirrer Voltage 3v



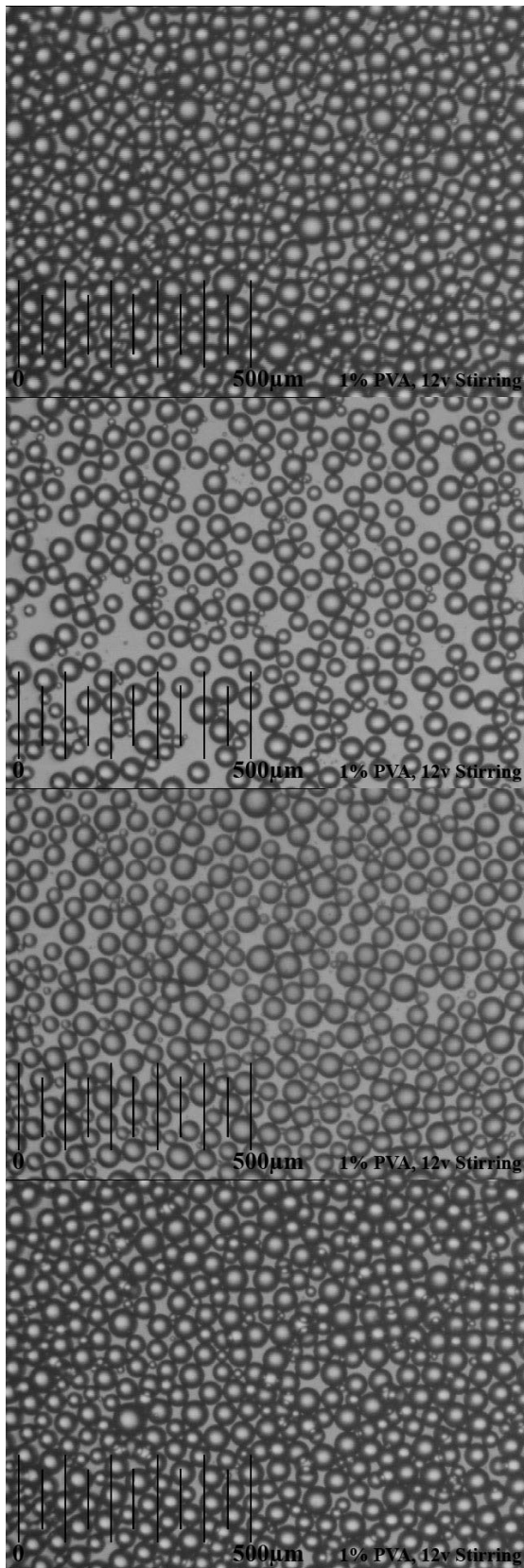
PVA Concentration 1%, Stirrer Voltage 6v



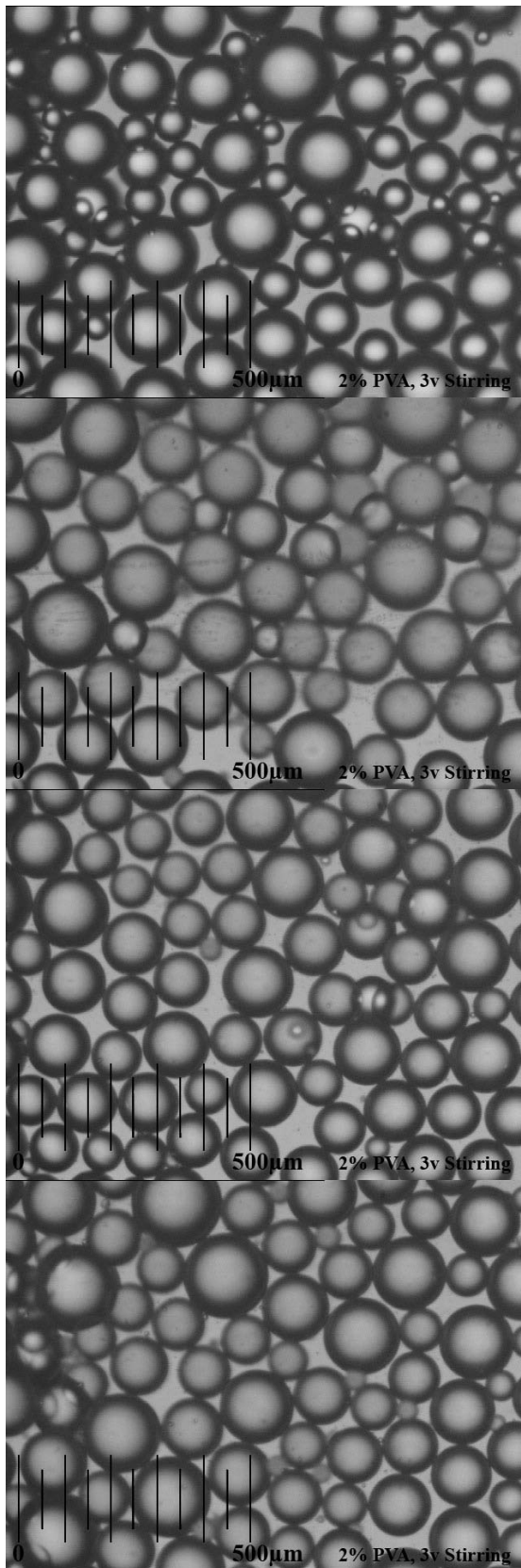
PVA Concentration 1%, Stirrer Voltage 9v



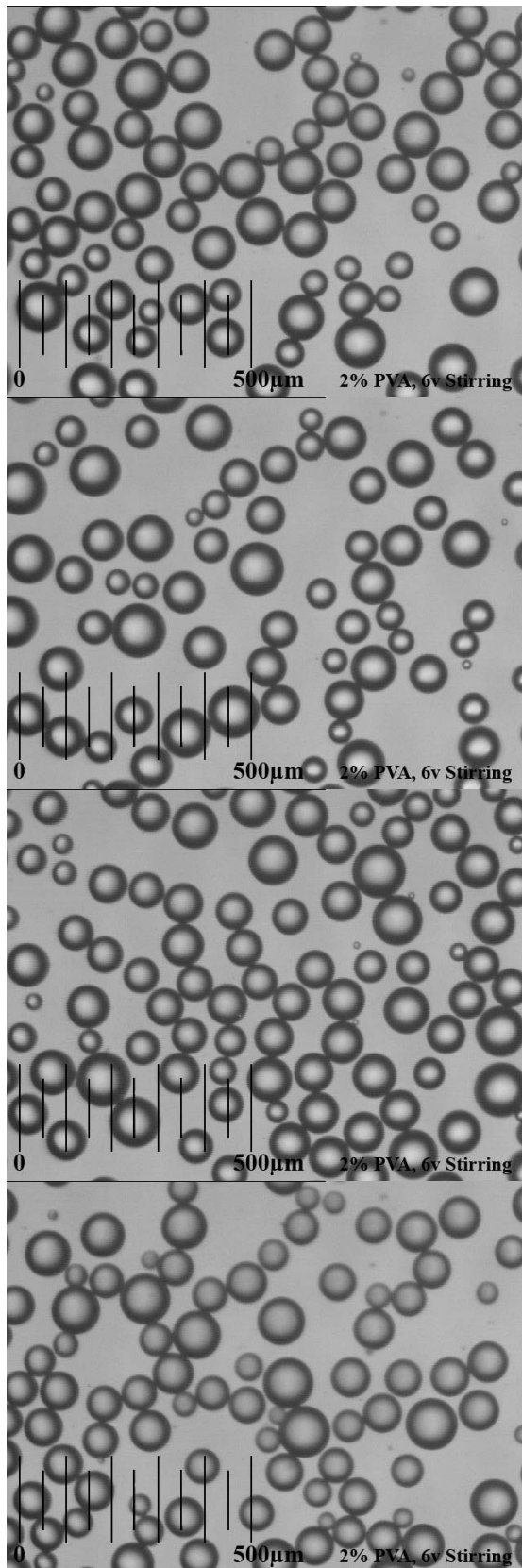
PVA Concentration 1%, Stirrer Voltage 12v



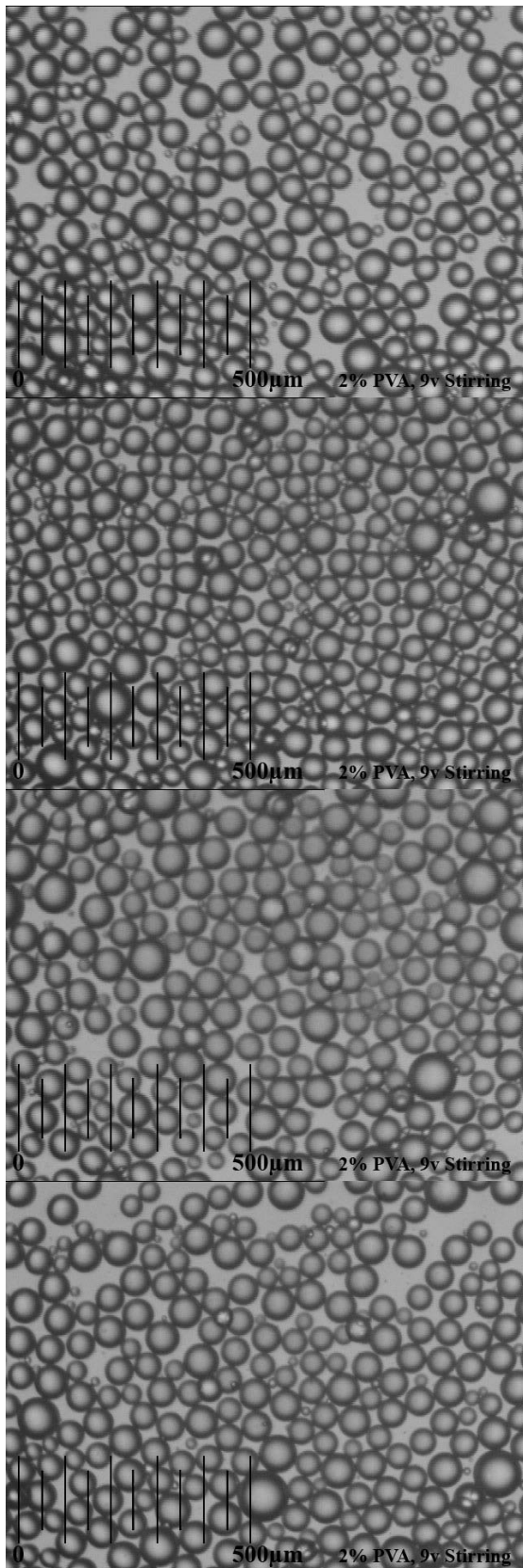
PVA Concentration 2%, Stirrer Voltage 3v



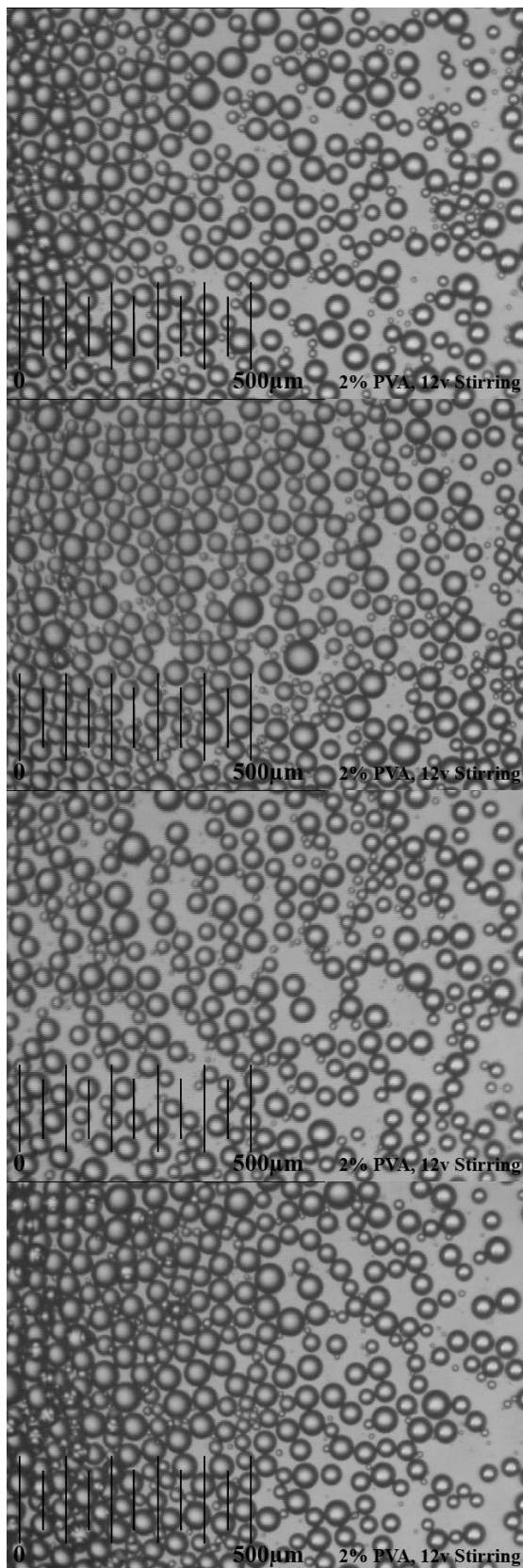
PVA Concentration 2%, Stirrer Voltage 6v



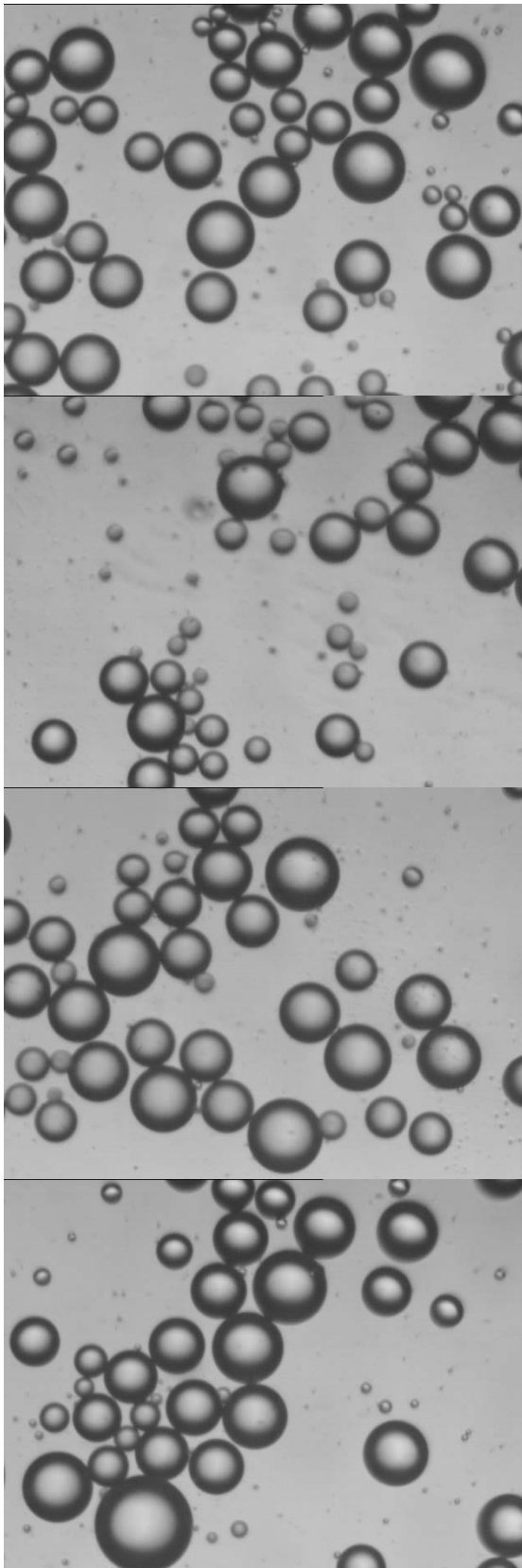
PVA Concentration 2%, Stirrer Voltage 9v



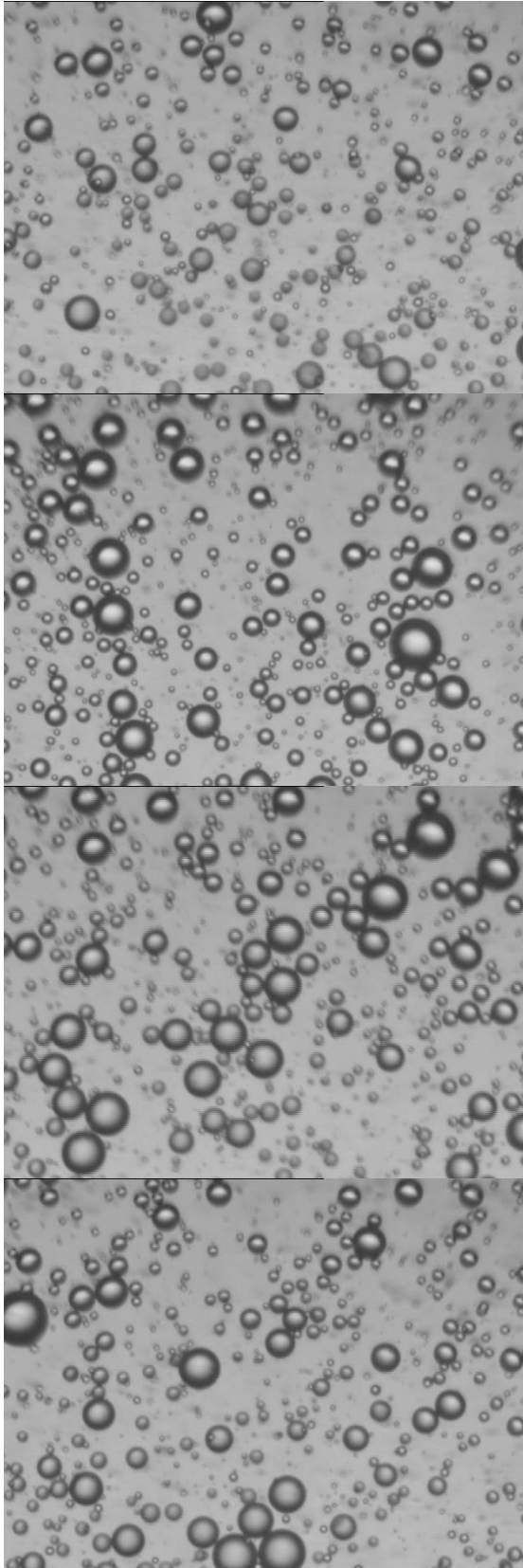
PVA Concentration 2%, Stirrer Voltage 12v



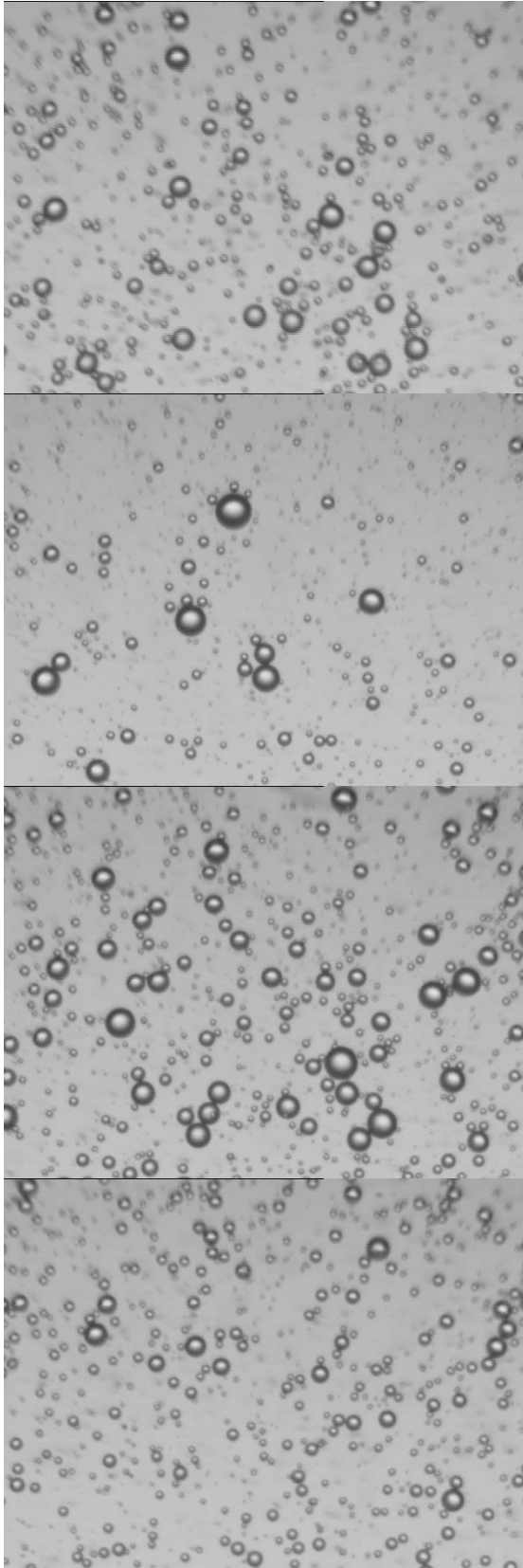
PVA Concentration 4%, Stirrer Voltage 3v



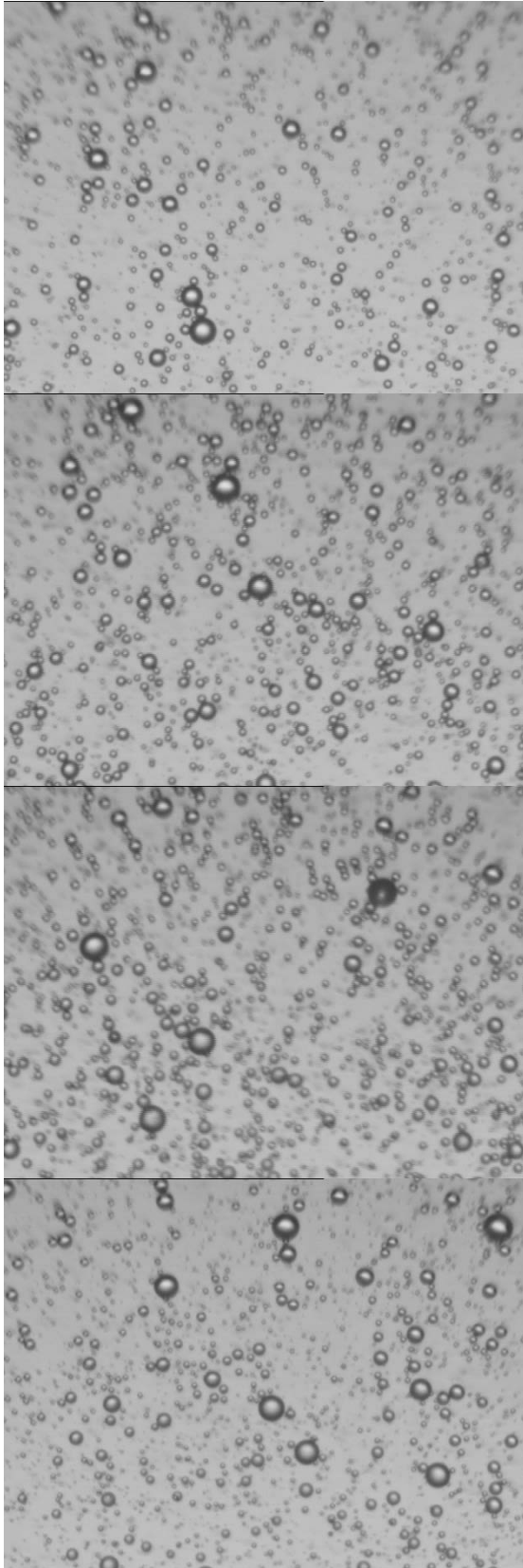
PVA Concentration 4%, Stirrer Voltage 6v



PVA Concentration 4%, Stirrer Voltage 9v



PVA Concentration 4% Stirrer Voltage 12v



8.3 Appendix III Irreversible adsorption batch kinetics model

Courtesy of Danish Malik, Chemical Engineering Dept. Loughborough University.

The usual shell balance for mass transfer within the adsorbent particle:

$$JA|_r - JA|_{r+\delta r} = \frac{\partial [q(1-\varepsilon)\rho_s 4\pi r^2 \delta r]}{\partial t} + \frac{\partial [\bar{c}\varepsilon\rho_s 4\pi r^2 \delta r]}{\partial t} \quad [1]$$

Applying Fick's Law:

$$J = -D_e \frac{\partial \bar{c}}{\partial r}$$

For irreversible adsorption, the solute uptake at equilibrium, q^* , is independent of the solute solution concentration \bar{c} , i.e. if there is solute in solution, adsorption will continue until the solute runs out or the adsorbent gets saturated.

Between $r_i \leq r \leq R$:

$$\frac{\partial q}{\partial t} = 0$$

Ignoring solute hold-up in the adsorbent pores, eq. 1 simplifies to:

$$\frac{\partial}{\partial r} \left[r^2 \frac{\partial \bar{c}}{\partial r} \right] = 0 \quad [2]$$

Integrating eq. 2 once gives:

$$r^2 \frac{\partial \bar{c}}{\partial r} = A(t) \quad [3]$$

A boundary condition may be as follows:

At $r = R$;

$$\left. \frac{\partial \bar{c}}{\partial r} \right|_{r=R} = \frac{\partial \bar{c}}{\partial r} \quad [4]$$

Where:

$$D_e \left. \frac{\partial \bar{c}}{\partial r} \right|_{r=R} = k_f (C_b - \bar{c}_R) \quad [5]$$

Therefore:

$$\left. \frac{\partial \bar{c}}{\partial r} \right|_{r=R} = \frac{k_f}{D_e} (C_b - \bar{c}_R)$$

And hence:

$$A(t) = \frac{R^2 k_f}{D_e} (C_b - \bar{c}_R) \quad [6]$$

Integrating eq. 3 requires a second boundary condition which is as follows:

At $r = r_i$, $\bar{c} = 0$, thus:

$$\int_{\bar{c}=0}^{\bar{c}} d\bar{c} = \int_{r=r_i}^{r=R} \frac{A(t)}{r^2} dr \quad [7]$$

Yielding:

$$\bar{c} = A(t) \left[\frac{1}{r_i} - \frac{1}{r} \right] \quad [8]$$

Therefore, combining the results in [6] and [8]:

$$\bar{c} = \frac{R^2 k_f}{D_e} \left[C_b - \bar{c}_R \right] \left[\frac{r - r_i}{r r_i} \right] \quad [9a]$$

Hence at $r=R$:

$$\bar{c}_R = \frac{R k_f}{D_e} \left[C_b - \bar{c}_R \right] \left[\frac{R - r_i}{r_i} \right] \quad [9b]$$

Define the following variables:

$$\phi = \frac{r_i}{R} \quad \text{and} \quad Bi = \frac{k_f R}{D_e};$$

Therefore, [9b] may be represented as:

$$\bar{c}_R = Bi \left[C_b - \bar{c}_R \right] \left[\frac{1 - \phi}{\phi} \right] \quad [10]$$

Express \bar{c}_R in terms of C_b :

$$\bar{c}_R = C_b \left[\frac{Bi(1-\phi)}{Bi + \phi(1-Bi)} \right] \quad [11]$$

Applying a mass balance on the solute in the stirred vessel:

$$-V \frac{dC_b}{dt} = \frac{d}{dt} \left\{ \bar{q} \rho_s (1-\varepsilon) \left(\frac{4}{3} \pi R^3 \right) N_p \right\} = A_p k_f (C_b - \bar{c}_R) \quad [12]$$

The average solute composition in the adsorbent is:

$$\bar{q} = \frac{\frac{4}{3} \pi [R^3 - r_i^3] q^*}{\frac{4}{3} \pi R^3} = q^* (1 - \phi^3) \quad [13]$$

And:

$$q^* = \frac{(C_{bo} - C_{bf})V}{m_p} \quad [14a]$$

$$\bar{q} = \frac{(C_{bo} - C_b)V}{m_p} \quad [14b]$$

Dividing eq. 14b by eq. 14a and using the result in eq. 13:

$$\frac{\bar{q}}{q^*} = \frac{C_{bo} - C_b}{C_{bo} - C_{bf}} = 1 - \phi^3 \quad [15]$$

Thus:

$$C_b = C_{bo} - \left\{ (1 - \phi^3) (C_{bo} - C_{bf}) \right\} \quad [16]$$

From eq. 14a:

$$C_{bo} - C_{bf} = \frac{q^* m_p}{V} \quad [17]$$

Replacing eq. 17 in eq. 16:

$$C_b = C_{bo} - \left\{ (1 - \phi^3) \left(\frac{q^* m_p}{V} \right) \right\} \quad [18]$$

Combining [11], [12], [13] and [18] yields a first order ordinary differential equation:

$$-\frac{d\phi}{dt} = \frac{m_p D_e B_i}{\rho_s (1 - \varepsilon) \phi^2 q^* R^2} \left\{ \left[C_{bo} + \frac{(\phi^3 - 1) q^* m_p}{V} \right] \left[\frac{\phi}{Bi + \phi(1 - Bi)} \right] \right\} \quad [19]$$

The o.d.e. in eq. 19 was solved numerically using an explicit 4th order Runge-Kutta method in Matlab (release 2007b) using the initial condition:

$$\text{At } t = 0; \phi = 1$$

The value of the film mass transfer coefficient was evaluated using the correlation in Middleman [1]:

$$Sh = 0.418 Sc^{0.25} Re^{0.75} \left(\frac{D_t^4}{VD_i} \right)^{\frac{1}{4}} \quad [20]$$

¹ Middleman, S. 1998, An introduction to mass and heat transfer – Principles of analysis and design. John Wiley & Sons, Inc.

Nomenclature

Symbol	Descriptor	Units
A	Area	(m ²)
A(t)	Time dependent integration constant	(-)
A _p	External area of adsorbent particles	(m ²)
Bi	Biot number ($\equiv k_f R/D_e$)	(-)
C _b	Bulk solute concentration in the stirred tank	(kg m ⁻³)
C _{bo}	Initial solute concentration (t = 0) in the stirred tank	(kg m ⁻³)
	Final solute concentration (t = ∞) in the stirred tank	(kg m ⁻³)
\bar{C}_R	Solute concentration in solution within particle at the external surface	(kg m ⁻³)
\bar{c}	Concentration of solute within the adsorbent pores	(kg m ⁻³)
D _e	Effective solute diffusivity in adsorbent	(m ² s ⁻¹)
D _v	Molecular diffusivity in solution	(m ² s ⁻¹)
D _t	Tank diameter	(m)
D _i	Impeller diameter	(m)
ε	Adsorbent porosity	(-)
J	Mass flux	(kg m ⁻² s ⁻¹)
k _f	External film mass transfer coefficient	(m ² s ⁻¹)
m _p	Mass of adsorbent particles in stirred tank reactor	(kg)
μ	Solution viscosity	(Pa.s)
N _p	Number of adsorbent particles in the stirred tank	(-)

N_s	Impeller rotational speed	(s^{-1})
ϕ	Reduced radius length scale ($\equiv r_i/R$)	(-)
Q	Adsorption uptake	($kg\ kg^{-1}$)
Q^*	Saturation adsorption capacity	($kg\ kg^{-1}$)
\bar{q}	Average solid phase solute composition	($kg\ m^{-3}$)
r	Radial position within spherical adsorbent particle	(m)
r_i	Radial position of adsorption front within spherical adsorbent particle	(m)
R	Radius of adsorbent particle	(m)
Re	Rotational Reynolds number ($\equiv \frac{\rho_f N_s D_i^2}{\mu}$)	(-)
ρ_f	Fluid density	($kg\ m^{-3}$)
ρ_s	Polymer solid density	($kg\ m^{-3}$)
Sc	Schmidt number ($\equiv \mu/\rho D_v$)	(-)
Sh	Sherwood number ($\equiv k_f R/D_v$)	(-)
V	Volume of solution in the stirred tank	(m^3)

8.4 Appendix IV Publications

Peer Reviewed Journal Article

Malik, D.J., Webb, C., Holdich, R.G., Ramsden, J.J., Warwick, G.L., Roche, I., Williams, D.J., Trochimczuk, A.W., Dale, J.A. and Hoenich, N.A., *Synthesis and characterization of size-selective nanoporous polymeric adsorbents for blood purification*, Separation and Purification Technology, 66, 2009, 578-585.

Conferences

Webb, C., Malik, D.J. and Holdich, R.G., *Engineering of the internal pore structure of poly(styrene-divinylbenzene) adsorbents for the removal of middle molecular weight proteins from blood and the exclusion of albumin*, Proceedings of the XXIInd International Symposium on Physicochemical Methods of Separations "Ars Separatoria 2007", June 10-14 2007, Szklarska Poreba, Poland., pp 88 – 92.

Webb, C., Malik, D.J. and Holdich, R.G., Synthesis and control of nanoporous polymeric adsorbents for the removal middle molecular weight molecules, Presented at IChemE Fluid Separation Subject Group Meeting 18/05/2007 at GlaxoSmithKline Stevenage.